



1 A synthesis of SNAPO-CO₂ ocean total alkalinity and total dissolved
2 inorganic carbon measurements from 1993 to 2022.

3

4 Nicolas Metzl¹, Jonathan Fin^{1,2}, Claire Lo Monaco¹, Claude Mignon¹, Samir Alliouane³,
5 David Antoine^{3,4}, Guillaume Bourdin⁵, Jacqueline Boutin¹, Yann Bozec⁶, Pascal Conan^{7,8},
6 Laurent Coppola^{3,8}, Frédéric Diaz^{*}, Eric Douville⁹, Xavier Durrieu de Madron¹⁰, Jean-Pierre
7 Gattuso^{3,11}, Frédéric Gazeau³, Melek Golbol^{8,12}, Bruno Lansard⁹, Dominique Lefèvre¹³,
8 Nathalie Lefèvre¹, Fabien Lombard^{3,14}, Férial Louanchi¹⁵, Liliane Merlivat¹, Léa Olivier¹,
9 Anne Petrenko¹³, Sébastien Petton¹⁶, Mireille Pujo-Pay⁷, Christophe Rabouille⁹, Gilles
10 Reverdin¹, Céline Ridame¹, Aline Tribollet¹, Vincenzo Vellucci^{8,12}, Thibaut Wagener¹³, Cathy
11 Wimart-Rousseau^{13,17}

12

13 ¹ Laboratoire LOCEAN/IPSL, Sorbonne Université-CNRS-IRD-MNHN, Paris, 75005, France

14 ² OSU Ecce Terra, Sorbonne Université-CNRS, Paris, 75005, France

15 ³ Sorbonne Université, CNRS, Laboratoire d'Océanographie de Villefranche, LOV, F-06230 Villefranche-sur-
16 Mer, France

17 ⁴ Remote Sensing and Satellite Research Group, School of Earth and Planetary Sciences, Curtin University,
18 Perth WA 6845, Australia

19 ⁵ School of Marine Sciences, University of Maine, Orono, USA

20 ⁶ Station Biologique de Roscoff, UMR 7144 – EDYCO-CHIMAR, Roscoff, France

21 ⁷ Sorbonne Université, CNRS, Laboratoire d'Océanographie Microbienne, LOMIC, F-66650 Banyuls-sur-Mer,
22 France

23 ⁸ Sorbonne Université, CNRS, OSU Station Marines, STAMAR, Paris, F-75006, France

24 ⁹ Laboratoire des Sciences du Climat et de l'Environnement, LSCE/IPSL, UMR 8212 CEA- CNRS-UVSQ,
25 Université Paris-Saclay, 91191 Gif-sur-Yvette, France

26 ¹⁰ CEFREM, CNRS-Université de Perpignan Via Domitia, 52 Avenue Paul Alduy, 66860 Perpignan, France

27 ¹¹ Institute for Sustainable Development and International Relations, Sciences Po, 27 rue Saint Guillaume, F-
28 75007 Paris, France

29 ¹² Sorbonne Université, CNRS, Institut de la Mer de Villefranche, IMEV, Villefranche-sur-Mer, F-06230, France

30 ¹³ Aix Marseille Univ, Université de Toulon, CNRS, IRD, MIO, Marseille, France

31 ¹⁴ Research Federation for the study of Global Ocean Systems Ecology and Evolution, FR2022/Tara GOSEE,
32 75000, Paris, France.

33 ¹⁵ CVRM: Laboratoire de Conservation et de Valorisation des Ressources Marines, Ecole Nationale Supérieure
34 des Sciences de la Mer et de l'Aménagement du Littoral (ENSSMAL), Station de recherche de Sidi Fredj,
35 Algeria

36 ¹⁶ Ifremer, Univ Brest, CNRS, IRD, LEMAR, F-29840 Argenton, France

37 ¹⁷ Marine Biogeochemistry, GEOMAR Helmholtz Centre for Ocean Research Kiel, 24105 Kiel, Germany

38 ^{*} Passed away 14/3/2021

39 *Correspondence to:* Nicolas Metzl (nicolas.metzl@locean.ipsl.fr)

40 **Abstract.** Total alkalinity (A_T) and total dissolved inorganic carbon (C_T) in the oceans are important properties
41 to understand the ocean carbon cycle and its link with climate change (ocean carbon sinks and sources) or global
42 change (ocean acidification). We present a data-base of more than 44 400 A_T and C_T observations in various
43 ocean regions obtained since 1993 mainly in the frame of French projects. This includes both surface and water
44 columns data acquired in open oceans, coastal zones and in the Mediterranean Sea and either from time-series or
45 punctual cruises. Most A_T and C_T data in this synthesis were measured from discrete samples using the same
46 closed-cell potentiometric titration calibrated with Certified Reference Material, with an overall accuracy of ± 4
47 $\mu\text{mol kg}^{-1}$ for both A_T and C_T . Given the lack of observations in the Indian and Southern Oceans, we added sea



48 surface underway A_T and C_T data obtained in 1998-2018 in the frame of OISO cruises and in 2019 during the
49 CLIM-EPARSEs cruise measured onboard using the same technique. Separate datasets for the global ocean, and
50 for the Mediterranean Sea are provided in a single format (<https://doi.org/10.17882/95414>, Metzl et al., 2023)
51 that offers a direct use for regional or global purposes, e.g. A_T /Salinity relationships, long-term C_T estimates,
52 constraint and validation of diagnostics C_T - A_T reconstructed fields or ocean carbon and coupled climate/carbon
53 models simulations, as well as data derived from BG-ARGO floats. When associated with other properties, these
54 data can also be used to calculate pH, fugacity of CO_2 ($f\text{CO}_2$) and other carbon systems properties to derive
55 ocean acidification rates or air-sea CO_2 fluxes.

56

57 **1 Introduction**

58

59 Since 1750, humans activities have added 700 (± 75) PgC to the atmosphere by burning fossil fuels,
60 producing cement and changing land use (Friedlingstein et al., 2022) driving up the atmospheric carbon dioxide
61 (CO_2) concentration and leading to unequivocal global warming. The ocean plays a major role in reducing the
62 impact of climate change by absorbing more than 90% of the excess heat in the climate system (Cheng et al.,
63 2020; von Schuckmann et al., 2020, 2023; IPCC, 2022) and about 25% of human released CO_2 (Friedlingstein et
64 al., 2022). However, the oceanic CO_2 uptake changes the chemistry of seawater reducing its buffering capacity
65 (Revelle and Suess, 1957) and leading to a process known as ocean acidification with potential impacts on
66 marine organisms (Fabry et al., 2008; Doney et al., 2009, 2020; Gattuso et al., 2015). With atmospheric CO_2
67 concentrations, surface ocean temperature and ocean heat content, sea-level, sea-ice and glaciers, the ocean
68 acidification (decrease of pH) is now recognized as one of the 7 key properties for global climate indicators
69 (WMO, 2018). In the frame of the 2030 Agenda, the United Nations established a set of Sustainable
70 Development Goals (SDG; United Nations, 2020), including a goal dedicated to the ocean (SDG 14, "Life below
71 water") which calls to "conserve and sustainably use the oceans, seas and marine resources for sustainable
72 development". Ocean acidification is specifically referred in the SDG indicator 14.3.1 coordinated at the
73 Intergovernmental Oceanographic Commission (IOC) of UNESCO. Observing the carbonate system in the
74 oceans and marginal seas and understanding how this system changes over time is thus highly relevant not only
75 to quantify the global ocean carbon budget, the anthropogenic CO_2 inventories or ocean acidification rates, but
76 also to understand and simulate the processes that govern the complex CO_2 cycle in the ocean and to better
77 predict future climate and global changes (Eyring et al., 2016; Kwiatkowski et al., 2020; Jiang et al., 2023a).

78 The number and quality of ocean $f\text{CO}_2$, A_T , C_T and pH measurements has increased substantially over
79 the past few decades. Quality-controlled observations are now regularly assembled in global data syntheses such
80 as SOCAT (Surface Ocean CO_2 Atlas, Pfeil et al., 2013; Bakker et al., 2014, 2016) and GLODAP (Global Ocean
81 Data Analysis Project, Key et al., 2004; Olsen et al., 2016, 2019, 2020; Lauvset et al., 2021). These datasets
82 allow evaluation of properties trends in the global ocean, including the change of the ocean CO_2 sink (e.g.
83 Wanninkhof et al., 2013; Friedlingstein et al., 2022; Watson et al., 2020), anthropogenic CO_2 inventories (e.g.
84 Sabine et al., 2004; Khatiwala et al., 2013; Gruber et al., 2019) and ocean acidification (Lauvset et al., 2015,
85 2020; Jiang et al., 2019). Thanks to the GLODAP data-base, new methods were recently developed (Sauzède et
86 al., 2017; Bittig et al., 2018) to reproduce A_T and C_T distributions from other properties like temperature, salinity
87 and oxygen more often observed in the water column especially from autonomous floats (Claustre et al., 2020;
88 Mignot et al., 2023). These methods (named CANYON-B and CONTENT, Bittig et al., 2018) are now also used
89 to help decisions on GLODAP data quality control or to fill in observational gaps (Olsen et al., 2019, 2020;



90 Tanhua et al., 2019, 2021). The GLODAP data-products were also successfully used to construct new global
91 ocean A_T and C_T climatological monthly fields in surface and water column using neural network method (e.g.
92 Broullón et al., 2019, 2020).

93 Following pioneer works that produced various global-ocean climatologies of the sea-surface carbonate
94 system (Millero et al., 1998; Lee et al., 2000, 2006; Takahashi et al., 2002, 2009, 2014; Sasse et al., 2013; Jiang
95 et al., 2019), the coupling of fCO_2 data (from SOCAT) and A_T data (from GLODAP) now enables reconstruction
96 of the full carbonate system in the surface ocean at monthly scale to investigate temporal trends at decadal scale
97 (e.g. Gregor and Gruber, 2021; Keppler et al., 2023).

98 International projects such as SOCAT and GLODAP offer important way to synthesize ocean carbon
99 data. In these projects, each observation is quality controlled offering to users high quality observations for
100 regional or global analysis, either for processes analysis or to constraint or validate of ocean and coupled
101 climate/carbon models (CMIP6, e.g. Lerner et al., 2021). SOCAT is a publicly available synthesis product
102 initiated in 2007 (Metzl et al., 2007) for quality-controlled, surface ocean fCO_2 (fugacity of carbon dioxide)
103 observations made by the international marine carbon research community (Bakker et al., 2016). The first
104 SOCAT version was released in 2011 (Pfeil et al., 2013; Sabine et al., 2013), followed by 6 SOCAT versions
105 (Bakker et al., 2014, 2016). The last version in 2023 includes more than 40 million fCO_2 data with accuracy
106 better than $5 \mu atm$ (Bakker et al., 2023). One important product from SOCAT is the use of data to estimate
107 global air-sea CO_2 fluxes based on reconstructed pCO_2 fields (e.g. SOCOM project, Surface Ocean pCO_2
108 Mapping Intercomparison, Rödenbeck et al., 2015). Since 2015, these results are included each year for the
109 global carbon budget (Le Quere et al., 2015; Friedlingstein et al., 2022).

110 On the other hand, following WOCE/JGOFS era in the 90s when almost all observations were started to
111 be synthesized in a specific recommended format (Joyce and Corry, 1994), GLODAP focusses on water-column
112 carbon observations (and other properties). Following the original GLODAP data-product (Key et al., 2004), the
113 project accumulated many new quality controlled observations. One important achievement from GLODAP is
114 the use of data to estimate the anthropogenic CO_2 inventory or its change over decades (Sabine et al., 2004;
115 Gruber et al., 2019). Both products, SOCAT and GLODAP, are relevant tools to detect oceanic acidification
116 rates (Lauvset et al., 2015; Jiang et al., 2019).

117 Although these projects include many international ocean observations there are ocean CO_2 related
118 observations all around the world (published or not published), such as total alkalinity and dissolved inorganic
119 carbon, not included in SOCAT or GLODAP. This is because SOCAT accepts and controls only fCO_2 data,
120 whereas GLODAP includes and controls water-columns data mainly from WOCE/GO-SHIP/CLIVAR cruises. It
121 should be noticed that many ocean carbon observations in various formats can be also found in dedicated data-
122 base such as NCEI/OCADS (former CDIAC-Ocean, Jiang et al., 2013b,
123 <https://www.ncei.noaa.gov/products/ocean-carbon-acidification-data-system>), PANGAEA
124 (<https://www.pangaea.de/>) or SeaNoe (<https://www.seanoe.org/>). In this context it is recommended to progress in
125 data synthesis of the ocean carbon observations that would offer new high quality products for the community
126 (e.g. for GOA-ON, www.goa-on.org, IOC/SDG 14.1.3, <https://oa.iode.org/>, Tilbrook et al., 2019).

127 In this work, we present a synthesis of more than 44 400 A_T and C_T observations obtained over the
128 1993-2022 period during various cruises or at time-series stations mainly supported by French projects. This
129 dataset merges observations measured with the same instruments thus being analytically coherent. Most of the
130 data have accuracy better than $\pm 4 \mu mol kg^{-1}$, i.e. between the climate ($\pm 2 \mu mol kg^{-1}$) and weather ($\pm 10 \mu mol kg^{-1}$)



131 ¹) goals (Bockmon and Dickson, 2015). Hereafter this dataset will be cited as SNAPO-CO₂. We describe the
132 data assemblage and associated quality control and discuss some potential uses of this dataset.

133

134 **2 Data collections**

135

136 The time series projects and research cruises from which data were collated are listed in Table 1 with
137 references in the Supplementary file (SNAPO-CO₂-cruises) and the sampling locations displayed in Figure 1.
138 Sampling was performed either from CTD-Rosette casts (Niskin bottles) or from the ship's seawater supply
139 (intake at about 5m depth depending the ship and swell). Samples collected in 500 mL borosilicate glass bottles
140 were poisoned with 100 to 300 µL of HgCl₂ depending on the cruises, closed with greased stoppers (Apiezon®)
141 and held tight using elastic band following the SOP protocol (Dickson et al., 2007). Some samples were also
142 collected in 500 mL bottles closed with screw caps. After completion of each cruise, discrete samples were
143 returned back to the LOCEAN laboratory (Paris, France) and stored in a dark room at 4 °C before analysis
144 generally within 2-3 months after sampling (sometimes within a week). Some samples were also measured for
145 specific processes studies on benthic corals (e.g. Maier et al., 2012; McCulloch et al., 2012) or for mesocosm
146 and culture experiments but the data are not included in this synthesis as they do not represent natural ocean state
147 (e.g. addition of Sahara dust during the DUNE project, Ridame et al., 2014).

148 As opposed to pCO₂, surface A_T or C_T observations are generally obtained from discrete sampling
149 (measured onboard or onshore). Few cruises offer sea-surface semi-continuous A_T or C_T observations (e.g. Metzl
150 et al., 2006) but new instrumental developments now enable A_T measurements on SOOP lines, Ship of
151 Opportunity Program (Seelmann et al., 2020). In addition to discrete samples analyzed for various projects
152 conducted mainly in the North Atlantic, Tropical Atlantic, Tropical Pacific, Mediterranean sea and coastal
153 regions (Table 1), we complemented this synthesis with A_T and C_T surface observations obtained in the Indian
154 and Southern oceans during the OISO cruises in 1998-2018 (Metzl et al., 2006; Leseurre et al., 2022; data also
155 available at NCEI/OCADS: www.nodc.noaa.gov/ocads/oceans/VOS_Program/OISO.html) and the recent CLIM-
156 EPARSEES cruise conducted in the Mozambique Channel in April 2019 (Lo Monaco et al., 2020, 2021). For
157 OISO cruises the water-column observations are part of the CARINA (CARbon IN the Atlantic) and GLODAP
158 synthesis products (Lo Monaco et al., 2010; Olsen et al., 2016, 2019, 2020) and not included here. Excepted
159 when specified, all data in this synthesis were obtained using the same technique used either in laboratory or at
160 sea (for OISO 1998-2018 and CLIM-EPARSEES 2019 cruises).

161



162 **Table 1:** List of cruises in the SNAPO-CO2 dataset. This is organized by region: Global Ocean and coastal
 163 zones, and Mediterranean Sea (MedSea). See Tables S1, S2, S4 and S4 in the Supplementary Material for a list
 164 of laboratories, of CRMs used, for references and for DOI of cruises. Nb = the number of data for each cruise or
 165 time-series.

166	Cruise/Project	Start	End	Region	Sampling	Nb
167						
168						
169						
170						
171	AWIPEV	2015	2021	Arctic	Surface and sub-surface	195
172	SURATLANT+RREX	1993	2017	North Atlantic	Surface	2832
173	OVIDE	2006	2018	North Atlantic	Surface, Water Column	397
174	STRASSE	2012		North Atlantic	Water Column	205
175	EUREC4A-OA	2020		North Atlantic	Surface, Water Column	135
176	PROTEUS	2010		North Atlantic	Water Column	27
177	CHANNEL	2012	2015	English Channel	Surface	696
178	SOMLIT-Brest	2008	2019	Coastal North Atl	Surface	1174
179	SOMLIT-Roscoff	2009	2019	Coastal North Atl	Surface and 60m	801
180	ECOSCOPIA	2017	2019	Coastal North Atl	Surface	67
181	PENZE	2011	2020	River Brittany	Surface and sub-surface	148
182	AULNE	2009	2010	River Brittany	Surface	27
183	ELORN	2009	2009	River Brittany	Surface	28
184	BIOZAIRE	2003	2004	Trop Atlantic	Water Column	87
185	EGEE	2005	2007	Trop Atlantic	Surface	199
186	PIRATA-FR	2009	2017	Trop Atlantic	Surface, Water Column	513
187	PLUMAND	2007		Trop Atlantic	Surface	38
188	OUTPACE	2015		Trop Pacific	Water Column	240
189	PANDORA	2012		Solomon Sea	Water Column	178
190	TARA-Pacific	2016	2018	Trop Pac, NATL	Surface and sub-surface	325
191	TARA-Ocean	2009	2012	Global Ocean	Surface + 400m	123
192	TARA-Microbiome	2021	2022	Atlantic	Surface, Water Column	216
193	ACE	2016	2017	Southern Ocean	Surface, Water Column	135
194	MOBYDICK	2019		Southern Ocean	Water Column	64
195	CLIM-EPARSESES	2019		Indian	Surface	790
196	OISO	1998	2018	South Indian	Surface	24950
197						
198	DYFAMED	1998	2017	MedSea	Water Column	2118
199	BOUSSOLE	2014	2019	MedSea	Surface + 10m	172
200	SOMLIT-PointB	2007	2015	MedSea Coastal	Surface + 50m	2397
201	ANTARES	2010	2016	MedSea	Water Column	502
202	MOLA	2010	2013	MedSea Coastal	Water Column	66
203	SOLEMIO	2016	2018	MedSea Coastal	Water Column	212
204	MOOSE-GE	2010	2019	MedSea	Water Column	1847
205	LATEX	2010		MedSea	Water Column	51
206	CARBORHONE	2011	2012	MedSea	Water Column	706
207	CASCADE	2011		MedSea	Water Column	218
208	DEWEX	2013		MedSea	Water Column	367
209	SOMBA	2014	2014	MedSea	Water Column	203
210	AMOR-BFLUX	2015		MedSea Coastal	Water Column	6
211	PEACETIME	2017	2017	MedSea	Water Column	233
212	PERLE	2018	2021	MedSea	Water Column	805

213
 214

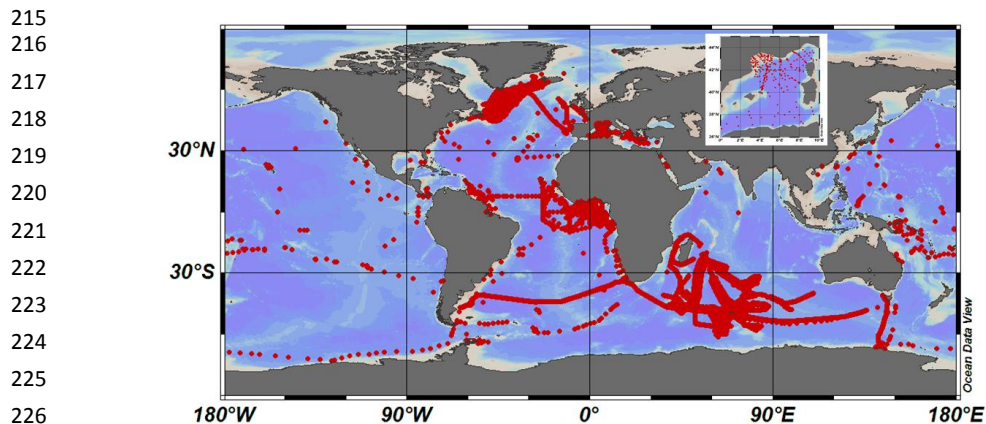


Figure 1: Locations of A_T - C_T data (1993-2022) in the Global Ocean and the Western Mediterranean Sea (insert).
Figure produced with ODV (Schlitzer, 2018).

3 Method, accuracy, reproducibility, intercomparison and quality control

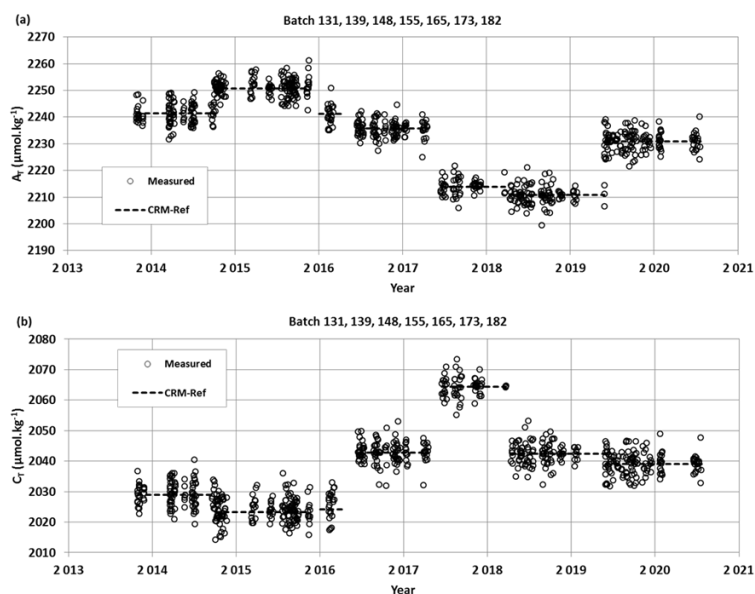
3.1 Method and accuracy

Except for the DYFAMED time-series observations measured between in 1998 and 2000 in the Mediterranean Sea (Copin-Montégut and Bégovic, 2002; Coppola et al., 2020; Lange et al., 2023), the SURATLANT time-series values acquired from 1993 to 1997 in the North Atlantic subpolar gyre (Reverdin et al., 2018) and samples measured in the river Penzé (Brittany) in 2019-2020 (Yann Bozec, SBR/Roscoff, pers. comm.), all discrete samples were measured at LOCEAN laboratory in Paris (SNAPO-CO₂ Service facilities) using the same technique. A_T and C_T were analyzed simultaneously by potentiometric titration using a closed cell (Edmond, 1970; Goyet et al., 1991). In the late 1980s the so-called “JGOFS-IOC Advisory Panel on Ocean CO₂” recommended the need for standard analysis protocols and for developing Certified Reference Materials (CRMs) for inorganic carbon measurements (Poisson et al., 1990; UNESCO, 1990, 1991). The CRMs were provided to international laboratories by Pr. A. Dickson (Scripps Institution of Oceanography, San Diego, USA), starting in 1990 for C_T and 1996 for A_T , respectively. These CRMs were thus always available to us and used to calibrate the measurements (CRM Batch numbers used for each cruise are listed in Supplementary file (Table S2)).

Results of analyses performed on 724 CRM bottles (different Batches) in 2013-2020 are presented in Figure 2. The standard deviations of the differences of measurements were on average around $\pm 3.5 \mu\text{mol kg}^{-1}$ for both A_T and C_T . For unknown reasons, the differences were occasionally up to $10\text{--}15 \mu\text{mol kg}^{-1}$ (0.8% of the data, Figure S2). These few CRM measurements were discarded for the data processing. On average, and excluding some outliers, standard-deviations of the differences for 985 CRM analyses were $\pm 2.95 \mu\text{mol kg}^{-1}$ for A_T and $\pm 3.30 \mu\text{mol kg}^{-1}$ for C_T , respectively. We did not detect any specific signal for these CRM analyses (e.g., larger uncertainty depending on the Batch number or temporal drifts during analyses, Figure 2) but for some cruises and specific series of samples analyzed over 2 to 7 consecutive days, the accuracy based on CRMs could



256 be slightly better than $3 \mu\text{mol kg}^{-1}$ ($\pm 2.5 \mu\text{mol kg}^{-1}$ for both A_T and C_T , e.g. Marrec et al., 2014; Touratier et al.,
257 2016; Ganachaud et al., 2017; Wimart-Rousseau et al., 2020a).



278 **Figure 2:** A_T (a) and C_T (b) analyses for different CRM Batches measured in 2013-2020. For these 724 analyses
279 the mean and standard-deviations of the differences with the CRM reference were $-0.08 (\pm 3.35) \mu\text{mol.kg}^{-1}$ for A_T
280 and $0.15 (\pm 3.61) \mu\text{mol.kg}^{-1}$ for C_T .

281 282 3.2 Reproducibility and repeatability

283
284 For some projects, duplicates have been regularly sampled (SOMLIT-Point-B, SOMLIT-BREST,
285 BOUSSOLE/DYFAMED) or replicate bottles sampled at selected depths at fixed stations during the cruises (e.g.
286 OUTPACE-2015, Wagener et al., 2018; SOMBA-2014, Keraghel et al., 2020). Results of A_T and C_T
287 reproducibility or repeatability are synthesized in Table 2. Figure 3 shows example of regular duplicates from the
288 times-series SOMLIT-Point-B in the coastal Mediterranean Sea (Kapsenberg et al., 2017), SOMLIT-Brest in the
289 Bay of Brest, coastal Iroise Sea (Salt et al., 2016) and BOUSSOLE/DYFAMED in the Ligurian Sea (Merlivat et
290 al., 2018; Golbol et al., 2000, 2020). For the 26 OISO cruises conducted between 1998 and 2018 and the CLIM-
291 EPARSES cruise in April 2019 (Lo Monaco et al., 2020, 2021), the repeatability was evaluated from duplicate
292 analyses (within 20 minutes time) of continuous sea surface underway sampling at the same location (when the
293 ship was stopped). Similarly to what was found for the CRM measurements (Figure S2), differences in
294 duplicates are occasionally higher than $10\text{-}15 \mu\text{mol kg}^{-1}$ (Figure 3) but most of the duplicates for all projects are
295 within 0 to $3 \mu\text{mol kg}^{-1}$. Based on the CRM analyses and replicates for different projects, different regions and
296 different periods, we estimated the accuracy for both A_T and C_T of $\pm 4 \mu\text{mol kg}^{-1}$.

297



298
299
300
301
302
303
304
305
306
307
308
309
310
311
312
313
314
315
316
317
318
319
320
321
322
323
324
325
326
327
328
329
330
331
332
333
334
335
336
337
338
339
340
341
342

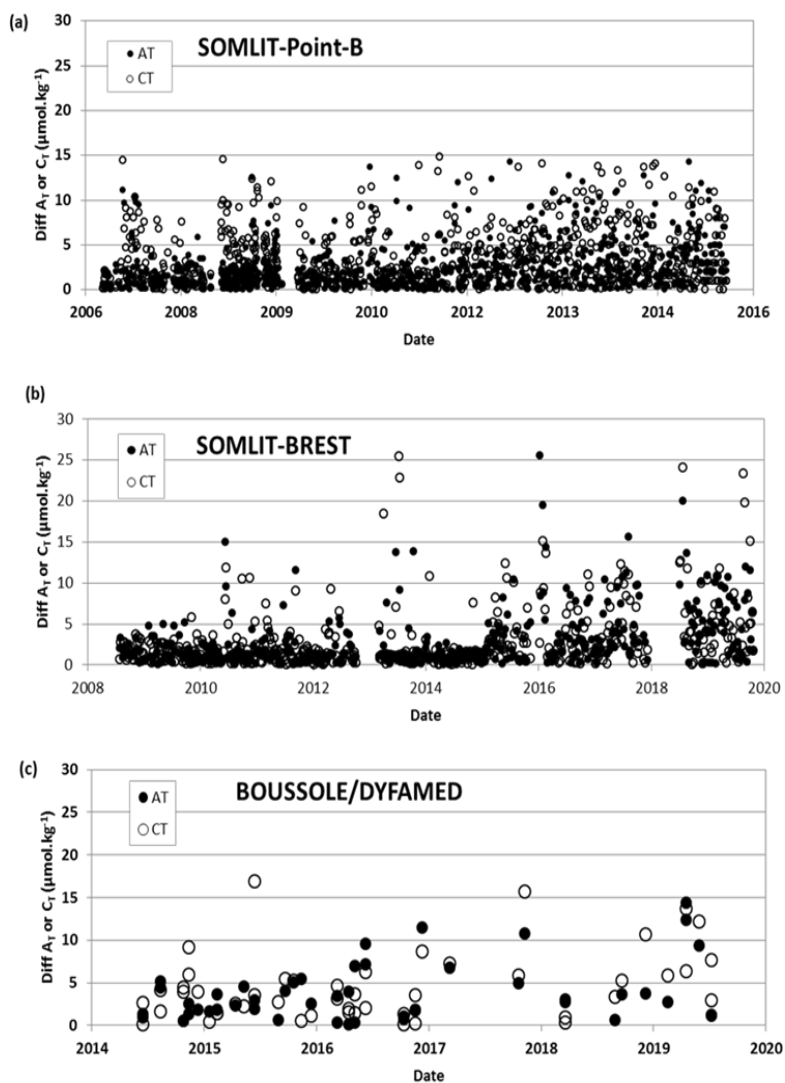


Figure 3: Results of duplicate A_T and C_T analyses from the time-series (a) SOMLIT-Point-B in the coastal Mediterranean Sea (Kapsenberg et al., 2017), (b) SOMLIT-BREST in the Bay of Brest, coastal Iroise Sea (Salt et al., 2016 and unpublished) and (c) BOUSSOLE/DYFAMED in the Ligurian Sea (Merlivat et al., 2018; Golbol et al., 2020). The plots show differences in duplicates for both A_T (filled circles) and C_T (open circles). Standard-deviations of these duplicates are listed in Table 2.



343

344 **Table 2:** Reproducibility of A_T and C_T analyses for cruises with duplicate analysis. The results are expressed as
345 the standard-deviations (Std) of the analysis of replicated samples. Nb = the number of replicates for each Time-
346 series or Cruise. See Figure 4 for the results of regular duplicates for 3 Time-series (SOMLIT-Point-B,
347 SOMLIT-BREST, and BOUSSOLE). For OISO and CLIM-EPARSE cruises the results correspond to repeated
348 measurements from continuous sea surface underway sampling at the same location (i.e. within 20 minutes time
349 and when the ship was stopped). For the 26 OISO cruises (1998-2018) and for simplicity we list the mean
350 repeatability obtained for all cruises. Detail for each OISO cruise could be consulted in the associated metadata
351 online at NCEI/OCADS, www.nodc.noaa.gov/ocads/oceans/VOS_Program/OISO.html
352

353

354

355

356

357

358

359

360

361

362

363

364

365

366

367

368

Project-Cruise	Nb	Std A_T $\mu\text{mol kg}^{-1}$	Std C_T $\mu\text{mol kg}^{-1}$	Reference
OUTPACE	12	3.64	3.68	Wagener et al. (2018)
SOMBA	13	2.00	3.30	Keraghel et al. (2020)
SOMLIT-Point-B	786	2.63	3.10	Kapsenberg et al. (2017)
SOMLIT-Brest	446	3.34	3.67	Salt et al. (2016) + unpub
BOUSSOLE	48	3.47	4.02	Merlivat et al. (2018); Golbol et al. (2020)
CLIM-EPARSE	122	2.20	2.30	Lo Monaco et al. (2020, 2021)
OISO 1998-2018	1162	2.06	2.28	Metzl et al. (2006) and (*)

367

368

(*) Data available at www.nodc.noaa.gov/ocads/oceans/VOS_Program/OISO.html

369

370

371

372

373

374

375

376

377

378

379

380

381

382

383

384

385

386

387

388

389

390

391

392

3.3 Inter-comparisons

Inter-comparisons of measurements performed with different technics help to evaluate the quality of the data and detect potential shifts (if any) when merging the data in the same region obtained by different laboratories at different periods. This is especially important to interpret long-term trends of A_T and C_T as well as for pCO_2 and pH calculated with A_T/C_T pairs. For ocean acidification studies, this also refers to the “climate goal” for which an accuracy for A_T and C_T better than $\pm 2 \mu\text{mol kg}^{-1}$ is needed (Newton et al., 2015; Tilbrook et al., 2019). Such inter-comparison thus helps to reflect the quality of the data to achieve either the so-called “weather goal” (for A_T and C_T , $\pm 10 \mu\text{mol kg}^{-1}$) or the “climate goal” ($\pm 2 \mu\text{mol kg}^{-1}$) (Bockmon and Dickson, 2015). For the projects in this data synthesis, inter-laboratory comparisons were performed occasionally and summarized below.

As part of the time-series CHANNEL (2012-2015) in the Western English Channel, Marrec et al. (2014) analyzed surface samples collected bi-monthly in 2011-2013. A_T analyses were performed with a TA-ALK-2 system (Appolo SciTech.) while C_T measurements were acquired with an AIRICA system (Marianda Inc.) Based on CRM analyses (Batch #92) the accuracy was estimated $\pm 3 \mu\text{mol kg}^{-1}$ for A_T and $\pm 1.5 \mu\text{mol kg}^{-1}$ for C_T (Marrec et al., 2014). When comparing with the samples measured at LOCEAN/Paris for the year 2012, Marrec et al. (2014) concluded that between the two methods the concentrations were within $\pm 2 \mu\text{mol kg}^{-1}$ and $\pm 3 \mu\text{mol kg}^{-1}$ for A_T and C_T respectively. This is close to the “climate goal” offering confident results for long-term trend analysis of the carbonate system in this region.

In the frame of the SURATLANT project in the Sub-Polar North Atlantic gyre, some samples collected at the same time (in 2005, 2006, 2010, 2015, and 2016) were also analyzed onshore for A_T and/or C_T by other laboratories using different technics (e.g. coulometric method) and the results summarized by Reverdin et al. (2018). For C_T , the mean differences between LOCEAN values and from 4 other laboratories range between -0.7 (± 4.6) and -6.5 (± 3.4) $\mu\text{mol kg}^{-1}$ depending on the cruise. For A_T the mean differences with 2 other laboratories



393 range from $-0.6 (\pm 4.1) \mu\text{mol kg}^{-1}$ to $+2.3 (\pm 4.8) \mu\text{mol kg}^{-1}$. These results range between the “climate goal” and
394 the “weather goal”. See Reverdin et al. (2018) for details on these inter-comparisons.

395 During OVIDE cruises conducted since 2002 in the North Atlantic along a section from Greenland to
396 Portugal (Lherminier et al., 2007; Mercier et al., 2015) samples have been taken (since 2006) to complement, for
397 summer, the SURATLANT time-series in the North Atlantic Sub-Polar gyre (NASPG). The OVIDE samples at
398 the surface and along the water-column at a few stations were measured back at LOCEAN for A_T and C_T (Metzl
399 et al., 2018). This enables us to compare our data with the measurements performed on-board by the IIM group
400 in Vigo/Spain (e.g. Pérez et al., 2010, 2013, 2018; Vazquez-Rodriguez et al., 2012). The OVIDE data have been
401 regularly quality controlled in CARINA and GLODAP data products (Velo et al., 2009; Key et al., 2010; Olsen
402 et al., 2016, 2019, 2020). The results of inter-comparisons are gathered in Table 3. For OVIDE in 2006 we
403 identified (for unknown reason) a large difference between our original A_T values compared to the A_T data
404 qualified in GLODAP and we thus corrected our A_T data by $+7.2 \mu\text{mol kg}^{-1}$. However, no correction was applied
405 for C_T . For other OVIDE cruises, differences for A_T range between $-4.5 (\pm 4.11) \mu\text{mol kg}^{-1}$ and $-0.05 (\pm 3.43)$
406 $\mu\text{mol kg}^{-1}$ depending on the cruise (i.e. A_T measured at LOCEAN was always slightly lower than onboard
407 measurements). For C_T , we compared our measurements onshore with C_T values calculated with A_T and pH
408 measured onboard. Most of the mean C_T differences are slightly positive (i.e. C_T measured at LOCEAN was
409 always higher, except for 2010). Taking into account all errors associated with the sampling, the transport of
410 samples, the instrumentations, the data processing, or the calculations for C_T , the comparisons between
411 LOCEAN and IIM data for OVIDE cruises are deemed acceptable and large differences for both A_T and C_T (> 4
412 $\mu\text{mol kg}^{-1}$) are far from being systematic (Table 3). The data from SURATLANT and OVIDE can then be
413 merged to complete the time-series in the NASPG in summer and to better describe the seasonality of the
414 oceanic carbonate system. For example, in 2010, when the North Atlantic Oscillation (NAO) was strongly
415 negative, the SURATLANT data showed a rapid decrease of C_T concentrations in the NASPG between early
416 June and August (Figure 4), with C_T concentrations in August much lower than other years (Racapé et al., 2014).
417 This leads to a rapid drop in $f\text{CO}_2$ in 2009-2010, such that the NASPG was a strong CO_2 sink (Leseurre et al.,
418 2020). The winter-to-summer seasonal decrease of C_T in 2010 in the north NASPG was on average $-77 \mu\text{mol}$
419 kg^{-1} (Figure 4) much larger than in the climatology (range -50 to $-55 \mu\text{mol kg}^{-1}$, Takahashi et al., 2014; Reverdin
420 et al., 2018). The OVIDE data in late June 2010 and SURATLANT in August 2010 confirmed this signal that
421 was linked to a pronounced primary productivity in that period (Figure 4, Henson et al., 2013; Racapé et al.,
422 2014; Mc Kinley et al., 2018). Notice that for this period no $p\text{CO}_2$ observations were available in July-September
423 2010 in SOCAT data-product and the A_T - C_T data presented here could be used to calculate $p\text{CO}_2$ to complement
424 the $p\text{CO}_2$ dataset in this region like was done for other periods (Mc Kinley et al., 2011).

425



426
 427
 428
 429
 430
 431
 432
 433
 434
 435
 436
 437
 438
 439
 440
 441
 442
 443
 444
 445
 446
 447
 448
 449
 450
 451
 452
 453
 454
 455
 456
 457
 458
 459
 460
 461
 462
 463
 464
 465
 466
 467
 468
 469
 470
 471
 472
 473
 474
 475
 476
 477
 478
 479
 480
 481

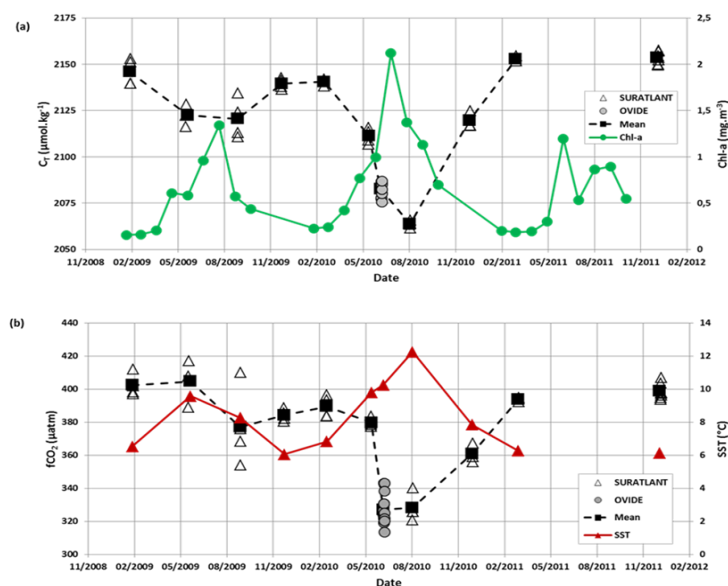


Figure 4: (a) Time-series of C_T concentrations ($\mu\text{mol.kg}^{-1}$) for 2009-2011 in surface waters in the North Atlantic Sub-Polar gyre (zone 59°N - 33°W) based on SURATLANT (open triangles) and OVIDE-2010 (grey circles) data. In 2009, SURATLANT data were available in February, June, September and December, while in 2010 data available in March, June, August and December and in 2011 data only available for March and December. The OVIDE data in late June 2010 completed the temporal cycle and confirmed the strong seasonal signal and low C_T concentrations in summer 2010 not seen in 2009 (or in 2011 as there is no data in summer). The mean observations for each period describe the C_T seasonal cycles in 2009 and 2010 (Black squares, dashed line). The monthly surface chlorophyll-a concentrations (Chl-a, mg.m^{-3}) averaged in the same region based on MODIS are also shown (Green dots and line) highlighting the high productivity during the summer 2010. Chl-a monthly data extracted from MODIS (Giovanni/NASA, last access 3/5/19). (b): Time-series of $f\text{CO}_2$ (μatm) for the same cruises (same symbols) calculated with A_T - C_T . Mean SST ($^\circ\text{C}$) indicated (red triangles). In June 2010 oceanic $f\text{CO}_2$ decreased by $53 \mu\text{atm}$ in 2 weeks.

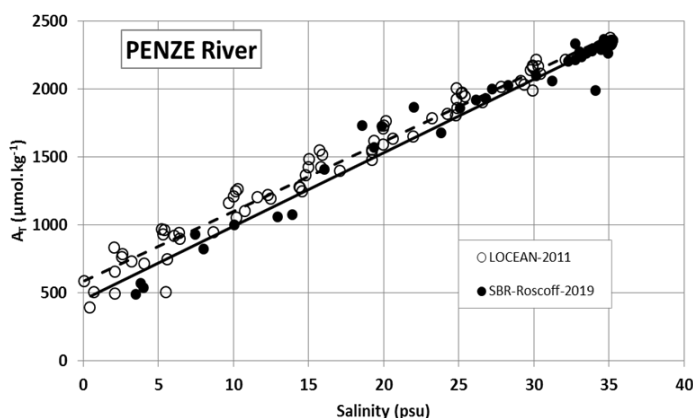
Table 3: Comparisons of A_T and C_T samples measured back at LOCEAN with measurements onboard by IIM Laboratory (F. Pérez, Vigo, Spain) for OVIDE cruises in the North Atlantic. Nb= Number of samples. ND= No Data. The results listed indicate the mean and standard deviations of the differences (LOCEAN-IIM). For A_T , IIM values were measured on-board. For C_T , IIM values were calculated from A_T and pH both measured onboard. The IIM data were quality controlled and here taken from the GLODAP data-products (Olsen et al, 2016, 2019).

Cruise Year	Nb A_T	A_T (LOCEAN) - A_T (IIM) $\mu\text{mol.kg}^{-1}$	Nb C_T	C_T (LOCEAN) - C_T (IIM) $\mu\text{mol.kg}^{-1}$
OVIDE-2006	14	-2.04 (\pm 5.84) (*)	14	1.12 (\pm 2.49)
OVIDE-2008	29	-4.53 (\pm 4.11)	29	3.76 (\pm 3.11)
OVIDE-2010	41	-1.96 (\pm 2.26)	41	-2.42 (\pm 3.35)
OVIDE-2012	37	-0.12 (\pm 8.85)	ND	ND
GEOVIDE-2014	57	-0.05 (\pm 3.43)	54	2.36 (\pm 7.89)

(*) for the OVIDE 2006 cruise original difference for A_T was $-9.0 (\pm 5.8) \mu\text{mol.kg}^{-1}$ and LOCEAN A_T data were corrected by $+7.2 \mu\text{mol.kg}^{-1}$ based on the mean concentrations in deep layers. No corrections were applied for A_T and C_T for other cruises.



482 The comparisons described above concern the open ocean region with A_T and C_T concentrations in a
483 range of concentrations close to the CRM references (used by the different laboratories). Another example of
484 comparison is presented here for samples obtained along a river and thus for waters with low salinity and A_T
485 concentrations (river Penzé in North Brittany). In 2019, A_T was measured at SBR laboratory (Station Biologique
486 de Roscoff) by a potentiometric method (using a Titrino-847 plus Metrohm) calibrated with CRM (Batch #131)
487 for a final accuracy of $\pm 2.1 \mu\text{mol kg}^{-1}$ (Gac et al., 2020). Although the samples were measured with different
488 technics the A_T /Salinity relationships are very coherent for both datasets (Figure 5). Therefore we added the A_T
489 data measured in 2019-2020 to complete the synthesis for this location (river Penzé).



491
492
493
494
495
496
497
498
499
500
501
502
503
504
505 **Figure 5:** Total alkalinity (A_T) versus salinity for samples measured in 2011 and 2019 in the river Penzé, North
506 Brittany (Gac et al., 2020). A_T samples were measured at LOCEAN in 2011 (open circles, dashed-line) and at
507 SBR laboratory (Roscoff) in 2019 (filled circles, black line).

508 509 3.4 Quality control and flags

510
511 Identifying each data with an appropriate flag is very convenient for selecting the data (good,
512 questionable or bad). Here we used 4 Flags for each property (Flags 2, 3, 4, and 9) following the WOCE
513 program and used in other data products such as SOCAT (Bakker et al., 2016) or GLODAP (Olsen et al., 2016,
514 2019, 2020; Lauvset et al., 2021). During the data-processing, we first assigned a flag for each A_T and C_T data
515 based on the standard error in the calculation of A_T and C_T concentrations (non-linear regression, Dickson et al.
516 2007). By default, if the standard-deviation on the regression is $> 1 \mu\text{mol kg}^{-1}$, we assigned a flag 3
517 (questionable) although the data could be acceptable and then used for interpretations. Flag 3 was also assigned
518 when salinity was doubtful or when differences of duplicates were large (e.g. $\pm 20 \mu\text{mol kg}^{-1}$). Flags 4 (bad or
519 certainly bad) were assigned when clear anomalies were detected for unknown reason (e.g. a sample probably
520 not fixed with HgCl_2). A secondary quality control was performed by the PIs of each project based on data
521 inspection, duplicates, A_T /Salinity relationship, or the mean observations in deep layers where large variability in
522 A_T and C_T is unlikely to occur from year to year. An example presents all data from the MOOSE-GE cruises
523 conducted in 2010-2019 in the Mediterranean Sea (Coppola et al., 2020; Testor et al., 2010) where clear outliers
524 have been identified (Figure S3). For the 10 MOOSE-GE cruises and a total of 1847 A_T and C_T analyses, 26 were
525 identified flagged as bad (flag 4), 139 for A_T and 141 for C_T listed as questionable (flag 3) and 1682 for A_T and



526 1680 for C_T considered as good data (flag 2, i.e. more than 90%). Similar control was performed for each
 527 project.

528 The synthesis of various cruises in the same region and period also offers verification and secondary
 529 control of the data. For example, several cruises were conducted in the Mediterranean Sea in 2014 (MOOSE-GE,
 530 SOMBA, ANTARES and DYFAMED). The mean values of C_T and A_T in the deep layers (> 1800m) for each
 531 cruise confirmed the coherence of the data (Table 4). This enabled to merge the different datasets for
 532 interpretations of the temporal trends and processes driving the CO_2 cycle (Coppola et al., 2019, 2020; Ulses et
 533 al., 2022) or to train and validate a regional neural network to reconstruct the carbonate system (e.g. CANYON-
 534 MED, Fourier et al., 2020, 2022).

535
 536
 537
 538
 539
 540
 541
 542

Table 4: Mean observations in the deep layers (> 1800m) of the western Mediterranean Sea for different cruises
 conducted in 2014. Results in deep layers (> 1800m) for the DEWEX cruise in 2013 and the PEACETIME
 cruise in 2017 in the same region are also listed. $N-A_T$ and $N-C_T$ are A_T and C_T normalized at Salinity = 38. Nb =
 number of data (with flag 2). Standard-deviations are in brackets. References for these cruises are listed in
 Supplementary Material.

Cruise	Period	Nb	Pot. Temp C	Salinity PSU	$N-A_T$ $\mu\text{mol kg}^{-1}$	$N-C_T$ $\mu\text{mol kg}^{-1}$
All cruises	Feb/Dec-2014	76	12.905 (0.007)	38.486 (0.005)	2562.9 (5.3)	2303.7 (4.7)
ANTARES	Feb/Nov-2014	14	12.913 (0.004)	38.488 (0.006)	2564.0 (3.8)	2301.9 (3.5)
DYFAMED	Mar/Dec-2014	9	12.905 (0.0016)	38.487 (0.004)	2560.1 (5.0)	2304.3 (6.8)
MOOSE-GE	Jul-2014	21	12.909 (0.004)	38.487 (0.005)	2565.6 (4.6)	2303.5 (4.1)
SOMBA	Aug/Sep-2014	32	12.899 (0.005)	38.483 (0.005)	2561.5 (5.6)	2304.6 (4.8)
DEWEX	Feb/Apr-2013	44	12.903 (0.010)	38.588 (0.006)	2556.0 (4.3)	2294.0 (5.7)
PEACETIME	May/Jun-2017	7	12.904 (0.002)	38.486 (0.003)	2567.2 (10.6)	2308.1 (8.9)

569
 570

571 The total number of data for the Global Ocean and the Mediterranean Sea are gathered in Table 5 with
 572 corresponding flags for each property. Overall, the synthesis includes more than 94% of good data for both A_T
 573 and C_T . About 5% are questionable and 2% are likely bad. Overall, we believe that all data (with Flag 2) in this
 574 synthesis have an accuracy better than $4 \mu\text{mol kg}^{-1}$ for both A_T and C_T , the same as for quality-controlled data in
 575 GLODAP (Olsen et al., 2020; Lauvset et al., 2021). The uncertainty ranges between the “Climate goal” ($2 \mu\text{mol}$
 576 kg^{-1}) and the “Weather Goal” ($10 \mu\text{mol kg}^{-1}$) for ocean acidification studies (Newton et al., 2015; Tilbrook et al.,
 577 2019). This accuracy is also relevant to validate or constraint data-based methods that reconstruct A_T and C_T



578 fields with an error of around 10-15 $\mu\text{mol kg}^{-1}$ for both properties (Bittig et al., 2018; Broullón et al., 2019, 2020;
579 Fourier et al., 2020; Chau et al., 2023).

580
581 **Table 5:** Number of Temperature, Salinity, A_T and C_T data in the synthesis identified for Flags 2, 3, 4, 9. The
582 data are given for the full data-set Global Ocean and for the Mediterranean Sea. Last column is the percentage of
583 Flag 2 (Good).

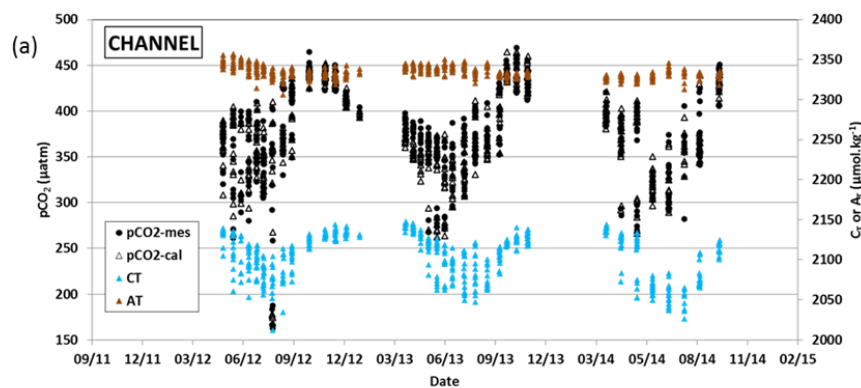
	Flag 2	Flag 3	Flag 4	Flag 9	% Flag 2
Global Ocean					
Temperature	43538	410	0	478	0.9907
Salinity	44033	319	2	71	0.9928
A_T	39331	2144	1165	1787	0.9224
C_T	39921	2091	1148	1279	0.9250
Mediterranean Sea					
Temperature	9843	1	0	65	0.9999
Salinity	9879	8	2	20	0.9999
A_T	8853	425	411	220	0.9137
C_T	8854	451	389	211	0.9133

3.5 Using A_T - C_T to calculate $p\text{CO}_2$ and pH and compare with $p\text{CO}_2$ and pH measurements

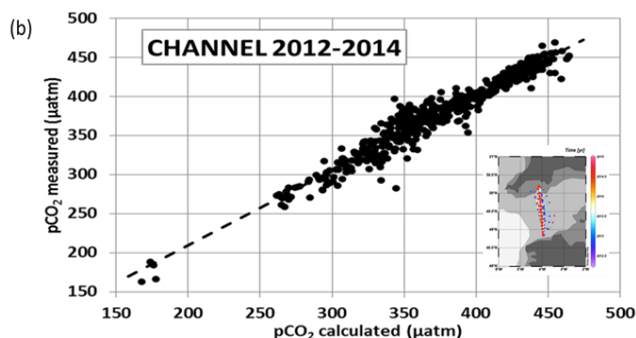
607
608 For some projects, the A_T - C_T data presented in this synthesis were used to calibrate or validate in situ
609 $p\text{CO}_2$ sensors (Bozec et al., 2011; Marrec et al., 2014; Merlivat et al., 2018). The A_T - C_T data were also used to
610 calculate $p\text{CO}_2$ and to derive associated air-sea CO_2 fluxes, especially during periods when no direct $p\text{CO}_2$
611 measurements were available (e.g. in the North Atlantic, Figure 4, Watson et al., 2009; Mc Kinley et al., 2011).
612 For example, Marrec et al. (2014) successfully used the calculated $p\text{CO}_2$ (with A_T - C_T pairs) to adjust the drift of
613 the $p\text{CO}_2$ data recorded with a Contros-HydroC/CO2 FT sensor mounted on a FerryBox for regularly sampling
614 the Western English Channel. Here we show the results for the period 2012-2014 (Figure 6). In this region the
615 alkalinity is relatively constant over time; the average of A_T for 528 samples at different seasons and years is
616 2334.4 (± 7.2) $\mu\text{mol kg}^{-1}$. On the opposite, the C_T concentrations show distinctive seasonality, with higher
617 concentrations in winter and lower in summer when biological activity is pronounced (Marrec et al., 2013, 2014;
618 Kitidis et al., 2019). This controls the seasonal $p\text{CO}_2$ distribution revealed each year in both measured and
619 calculated $p\text{CO}_2$ (Figure 6). For 528 co-located samples the mean difference between calculated and measured
620 $p\text{CO}_2$ is -1.9 (± 11.9) μatm with no distinct differences depending on the season and year.
621



622
623
624
625
626
627
628
629
630
631
632
633
634



635
636
637
638
639
640
641
642
643
644
645
646
647



648 **Figure 6:** (a): Time-series of A_T (brown triangles, right Y-axis), C_T (blue triangles, right Y-axis), pCO_2
649 calculated (open triangles, left Y-axis) and pCO_2 measured (filled circles) in the Western English Channel in
650 2012-2014 (Marrec et al., 2014). (b): Measured pCO_2 versus calculated pCO_2 for the same samples. The mean
651 difference ($pCO_{2cal} - pCO_{2mes}$) for 528 samples is $-1.9 \mu atm (\pm 11.9) \mu atm$. Data from Marrec and Bozec (2016
652 a,b; 2017). Localization of the samples is shown in the inserted map.
653

654 In the Ligurian Sea, following the first high frequency in situ fCO_2 measurements in 1995-1997 at the
655 DYFAMED time-series station (Hood and Merlivat, 2001), a new CARIOCA fCO_2 sensor was deployed at that
656 location in 2013 (BOUSSOLE project, Merlivat et al., 2018). The CARIOCA sensor was calibrated with regular
657 A_T - C_T analyses performed at LOCEAN. Based on these data, the mean difference between CARIOCA- fCO_2
658 measurements and calculated- fCO_2 data was estimated to be around $\pm 4.4 \mu atm$ for 2013-2015, i.e. the same
659 order than the precision of the CARIOCA sensor ($\pm 5 \mu atm$, Merlivat et al., 2018). Here we extend the results for
660 the period 2013-2018 (Golbol et al., 2020; data also in SOCAT version v2021, Bakker et al., 2016) and
661 compared the CARIOCA fCO_2 time-series with A_T and C_T data from different cruises (BOUSSOLE,
662 DYFAMED and MOOSE-GE) selected in the layer 0-20m at that location (Figure S4). For 67 co-located
663 samples at different seasons and years, the mean difference between calculated and measured fCO_2 (fCO_{2cal} -
664 fCO_{2mes}) was $-3.7 \mu atm (\pm 10.8) \mu atm$. At that location, the alkalinity is relatively constant over 2013-2018 with
665 an average concentration of $2569.8 (\pm 13.2) \mu mol kg^{-1}$. C_T concentrations show a clear seasonality, decreasing by
666 around $50 \mu mol kg^{-1}$ from winter to late summer driving the large seasonal cycle of fCO_2 (range $80 \mu atm$)
667 revealed in both measured and calculated values (here fCO_2 is normalized at $13^\circ C$, Figure S4). In addition to
668 calibration purposes, a regional A_T /Salinity relationship was derived from the A_T data measured at that location
669 and successfully used to construct time-series of C_T and pH calculated from the high-frequency CARIOCA fCO_2



670 data to investigate and interpret the long-term change of $f\text{CO}_2$ and acidification in the Ligurian Sea (Merlivat et
671 al., 2018; Coppola et al., 2020).

672 A CARIOCA sensor was also deployed in 2003 near the SOMLIT-Brest time-series site in the Bay of
673 Brest (Bozec et al., 2011; Salt et al., 2016). As for BOUSSOLE in the Ligurian Sea, samples collected for A_T - C_T
674 were used for validation of the $p\text{CO}_2$ recorded by the CARIOCA sensor and the comparison with calculated
675 $p\text{CO}_2$ showed a good agreement, i.e. $p\text{CO}_{2\text{cal}} = 0.98 * p\text{CO}_{2\text{mes}} + 7 \mu\text{atm}$ (Bozec et al., 2011). CARIOCA
676 sensors were also deployed on moorings in the Tropical Atlantic (PIRATA project, e.g. Lefèvre et al., 2008,
677 2016; Parard et al., 2010). With the discrete A_T and C_T data included in this synthesis (EGEE and PIRATA-FR
678 cruises), the $f\text{CO}_2$ data from CARIOCA sensor associated with an adapted A_T /Salinity relationship were used to
679 derive pH (Lefèvre et al., 2016) or C_T time-series to evaluate net community production in the eastern tropical
680 Atlantic (Parard et al., 2010; Lefèvre and Merlivat 2012).

681 Although this is not a direct instrumental inter-comparison, differences between $p\text{CO}_2$ (or $f\text{CO}_2$)
682 calculated using A_T - C_T pairs with direct $p\text{CO}_2$ measurements give a glimpse of the quality of A_T and C_T data in
683 this synthesis given the uncertainty attached to the $p\text{CO}_2$ or pH calculations (Orr et al., 2015). For example, in
684 the frame of the SURATLANT project in the North Atlantic, calculated $f\text{CO}_2$ data were compared with co-
685 located $f\text{CO}_2$ measurements for different seasons and years (Figure S5). The mean differences ($f\text{CO}_{2\text{cal}} - f\text{CO}_{2\text{mes}}$)
686 ranged between $-4.3 \mu\text{atm}$ (± 12.9) μatm (2004-2007, 74 co-located samples) and -3.0 (± 12.1) μatm (2014-2015,
687 98 co-located samples). The differences are almost the same for different years (and seasons) and are thus
688 attributed to method uncertainties (including sampling time, measurement errors, and data processing). Based on
689 these comparisons and the consistency between data we are confident that the A_T - C_T data presented in this
690 synthesis could be used to calculate $f\text{CO}_2$ (and pH) and interpret temporal changes and drivers of these
691 parameters as well as to estimate air-sea CO_2 fluxes in the North Atlantic (e.g. Corbière et al., 2007; Schuster et
692 al., 2009, 2013; Watson et al., 2009; Metzl et al., 2010; Mc Kinley et al., 2011; Reverdin et al., 2018, Kitidis et
693 al., 2019; Leseurre et al., 2020).

694 The A_T - C_T data in this synthesis have been also successfully used for $f\text{CO}_2$ and air-sea CO_2 fluxes
695 calculations in other regions: the tropical Atlantic (Koffi et al., 2010), the tropical Pacific (Moutin et al., 2018;
696 Wagener et al., 2018), the Solomon sea (Ganachaud et al., 2017) or the Mediterranean sea and coastal zones (De
697 Carlo et al., 2013; Marrec et al., 2015; Kapsenberg et al., 2017; Coppola et al., 2020; Keraghel et al., 2020;
698 Wimart-Rousseau et al., 2020a; Gattuso et al., 2023).

699 In addition, A_T - C_T data in the surface and the water-column are also relevant to calculate pH and
700 evaluate its rate of change for addressing ocean acidification topic in different regions (Kapsenberg et al., 2017;
701 Ganachaud et al., 2017; Wagener et al., 2018; Coppola et al., 2020; Leseurre et al., 2020; Lo Monaco et al.,
702 2021). At the time-series station ECOSCOPA in the Bay of Brest (Fleury et al., 2023; Petton et al., 2023), pH
703 calculated with A_T - C_T data were compared with direct pH measurements (Figure S6). In 2017-2019, pH (at
704 standard temperature 25°C , pH-25C) was always lower than 8 and presented a large seasonal signal of 0.3 (high
705 pH values in spring, low in winter). The mean difference between calculated and measured pH-25C for 46
706 samples was equal to $+0.013$ (± 0.010) which is in the range of the pH uncertainty evaluated by error
707 propagation when calculated from A_T - C_T pairs (A_T - C_T error of $\pm 3 \mu\text{mol kg}^{-1}$ leads to pH error of ± 0.0144). Part
708 of these A_T - C_T data used to calculate pH also helped for interpreting the response of marine species to
709 acidification, e.g. pteropodes or coccolithophores (*Emiliana huxleyi*) in the Mediterranean Sea (Howes et al.,
710 2015, 2017; Meier et al., 2014) or in the Southern Ocean (Beaufort et al., 2011). The A_T - C_T data were also



711 supporting environmental analysis in coral reef ecosystems in the tropical Pacific (TARA Expedition, Douville
712 et al., 2022; Lombard et al., 2023; Canesi et al., 2023).

713

714 4 Spatial distribution of A_T and C_T : a global view from the SNAPO-CO2 dataset

715

716 The surface distribution in the global ocean based on the SNAPO-CO2 dataset is presented in Figure 7
717 for A_T and C_T . In the open ocean, high A_T concentrations are identified in the subtropics in all basins (Jiang et al.,
718 2014; Takahashi et al., 2014) with highest concentrations up to $2484 \mu\text{mol kg}^{-1}$ in the central North Atlantic
719 (STRASSE cruise in August 2012, $26^\circ\text{N}/36^\circ\text{W}$). In surface and at depth, the A_T /Salinity and A_T/C_T relationships
720 are clearly identified and structured at regional scale (Figure 8).

721

722

723

724

725

726

727

728

729

730

731

732

733

734

735

736

737

738

739

740

741

742

743

744

745

746

747

748

749

750

751

752

753

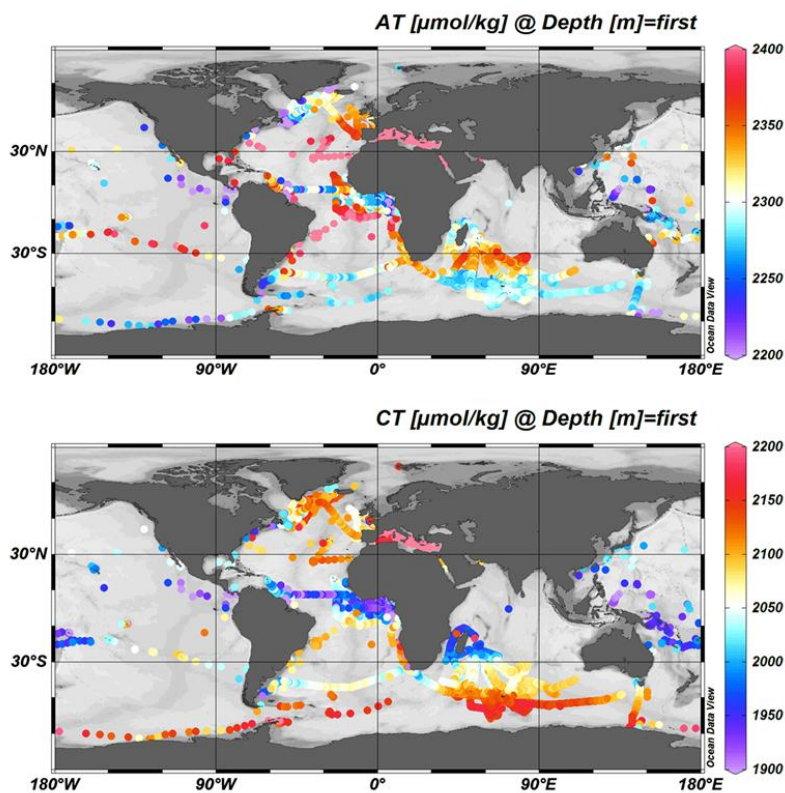


Figure 7: Distribution of A_T (top) and C_T (bottom) concentrations ($\mu\text{mol.kg}^{-1}$) in surface waters (0-10m). Only data with flag 2 are presented in these figures. Figures produced with ODV (Schlitzer, 2018).



754
 755
 756
 757
 758
 759
 760
 761
 762
 763
 764
 765
 766
 767
 768
 769
 770
 771
 772
 773
 774
 775
 776
 777
 778
 779
 780
 781
 782
 783
 784
 785
 786
 787
 788
 789
 790
 791
 792
 793
 794
 795
 796
 797
 798
 799
 800
 801
 802
 803
 804
 805
 806
 807
 808

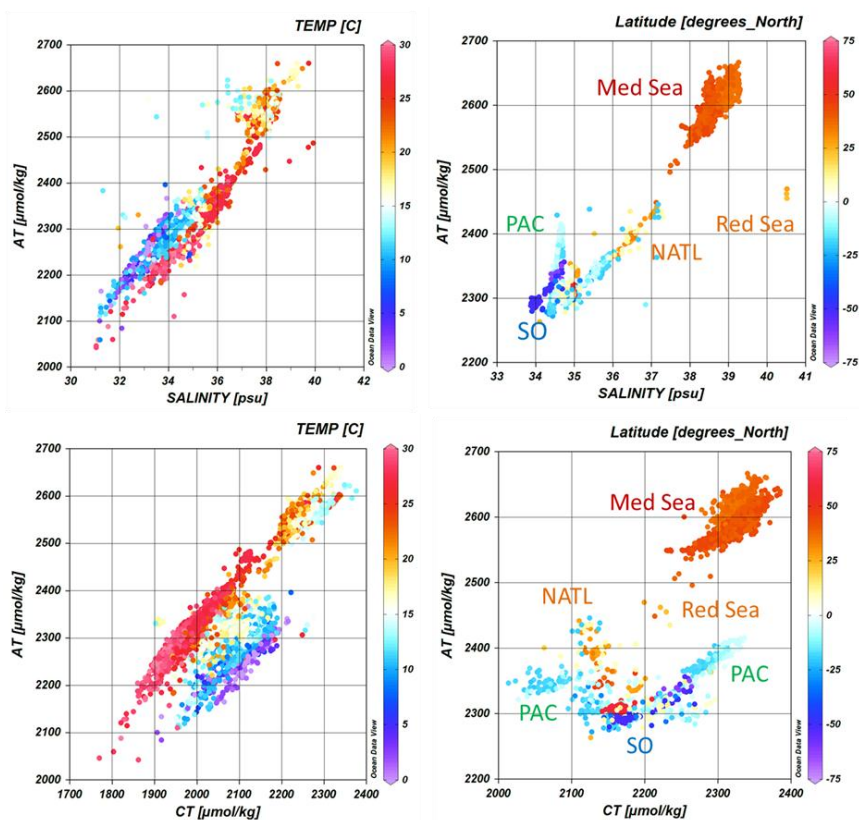


Figure 8: Relationships between A_T and Salinity (upper panel) and A_T versus C_T (lower panel) for samples in surface waters (0-10m and SSS > 31) (left) and in the water column below 100m (right). Only data with flag 2 are presented. The color scales correspond to the temperature (left) or the latitude (right). Some location of data are identified: Mediterranean Sea (Med Sea), Red Sea, Tropical Pacific (PAC), North Atlantic (NATL) and Southern Ocean (SO). Figures produced with ODV (Schlitzer, 2018).

In the eastern tropical Atlantic (ETA) where the Congo River impacts the salinity field (Vangriesheim et al., 2009), A_T concentrations range between 2100 and 2400 $\mu\text{mol kg}^{-1}$. The regional A_T /Salinity relationship in the ETA based on data from the EGEE cruises in 2005-2007 (Koffi et al., 2010) is robust and validated with more recent measurements from PIRATA-FR cruises in 2010-2019 (Lefevre et al., 2021). The strong A_T /Salinity relationship in the ETA was also recognized using data from the TARA-MICROBIOME cruise in May-July 2022 (Figure S7). Low salinity (< 30) and low A_T (1700-2200 $\mu\text{mol kg}^{-1}$) are also observed in the western tropical Atlantic near the Amazon River plume. The A_T /Salinity relationships in both river plume regions are very similar (Figure S7).

For C_T , the lowest concentrations were observed in the coastal regions of the Tropical Atlantic, on the eastern side in the Gulf of Guinea (BIOZAIRE cruise in 2003, 6°S/11°E, $C_T=1390 \mu\text{mol kg}^{-1}$, Vangriesheim et al., 2009) and on the western side in coastal zone off French Guyana (PLUMAND cruise in 2007, 5°N/51°W, $C_T=1512 \mu\text{mol kg}^{-1}$, Lefèvre et al., 2010). Such low C_T concentrations were also observed around 5°N/51°W in the Amazon River plume during the recent EUREC4A-OA cruise in 2020 and the TARA-MICROBIOME cruise in 2021 ($C_T=1451 \mu\text{mol kg}^{-1}$) leading to low oceanic $f\text{CO}_2$ (< 350 μatm) and a CO_2 sink in this region (Olivier et al., 2022).



809 The high C_T concentrations were mainly observed in the Southern Ocean (OISO and ACE cruises)
810 south of the Polar Front around 50°S linked to the upwelling of C_T -rich deep water (Figure 7, Metzl et al., 2006;
811 Wu et al., 2019; Chen et al., 2022). This leads to a high C_T/A_T ratio and a high Revelle factor in the Southern
812 Ocean (Figure 9, Fassbender et al., 2017). The high C_T content and low temperature in the Southern Ocean also
813 lead to low calcite and aragonite saturation state (Ω) (Takahashi et al., 2014; Jiang et al., 2015) but at present the
814 surface ocean is not under-saturated with regard to aragonite (Figure 10); however, under-saturation levels (Ω -
815 $Ar < 1$) were found around 500 m in the Southern Ocean (ACE cruise in 2017, MODYDICK cruise in 2018),
816 1000 m in the Tropical Pacific (PANDORA 2012 and OUTPACE 2015 cruises) and 2200 m in the North
817 Atlantic (OVIDE 2012 and 2014 cruises, see also Turk et al., 2017) (Figure 10). Samples at 400 m from the
818 TARA-Oceans cruise in 2009-2012 also indicated aragonite under-saturation in the Equatorial Atlantic,
819 Equatorial Pacific, as well as off South America (73°W - 34°S , Chile) associated to equatorial or eastern boundary
820 upwelling systems (Feely et al., 2012; Lauvset et al., 2020).

821 In surface, $\Omega - Ar > 3$ is found in the latitudinal band 45°S - 54°N and $\Omega - Ar < 3$, below the critical
822 threshold of $\Omega - Ar = 3.25$ that represents a limit for distribution of tropical coral reefs (Hoegh-Guldberg et al.,
823 2007) is observed at very few locations in the tropics.

824

825

826

827

828

829

830

831

832

833

834

835

836

837

838

839

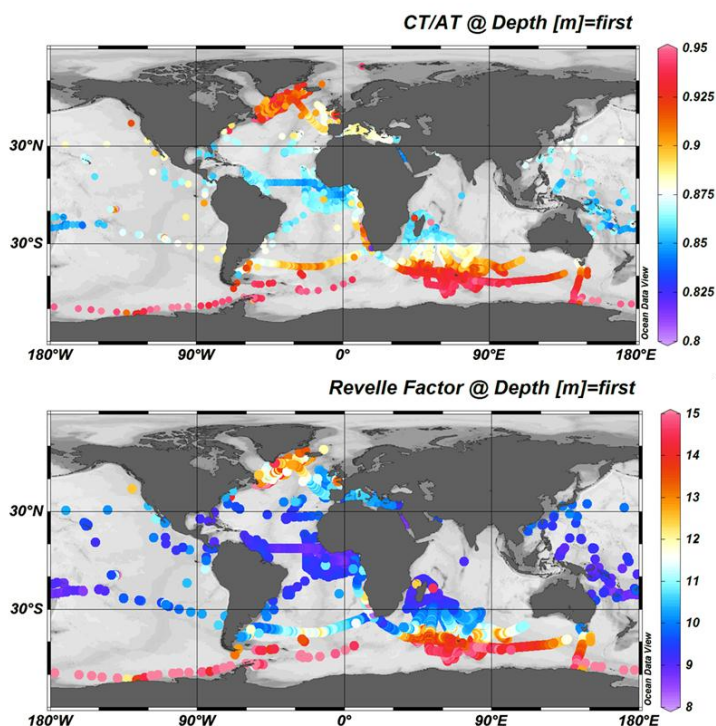
840

841

842

843

844



845 **Figure 9:** Distribution of the C_T/A_T ratio (top) and the Revelle factor (bottom) in surface waters (0-10m). Only
846 data with flag 2 were used. Figures produced with ODV (Schlitzer, 2018).



847
848
849
850
851
852
853
854
855
856
857
858
859
860
861
862
863
864
865
866
867
868
869
870
871
872
873
874
875
876
877
878
879
880
881
882
883
884
885
886
887
888
889
890
891
892
893
894
895

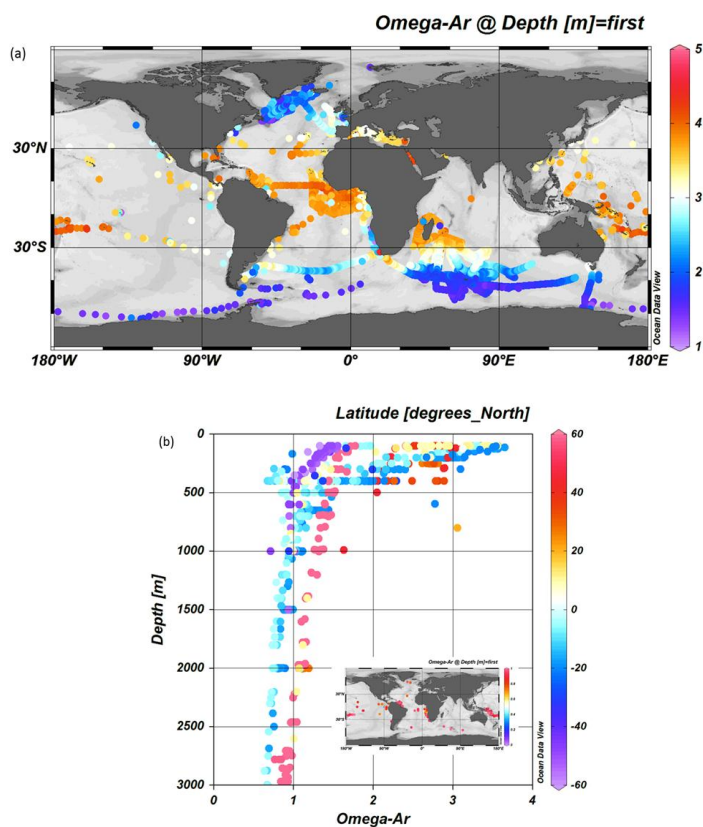


Figure 10: (a): Distribution of the aragonite saturation state (Ω -Ar) in surface waters (0-10m). Only data with flag 2 were used. (b): Depth profiles (100-3000m) of Ω -Ar at few locations in the Tropical Pacific, Atlantic and Southern Oceans. Stations where under-saturation is detected (Ω -Ar<1) at depth are identified in the inserted map. Figures produced with ODV (Schlitzer, 2018).

Compared to the open ocean, A_T concentrations are much higher in the Mediterranean Sea (Copin-Montégut, 1993; Schneider et al., 2007; Álvarez et al., 2023) with values up to $2600 \mu\text{mol kg}^{-1}$ (Figure 8). The A_T and C_T data obtained in 1998-2019 show on average a clear contrast between the northern and southern regions of the western Mediterranean sea (Figure 11 a, b) with higher concentration in the Ligurian Sea and the Gulf of Lion (Gemayel et al., 2015). However, the basin scale average distribution view smoothed the meso-scale signals recognized in the Mediterranean Sea (e.g. Bosse et al., 2017; Petrenko et al., 2017). In the Gulf of Lion the synthesis of 11 cruises conducted from May 2010 to June 2011 (CARBORHONE, CASCADE, LATEX, MOLA, MOOSE-GE) highlights the contrasting distributions of A_T and C_T in the coastal zones and off shore (Figure 11 c, d). The averaging of all data in 1998-2019 also smoothed the seasonal signal and the inter-annual variability described below.



896
897
898
899
900
901
902
903
904
905
906
907
908
909
910
911
912
913
914
915
916
917
918
919
920
921
922
923
924
925
926
927
928
929
930
931
932
933
934
935
936
937
938

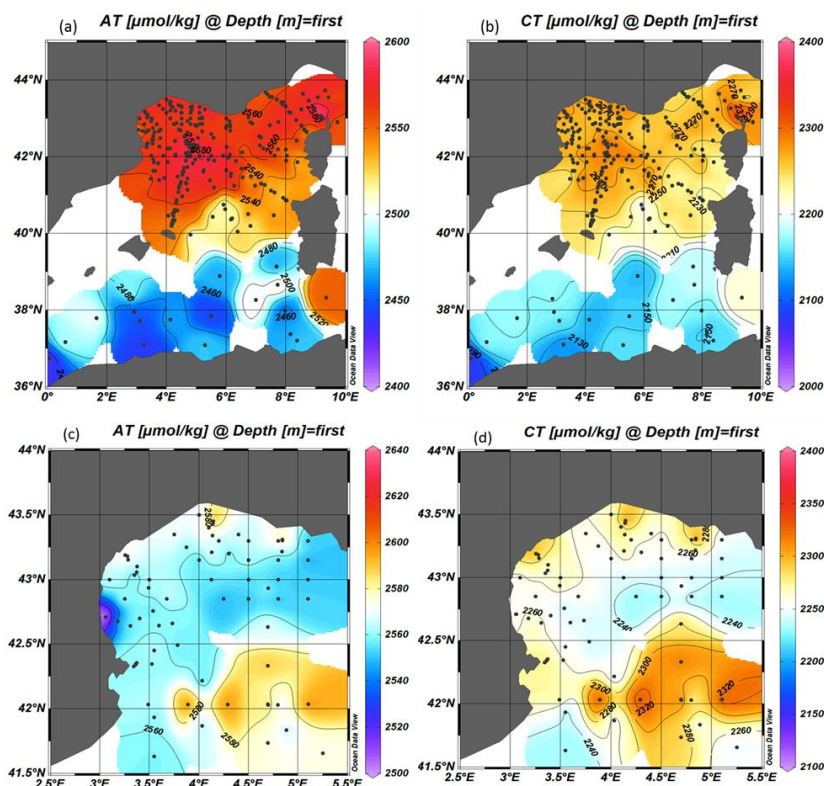


Figure 11: Distribution of A_T (a) and C_T (b) in $\mu\text{mol.kg}^{-1}$ in surface waters of the western Mediterranean Sea (0–10m) from all data for 1998–2019. Detailed distribution of A_T (c) and C_T (d) in $\mu\text{mol.kg}^{-1}$ in surface waters of the Gulf of Lion for the period 2010–2011 only (cruises CARBORHONE, CASCADE, LATEX, MOLA, MOOSEGE). Figures produced with ODV (Schlitzer, 2018).

5 Temporal variations of A_T and C_T : examples from the SNAPO-CO2 dataset

Time-series stations such as BATS, ESTOC, HOT, in the Irminger Sea or in the Iceland Sea are the only way to detect the long-term change in the ocean carbonate system in the surface and the water column (Bates et al., 2014). These important time-series help to understand driving processes (e.g. Hagens and Middelburg, 2016) and are often used to validate the $p\text{CO}_2$, A_T , C_T , or pH reconstructed fields (e.g. Rödenbeck et al., 2013; Broullón et al., 2019, 2020; Keppler et al., 2020; Gregor and Gruber, 2021; Chau et al., 2023; Ma et al., 2023).

Here we show examples of the temporal surface variations at locations where data were obtained for more than 10 years (Figure 12). We thus selected the following contrasting regions: the North Atlantic Subpolar Gyre (NASPG around $60^\circ\text{N}/30^\circ\text{W}$, period 1993–2018), the Equatorial Atlantic (at $2^\circ\text{N}-2^\circ\text{S}/12^\circ\text{W}-8^\circ\text{W}$, period 2005–2017), the Indian Ocean subtropical sector ($26-35^\circ\text{S}/50-56^\circ\text{E}$, period 1998–2018), the Indian Ocean high latitude ($54-60^\circ\text{S}/60-70^\circ\text{E}$, period 1998–2018), the Ligurian Sea (around DYFAMED station, $43.5-42.5^\circ\text{N}/5.5-9^\circ\text{E}$, period 1998–2019) and times-series stations in the coastal zones off Brittany (period 2008–2019).



939
 940
 941
 942
 943
 944
 945
 946
 947
 948
 949
 950
 951
 952
 953
 954
 955
 956
 957
 958
 959
 960
 961
 962

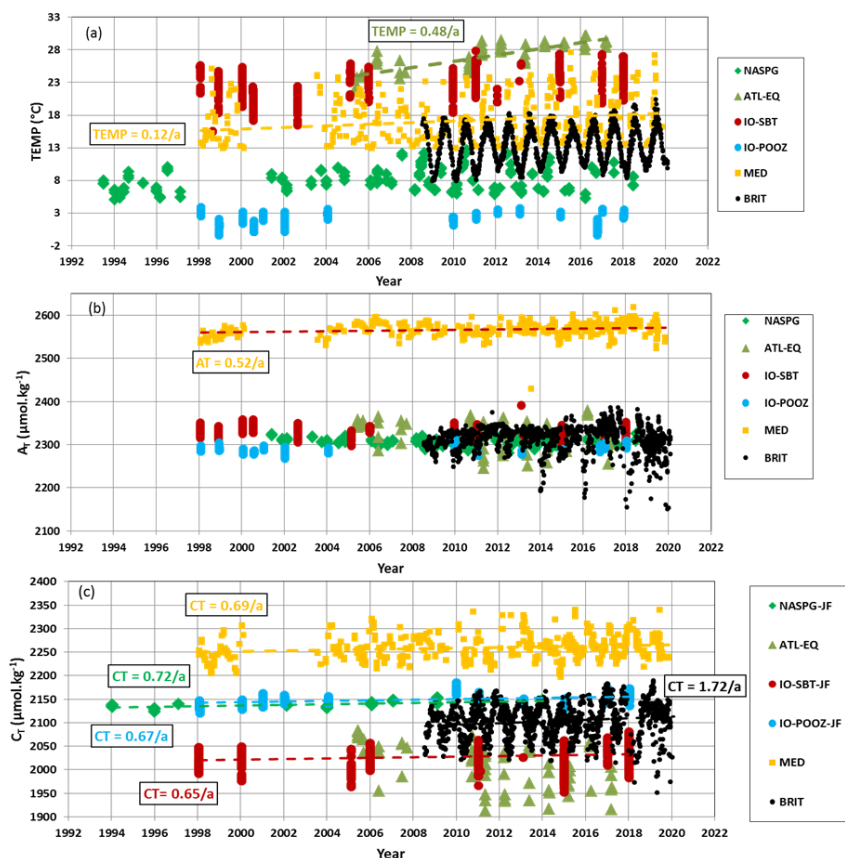


Figure 12: Time-series of (a) sea surface temperature ($^{\circ}\text{C}$), (b) A_T ($\mu\text{mol.kg}^{-1}$) and (c) C_T ($\mu\text{mol.kg}^{-1}$) in 6 regions: the North Atlantic Subpolar Gyre (NASPG 1993-2018, green diamond), the Equatorial Atlantic (ATL-EQ, 2005-2017, green triangle), the Indian subtropical sector (IO-SBT, red circle) and high latitude (IO-POOZ, blue circle) (1998-2018), the Ligurian Sea (MED, 1998-2019, orange square) and times-series stations in the coastal zones off Brittany (BRIT, period 2008-2019, black dots). Trends (dashed lines) are shown when relevant for the discussion (C_T trends listed in Table 6).

Table 6: Trend of C_T ($\mu\text{mol kg}^{-1} \text{ yr}^{-1}$) and corresponding standard error in 5 selected regions where data were available for more than 10 years (data are shown in Figure 12). The projects/cruises for selection of the data in each domain are indicated.

Region	Period	C_T trend $\mu\text{mol kg}^{-1} \text{ yr}^{-1}$	Season	Projects/Cruises
NASPG	1994-2014	+0.719 (0.168)	Jan-Feb	SURATLANT
Indian SBT	1998-2018	+0.646 (0.117)	Jan-Feb	OISO
Indian High Lat	1998-2018	+0.668 (0.042)	Jan-Feb	OISO
Ligurian Sea	1998-2019	+0.686 (0.181)	All seasons	DYFAMED, BOUSSOLE, MOOSE-GE
Coast Brittany	2008-2019	+1.720 (0.281)	All seasons	Brest, Roscoff, ECOSCOPIA, PENZE

985
 986



987 In the 6 regions, there was a progressive warming most clearly detected in the Mediterranean Sea (e.g.
988 Nykjaer, 2009). From 1998 to 2019 the warming in the Ligurian Sea was $+0.1208^{\circ}\text{C yr}^{-1}$ (± 0.0227) (Figure 12).
989 In the equatorial Atlantic, the apparent rapid increase of temperature of $+0.48^{\circ}\text{C yr}^{-1}$ (± 0.04) in 2005-2017 from
990 the selected data indicated a change in water masses and circulation. The colder sea surface in 2005 was
991 associated with the so-called Atlantic Cold Tongue (ACT) which was one of the most intense ATC since 1982
992 (Caniaux et al., 2011). The ACT also leads to significant changes in oceanic $f\text{CO}_2$ and air-sea CO_2 fluxes (Parard
993 et al., 2010; Koseki et al., 2023) and explained the high C_T concentrations observed in 2005 in this region
994 (Figure 12, Koffi et al., 2010).

995 Alkalinity presents rather homogenous concentrations in the NASGP and the south Indian Ocean. Inter-
996 annual variability of A_T is pronounced in the equatorial Atlantic ranging between 2245 and 2378 $\mu\text{mol kg}^{-1}$. This
997 is mainly related to salinity as normalized A_T values ($N-A_T$, for salinity= 35) do not show such inter-annual
998 variability (Mean $N-A_T = 2295.7 \pm 4.6 \mu\text{mol kg}^{-1}$, $n = 67$ for 2005-2017, not shown). In the coastal zones off
999 Brittany, the A_T is also highly variable (Salt et al., 2016; Gac et al., 2021) ranging between 2150 and 2386 μmol
1000 kg^{-1} (Figure 12).

1001 An interesting signal is the progressive increase of A_T in the Mediterranean Sea. The positive A_T trend
1002 of $+0.53$ (± 0.11) $\mu\text{mol kg}^{-1} \text{ yr}^{-1}$ ($n=538$) in 1998-2019 in the region offshore was also observed at the coastal
1003 station SOMLIT-Point-B in 2007-2015 but with a faster increase of $+2.08$ (± 0.19) $\mu\text{mol kg}^{-1} \text{ yr}^{-1}$ (Kapsenberg et
1004 al., 2017). Close to the DYFAMED site, at station SOMLIT-Point-B, the A_T trend was not linked to salinity
1005 temporal changes as a positive $N-A_T$ trend was also reported, $+0.52$ (± 0.07) $\mu\text{mol kg}^{-1} \text{ yr}^{-1}$ (not shown). Based
1006 on data from the PERLE cruises in 2018-2021 a significant increase in A_T was also identified in the Eastern
1007 Mediterranean Sea (Wimart-Rousseau et al., 2021). Along with the increase of C_T and the warming, the A_T
1008 increase would impact on the $f\text{CO}_2$, air-sea CO_2 fluxes and pH temporal changes (Merlivat et al., 2018).
1009 Processes explaining the A_T increase in the Mediterranean Sea are still unexplained and deserve further
1010 investigations (Coppola et al., 2019).

1011 As expected, because of the anthropogenic CO_2 uptake the C_T concentrations increased in most regions
1012 (Figure 12, Table 6). This is identified in the Indian Ocean (in the subtropics and the high latitude), in the
1013 Mediterranean Sea, and in coastal waters off Brittany. However, the signal is more complex in the NASPG. As
1014 previously shown the C_T trend in the NASPG depends on seasons and decades (Metzl et al., 2010; Reverdin et
1015 al., 2018; Fröb et al., 2019; Leseurre et al., 2020). Here we selected only the data in January-February from the
1016 SURATLANT cruises leading a C_T trend of $+0.719$ (± 0.168) $\mu\text{mol kg}^{-1} \text{ yr}^{-1}$. Compared to the regions further
1017 north the C_T trend in the NASPG is about half the C_T trends of $+1.44$ (± 0.23) $\mu\text{mol kg}^{-1} \text{ yr}^{-1}$ observed in the
1018 Iceland Sea (Olafsson et al., 2009) or $+1.48$ (± 0.22) $\mu\text{mol kg}^{-1} \text{ yr}^{-1}$ at station M in the Norwegian Sea (Skjelvan
1019 et al., 2022).

1020 In the coastal zones off Brittany, although there are large seasonal and inter-annual variabilities (Gac et
1021 al., 2021), an annual C_T trend of $+1.72$ (± 0.28) $\mu\text{mol kg}^{-1} \text{ yr}^{-1}$ is detected over 10 years (2009 to 2019). The same
1022 is observed in the Mediterranean Sea where the C_T offshore trend of $+0.69$ (± 0.18) $\mu\text{mol kg}^{-1} \text{ yr}^{-1}$ is low
1023 compared to what was observed in the coastal zone (SOMLIT-Point-B, $+2.97$ (± 0.20) $\mu\text{mol kg}^{-1} \text{ yr}^{-1}$, Kapsenberg
1024 et al., 2017).

1025 In the southern Indian Ocean, C_T concentrations also increased in both subtropical and high latitudes,
1026 two regions where the primary productivity is relatively low (oligotrophic regime in the subtropics and High
1027 Nutrient Low Chlorophyll regime, HNLC, south of the Polar Front). With the data selected for austral summer



1028 (January-February) the C_T trends appeared almost similar in these two regions, around $+0.65 \mu\text{mol kg}^{-1} \text{yr}^{-1}$
1029 (Table 6).

1030 Finally, in the Equatorial Atlantic the selected data around 0° - 10°W highlighted the large variability
1031 linked to the oceanic circulation. Detecting a C_T trend as well as a possible link with anthropogenic carbon
1032 uptake, at least with the data available in 2005-2017, appears to be intricate as it has been previously discussed
1033 for the period 2006-2013 (Lefèvre et al., 2016). However, the signal of the C_T increase is better identified north
1034 or south of the Equator in the eastern tropical Atlantic sector (Lefèvre et al., 2021).

1035 In the water column A_T - C_T data from dedicated cruises were used to evaluate the C_{ant} distribution and
1036 pH change since pre-industrial era (e.g. PANDORA cruise, Ganachaud et al., 2017; OUTPACE cruise, Wagener
1037 et al., 2018; SOMBA cruise, Keraghel et al., 2020). Time-series at DYFAMED station also enabled to
1038 investigate the temporal variability of C_T , A_T and C_{ant} in the water column (Touratier and Goyet, 2009; Coppola
1039 et al., 2020; Fourrier et al., 2022). As an example of the observed temporal variations at depth we selected the
1040 data in the layer 950-1050m in the Ligurian Sea from different cruises (Figure 13). At that depth both A_T and C_T
1041 present some large anomalies especially noticed in 2013 (lower A_T and C_T in February 2013, DEWEX cruise)
1042 and in 2018 (lower A_T and C_T in May 2018, MOOSE-GE cruise) the later probably linked to episodic convective
1043 process that occurred in winter 2018 (Fourrier et al., 2022). In this region the long-term increase of A_T indicates
1044 that in addition to the anthropogenic CO_2 signal another process is at play to explain the rapid C_T trend of $+1.20$
1045 (± 0.12) $\mu\text{mol kg}^{-1} \text{yr}^{-1}$ at depth compared to that observed in surface (Figure 12). The signal at depth is probably
1046 linked to the variations of the deep convection and mixing with Levantine intermediate water (LIW, Margirier et
1047 al., 2020) with higher A_T and C_T concentrations. The long-term increase of A_T and C_T at depth (here at 1000m,
1048 Figure 13) was also observed below 2000m (Coppola et al., 2020) a signal that has to be investigated in
1049 dedicated analysis using other properties (O_2 , nutrients, following Fourrier et al. (2022) for the period 2012-
1050 2020) and a larger dataset in the Mediterranean Sea (e.g. CARIMED).

1051

1052

1053

1054

1055

1056

1057

1058

1059

1060

1061

1062

1063

1064

1065

1066

1067

1068

1069

1070

1071

1072

1073

1074

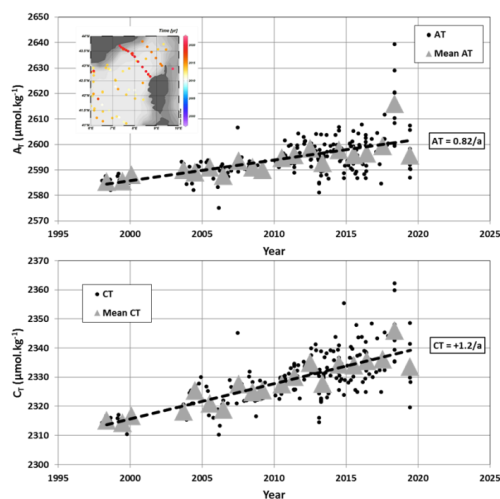


Figure 13: Time-series of A_T ($\mu\text{mol.kg}^{-1}$) and C_T ($\mu\text{mol.kg}^{-1}$) in the Ligurian Sea (1998-2019) in the layer 950-1050m. Annual mean (grey triangles) was calculated from all data each year (black dots). The trends (dashed line) based on annual mean are $+0.82 (\pm 0.15) \mu\text{mol.kg}^{-1}.\text{yr}^{-1}$ for A_T and $+1.20 (\pm 0.12) \mu\text{mol.kg}^{-1}.\text{yr}^{-1}$ for C_T . In this layer data selected are from cruises ANTARES, CASCADE, DEWEX, DYFAMED, MOOSE-GE and PEACETIME (location of stations shown in the inserted map).



1075 **6 Using A_T and C_T data to validate observations from autonomous instruments**

1076

1077 The dataset presented in this synthesis would also offer interesting observations to validate properties
1078 (A_T and C_T) derived from BG-ARGO floats equipped with pH sensors (e.g. Bushinsky et al., 2019; Mazloff et
1079 al., 2023; Mignot et al., 2023). The water column in situ A_T - C_T data obtained during the Antarctic Circumpolar
1080 Expedition (ACE) in 2016-2017 were collected at location where SOCCOM floats were launched (Walton and
1081 Thomas, 2018). A SOCCOM float (WMO ID 5905069) was launched on January 11th 2017 at 55°S-96°E south
1082 of the Polar Front in the southern Indian Ocean. The pH, temperature and salinity data from the float were then
1083 used to derive A_T and C_T profiles (here using the MLR method, Williams et al., 2016, 2017). In the top layers the
1084 discrete ACE data (Figure 14) present large variability of A_T and C_T concentrations not captured in the records
1085 derived from the float (MLR method somehow smooth the profiles). However, given the uncertainty in
1086 reconstructed A_T from float data ($5.6 \mu\text{mol kg}^{-1}$) the average values in the first 100m were almost identical (A_T -
1087 $_{ACE} = 2285.1 (\pm 4.4) \mu\text{mol kg}^{-1}$ and A_T - $_{float} = 2278.3 (\pm 0.7) \mu\text{mol kg}^{-1}$; C_T - $_{ACE} = 2139.7 (\pm 9.2) \mu\text{mol kg}^{-1}$ and C_T -
1088 $_{float} = 2141.1 (\pm 3.2) \mu\text{mol kg}^{-1}$). Moreover below 200m, profiles from the float are coherent compared to the A_T -
1089 C_T measurements (Figure 14). This is encouraging for using float data to explore the seasonal variability of A_T
1090 and C_T in the Southern Ocean (e.g. Williams et al., 2018; Johnson et al., 2022) and the estimation of
1091 anthropogenic CO_2 in the water column in this sector (Figure 14). Here the C_{ant} concentrations were calculated
1092 below 200m (corresponding to the temperature minimum of the winter in the SO and using the TrOCA
1093 method, Touratier et al., 2007). The float data suggest that C_{ant} concentrations are positive down to about 1000m,
1094 with maximum values in subsurface. In 2017 the mean C_{ant} concentration at 200m was $49.1 (\pm 9.0) \mu\text{mol kg}^{-1}$.
1095 Below that depth, C_{ant} decreased and reduced to $+29.8 (\pm 8.5) \mu\text{mol kg}^{-1}$ in the layer 300-400m. To complement
1096 the C_{ant} inventories based on GLODAP data-product (e.g. Gruber et al., 2019) C_{ant} estimates derived from BG-
1097 ARGO floats as evaluated here in the Southern Ocean could be applied in other locations as was previously
1098 tested in the North Pacific (Li et al., 2019).

1099 In surface water as the A_T derived from the float data are deduced using MLR or LIAR methods
1100 (Williams et al., 2017; Carter et al., 2016), the A_T data in the SNAPO-CO₂ synthesis could also be used to
1101 identify A_T anomalies not always captured from floats. This is particularly relevant in coccolithophores blooms
1102 areas when low A_T concentrations and high pCO₂ are observed (e.g. Balch et al., 2016 in the Southern Ocean;
1103 Robertson et al., 1994 in the North Atlantic).

1104

1105 **7 Summary and suggestions**

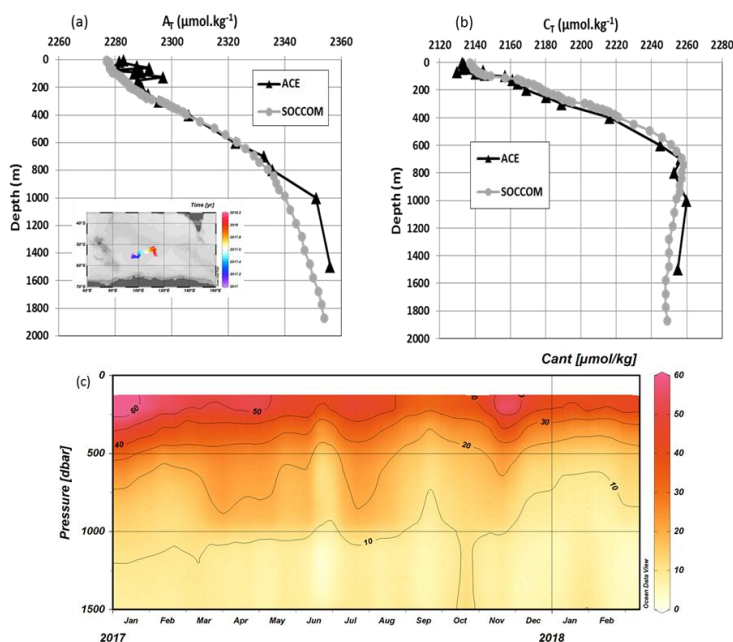
1106

1107 The ocean data synthesized in this product are based on measurements of A_T and C_T performed in 1993-
1108 2022 with an accuracy of $\pm 4 \mu\text{mol kg}^{-1}$. It offers a large data set of A_T and C_T for the global ocean and regional
1109 biogeochemical studies. It includes more than 44 400 surface and water column observations in all oceanic
1110 basins, in the Mediterranean Sea, in the coastal zones, near coral reef, and in rivers. For the open ocean this
1111 complements the SOCAT and GLODAP data-products (Bakker et al., 2016; Lauvset et al., 2021) and for the
1112 Mediterranean Sea the ongoing CARIMED dataset. For the coastal sites this also complements the synthesis of
1113 coastal time-series only done around North America (Fassbender et al., 2018; Jiang et al., 2020; OCADS, 2023).

1114



1115
1116
1117
1118
1119
1120
1121
1122
1123
1124
1125
1126
1127
1128
1129
1130
1131
1132
1133



1134 **Figure 14:** Profiles of (a) A_T ($\mu\text{mol.kg}^{-1}$) and (b) C_T ($\mu\text{mol.kg}^{-1}$) observed at station ACE-20 (55°S-95°E,
1135 11/1/17, black triangles) compared with the profiles deduced from the SOCCOM float (WMO code 5905069)
1136 launched at that location (first data on January 12th 2017, grey circles). The location/drift of the float in 2017-
1137 2018 is shown on the inserted map. (c) Hovmöller section (Pressure/time) of anthropogenic CO₂ concentrations
1138 (C_{ant} in $\mu\text{mol.kg}^{-1}$) estimated from the float data (A_T , C_T , O₂, T) below 200m (period January 2017-February
1139 2018). Section produced with ODV (Schlitzer, 2018).
1140

1141 The SNAPO-CO₂ dataset enables to investigate seasonal variations to decadal trends of A_T and C_T in
1142 various oceanic provinces. In regions where data are available for more than 2 decades in surface water (North
1143 Atlantic, Ligurian Sea, Southern Indian Ocean, and coastal regions), all time-series show an increase in C_T .
1144 Excepted in the Mediterranean Sea, A_T appears relatively constant over time, although the A_T content present
1145 significant inter-annual variability such as in the NASPG or in the coastal zones including near the Congo and
1146 Amazon Rivers plumes.

1147 This dataset represents independent data for validation of reconstructed A_T or C_T fields using various
1148 methods (e.g. Rödenbeck et al., 2013, 2015; Sauzède et al., 2017; Turk et al., 2017; Bittig et al., 2018; Broullón
1149 et al., 2019, 2020; Land et al., 2019; Keppler et al., 2020; Fourier et al., 2020; Gregor and Gruber, 2021; Sims et
1150 al., 2023; Chau et al., 2023). It is also useful to validate Earth System Models (ESM) that currently present bias
1151 to reproduce the seasonal cycle of C_T and A_T due to inadequate representation of biogeochemical cycles,
1152 including the coupling of biological and physical processes (e.g. Pilcher et al., 2015; Mongwe et al., 2018;
1153 Lerner et al., 2021). This should be resolved for confident in future projections of the productivity, ocean
1154 acidification, and the responses of the marine ecosystems (e.g. Kwiatowkki et al., 2020). Recall that OBG or
1155 ESM models calculate pCO₂ from A_T - C_T pairs and the simulated annual CO₂ flux might be correct when
1156 compared to observations but for wrong reasons (e.g. Goris et al., 2018, Lerner et al., 2021). For example, it has
1157 been shown that biases in A_T in ESM models led to an overestimation of the oceanic fCO₂ trend and thus
1158 uncertainty when predicting the oceanic anthropogenic CO₂ uptake (Lebehot et al., 2019). The simulated



1159 seasonal cycle of $p\text{CO}_2$ is also uncertain in ESM models especially in high latitudes (e.g. Joos et al., 2023). It is
1160 thus important to attempt validating ESM models with A_T - C_T data such as presented in this synthesis.

1161 This dataset would also serve for validating autonomous platforms capable of measuring pH and $p\text{CO}_2$
1162 variables and, along with SOCAT and GLODAP datasets, provides an additional reference dataset for the
1163 development and validation of regional biogeochemical models for simulating air-sea CO_2 fluxes. It is also
1164 essential for training and validating neural networks capable of predicting variables in the carbonate system,
1165 thereby enhancing observations of marine CO_2 at different spatial and temporal scales.

1166 The data presented here are available online on the Seanoë server (Metzl et al., 2023,
1167 <https://doi.org/10.17882/95414>) and is divided in two files: one for the Global Ocean, and one for the
1168 Mediterranean Sea. The sources of the original datasets (doi) with the associated references are listed in the
1169 Supplementary Material (Table S3, S4). We invite the users to comment on any anomaly that would have not
1170 been detected or to suggest potential misqualification of data in the present product (e.g. data probably good
1171 although assigned with Flag 3, probably wrong). The SNAPO-CO2 dataset will be regularly updated on Seanoë
1172 data server with new observations controlled and archived.

1173

1174 **8 Data availability**

1175 Data presented in this study are available at Seanoë: <https://www.seanoë.org>, <https://doi.org/10.17882/95414>
1176 (Metzl et al., 2023).

1177

1178 *Author contributions.* NM prepared the data synthesis, the figures and wrote the draft of the manuscript with
1179 contributions from all authors. JF measured the discrete samples since 2014, with the help from CM and CLM,
1180 and prepared the individual reports for each project. NM and JF pre-qualified the discrete A_T - C_T data. CLM and
1181 NM are co-Is of the ongoing OISO project and qualified the underway A_T - C_T data from OISO cruises. All
1182 authors have contributed either to organizing cruises, sample collection or data qualification.

1183

1184 *Competing interest.* The authors declare that they have no conflict of interest.

1185

1186 *Acknowledgments.* The A_T and C_T data presented in this study were measured at the SNAPO-CO2 facility
1187 (Service National d'Analyse des Paramètres Océaniques du CO_2) housed by the LOCEAN laboratory and part of
1188 the OSU ECCE Terra at Sorbonne University and INSU/CNRS analytical services. Support by INSU/CNRS, by
1189 OSU ECCE Terra and by LOCEAN, is gratefully acknowledged as well as support by different French "Services
1190 nationaux d'Observations", such as OISO/CARAUS, SOMLIT, PIRATA, SSS and MOOSE. We thank the
1191 research infrastructure ICOS (Integrated Carbon Observation System) France for funding a large part of the
1192 analyses. We acknowledge the MOOSE program (Mediterranean Ocean Observing System for the Environment,
1193 <https://campagnes.flotteoceanographique.fr/series/235/fr/>) coordinated by CNRS-INSU and the Research
1194 Infrastructure ILICO (CNRS-IFREMER). AWIPEV-CO2 was supported by the Coastal Observing System for
1195 Northern and Arctic Seas (COSYNA), the two Helmholtz large-scale infrastructure projects ACROSS and
1196 MOSES, the French Polar Institute (IPEV) as well as the European Union's Horizon 2020 research and
1197 innovation projects Jericho-Next (No 871153 and 951799), INTAROS (No 727890) and FACE-IT (No 869154).
1198 Support from the French *Agence Nationale de la Recherche* (ANR) is also acknowledged through their funding
1199 of the BIOCAREX project. The EURECA4-OA cruise was also supported by the EURECA4-OA JPI Ocean and
1200 Climate program. The OISO program was supported by the French institutes INSU (Institut National des



1201 Sciences de l'Univers) and IPEV (Institut Polaire Paul-Emile Victor), OSU Ecce-Terra (at Sorbonne Université),
1202 and the French program SOERE/Great-Gases. We thank the French oceanographic fleet ("Flotte
1203 océanographique française") for financial and logistic support for all cruises listed in this synthesis and for the
1204 OISO program (<https://campagnes.flotteoceanographique.fr/series/228/>). Data from the float launched during the
1205 ACE cruise were made freely available by the Southern Ocean Carbon and Climate Observations and Modeling
1206 (SOCCOM) Project funded by the National Science Foundation, Division of Polar Programs (NSF PLR -
1207 1425989), supplemented by NASA, and by the International Argo Program and the NOAA programs that
1208 contribute to it. The Argo Program is part of the Global Ocean Observing System
1209 (<http://doi.org/10.17882/42182>, <http://argo.jcompos.org>). We thank Frédéric Merceur (IFREMER) for preparing
1210 the page and data availability on Seanoe. We thank Patrick Raimbault (retired, former at MIO, Marseille) for
1211 managing the MOOSE project until 2019. We thank all colleagues and students who participated to the cruises
1212 and have carefully collected the precious seawater samples. We warmly acknowledge our colleague Christian
1213 Brunet (retired) for his supportive help for the analysis since the start of the Service facility SNAPO-CO2. We
1214 would like to pay tribute to our late colleague Frédéric Diaz who contributed to the LATEX cruise in 2010.

1215

1216 **References**

1217

1218 Álvarez, M., Catalá, T. S., Civitarese, G., Coppola, L., Hassoun, A. E.R., Ibello, V., Lazzari, P., Lefevre, D.,
1219 Macías, D., Santinelli, C. and Ulses, C.: Chapter 11 - Mediterranean Sea general biogeochemistry, Editor(s):
1220 Katrin Schroeder, Jacopo Chiggiato, Oceanography of the Mediterranean Sea, Elsevier, Pages 387-451,
1221 <https://doi.org/10.1016/B978-0-12-823692-5.00004-2>, 2023.

1222

1223 Bakker, D. C. E., Pfeil, B., Smith, K., Hankin, S., Olsen, A., Alin, S. R., Cosca, C., Harasawa, S., Kozyr, A.,
1224 Nojiri, Y., O'Brien, K. M., Schuster, U., Telszewski, M., Tilbrook, B., Wada, C., Akl, J., Barbero, L., Bates, N.
1225 R., Boutin, J., Bozec, Y., Cai, W.-J., Castle, R. D., Chavez, F. P., Chen, L., Chierici, M., Currie, K., De Baar, H.
1226 J. W., Evans, W., Feely, R. A., Fransson, A., Gao, Z., Hales, B., Hardman-Mountford, N. J., Hoppema, M.,
1227 Huang, W.-J., Hunt, C. W., Huss, B., Ichikawa, T., Johannessen, T., Jones, E. M., Jones, S., Jutterstrøm, S.,
1228 Kitidis, V., Körtzinger, A., Landschützer, P., Lauvset, S. K., Lefèvre, N., Manke, A. B., Mathis, J. T., Merlivat,
1229 L., Metzl, N., Murata, A., Newberger, T., Omar, A. M., Ono, T., Park, G.-H., Paterson, K., Pierrot, D., Ríos, A.
1230 F., Sabine, C. L., Saito, S., Salisbury, J., Sarma, V. V. S. S., Schlitzer, R., Sieger, R., Skjelvan, I., Steinhoff, T.,
1231 Sullivan, K. F., Sun, H., Sutton, A. J., Suzuki, T., Sweeney, C., Takahashi, T., Tjiputra, J., Tsurushima, N., Van
1232 Heuven, S. M. A. C., Vandemark, D., Vlahos, P., Wallace, D. W. R., Wanninkhof, R. and Watson, A. J.: An
1233 update to the Surface Ocean CO₂ Atlas (SOCAT version 2). Earth System Science Data, 6, 69-90.
1234 doi:10.5194/essd-6-69-2014. 2014

1235

1236 Bakker, D. C. E., Pfeil, B., Landa, C. S., Metzl, N., O'Brien, K. M., Olsen, A., Smith, K., Cosca, C., Harasawa,
1237 S., Jones, S. D., Nakaoka, S.-I., Nojiri, Y., Schuster, U., Steinhoff, T., Sweeney, C., Takahashi, T., Tilbrook, B.,
1238 Wada, C., Wanninkhof, R., Alin, S. R., Balestrini, C. F., Barbero, L., Bates, N. R., Bianchi, A. A., Bonou, F.,
1239 Boutin, J., Bozec, Y., Burger, E. F., Cai, W.-J., Castle, R. D., Chen, L., Chierici, M., Currie, K., Evans, W.,
1240 Featherstone, C., Feely, R. A., Fransson, A., Goyet, C., Greenwood, N., Gregor, L., Hankin, S., Hardman-
1241 Mountford, N. J., Harlay, J., Hauck, J., Hoppema, M., Humphreys, M. P., Hunt, C. W., Huss, B., Ibánhez, J. S.
1242 P., Johannessen, T., Keeling, R., Kitidis, V., Körtzinger, A., Kozyr, A., Krasakopoulou, E., Kuwata, A.,
1243 Landschützer, P., Lauvset, S. K., Lefèvre, N., Lo Monaco, C., Manke, A., Mathis, J. T., Merlivat, L., Millero, F.
1244 J., Monteiro, P. M. S., Munro, D. R., Murata, A., Newberger, T., Omar, A. M., Ono, T., Paterson, K., Pearce, D.,
1245 Pierrot, D., Robbins, L. L., Saito, S., Salisbury, J., Schlitzer, R., Schneider, B., Schweitzer, R., Sieger, R.,
1246 Skjelvan, I., Sullivan, K. F., Sutherland, S. C., Sutton, A. J., Tadokoro, K., Telszewski, M., Tuma, M., Van
1247 Heuven, S. M. A. C., Vandemark, D., Ward, B., Watson, A. J., and Xu, S.: A multi-decade record of high-quality
1248 fCO₂ data in version 3 of the Surface Ocean CO₂ Atlas (SOCAT), Earth Syst. Sci. Data, 8, 383-413,
1249 doi:10.5194/essd-8-383-2016. 2016.

1250



- 1251 Bakker, D.C.E., Alin, S.R., Bates, N.R., Becker, M., Feely, R. A., Gritzalis, T., Jones, S. D., Kozyr, A., Lauvset,
1252 S. K., Metzl, N., Munro, D.R., Nakaoka, S.-I., Nojiri, Y., O'Brien, K., Olsen, A., Pierrot, D., Rehder, G.,
1253 Steinhoff, T., Sutton, A., Sweeney, C., Tilbrook, B., Wada, C., Wanninkhof, R., and all >100 SOCAT
1254 contributors: An alarming decline in the ocean CO₂ observing capacity. Available at www.socat.info, 2023.
1255
- 1256 Balch, W.M., Bates, N.R., Lam, P.J., Twining, B.S., Rosengard, S. Z., Bowler, B.C., Drapeau, D.T., Garley, R.,
1257 Lubelczyk, L.C., Mitchell, C. and Rauschenberg S.: Factors regulating the Great Calcite Belt in the Southern
1258 Ocean and its biogeochemical significance. *Global Biogeochem. Cycles*, 30, doi:10.1002/2016GB005414, 2016
1259
- 1260 Beaufort, L., Probert, I., de Garidel-Thoron, T., Bendif, E.M., Ruiz-Pino, D., Metzl, N., Goyet, C., Buchet, N.,
1261 Coupel, P., Grelaud, M., Rost, B., Rickaby, R.E.M., and de Vargas C.: Sensitivity of coccolithophores to
1262 carbonate chemistry and ocean acidification. *Nature*, doi:10.1038/nature10295. 2011
1263
- 1264 Bittig, H.C., Steinhoff, T., Claustre, H., Fiedler, B., Williams, N.L., Sauzède, R., Körtzinger, A. and Gattuso, J.-
1265 P.: An Alternative to Static Climatologies: Robust Estimation of Open Ocean CO₂ Variables and Nutrient
1266 Concentrations From T, S, and O₂ Data Using Bayesian Neural Networks. *Front. Mar. Sci.* 5:328. doi:
1267 10.3389/fmars.2018.00328, 2018
1268
- 1269 Bockmon, E. E., and Dickson, A. G.: An inter-laboratory comparison assessing the quality of seawater carbon
1270 dioxide measurements. *Marine Chemistry*, 171, 36-43, doi:10.1016/j.marchem.2015.02.002, 2015.
1271
- 1272 Bosse, A., Testor, P., Mayot, N., Prieur, L., D'Ortenzio, F., Mortier, L., Le Goff, H., Gourcuff, C., Coppola, L.,
1273 Lavigne, H. and Raimbault, P.: A submesoscale coherent vortex in the Ligurian Sea: From dynamical barriers to
1274 biological implications. *J. Geophys. Res. Oceans*, 122, doi:10.1002/2016JC012634., 2017.
1275
- 1276 Bozec, Y., Merlivat, L., Baudoux, A.-C., Beaumont, L., Blain, S., Bucciarelli, E., Danguy, T., Grosstefan, E.,
1277 Guillot, A., Guillou, J., Répécaud, M., and Tréguer, P.: Diurnal to inter-annual dynamics of pCO₂ recorded by a
1278 CARIOCA sensor in a temperate coastal ecosystem (2003–2009). *Marine Chemistry*, 126, 1-4, 13-26,
1279 10.1016/j.marchem.2011.03.003. 2011
1280
- 1281 Broullón, D., Pérez, F. F., Velo, A., Hoppema, M., Olsen, A., Takahashi, T., Key, R. M., Tanhua, T., González-
1282 Dávila, M., Jeansson, E., Kozyr, A., and van Heuven, S. M. A. C.: A global monthly climatology of total
1283 alkalinity: a neural network approach, *Earth Syst. Sci. Data*, 11, 1109–1127, [https://doi.org/10.5194/essd-11-](https://doi.org/10.5194/essd-11-1109-2019)
1284 1109-2019. 2019
1285
- 1286 Broullón, D., Pérez, F. F., Velo, A., Hoppema, M., Olsen, A., Takahashi, T., Key, R. M., Tanhua, T., Santana-
1287 Casiano, J. M., and Kozyr, A.: A global monthly climatology of oceanic total dissolved inorganic carbon: a
1288 neural network approach, *Earth Syst. Sci. Data*, 12, 1725–1743, <https://doi.org/10.5194/essd-12-1725-2020>.
1289 2020
1290
- 1291 Bushinsky, S. M., Landschützer, P., Rödenbeck, C., Gray, A. R., Baker, D., Mazloff, M. R., Resplandy L.,
1292 Johnson K. S., and Sarmiento, J. L.: Reassessing Southern Ocean air-sea CO₂ flux estimates with the addition of
1293 biogeochemical float observations. *Global Biogeochemical Cycles*, 33, doi: 10.1029/2019GB006176, 2019.
1294
- 1295 Canesi, M., Douville, E., Montagna, P., Taviani, M., Stolarski, J., Bordier, L., Dapoigny, A., Coulibaly, G. E. H.,
1296 Simon, A.-C., Agelou, M., Fin, J., Metzl, N., Iwankow, G., Allemand, D., Planes, S., Moulin, C., Lombard, F.,
1297 Bourdin, G., Troublé, R., Agostini, S., Banaigs, B., Boissin, E., Boss, E., Bowler, C., de Vargas, C., Flores, M.,
1298 Forcioli, D., Furla, P., Gilson, E., Galand, P. E., Pesant, S., Sunagawa, S., Thomas, O., Thurber, R. V., Voolstra,
1299 C. R., Wincker, P., Zoccola, D., and Reynaud, S.: Differences in carbonate chemistry up-regulation of long-lived
1300 reef-building corals. *Sci. Rep.* 13, 11589, Doi: 10.1038/s41598-023-37598-9, 2023.
1301
- 1302 Caniaux, G., Giordani, H., Redelsperger, J.-L., Guichard, F., Key, E. and Wade, M.: Coupling between the
1303 Atlantic cold tongue and the West African monsoon in boreal spring and summer. *J. Geophys. Res.*, 119,
1304 C04003, doi:10.1029/2010JC006570., 2011.



- 1305
1306 Cariou, T., and Bozec, Y.: COMOR-CARBORHONE 1 cruise, RV L'Europe,
1307 <https://doi.org/10.17600/11060060>, 2011a.
1308
1309 Cariou, T., and Bozec, Y.: COMOR-CARBORHONE 2 cruise, RV Téthys II,
1310 <https://doi.org/10.17600/11450150>, 2011b.
1311
1312 Cariou, T., and Bozec, Y.: CARBORHONE 3 cruise, RV Téthys II, <https://doi.org/10.17600/12450020>, 2012a.
1313
1314 Cariou, T., and Bozec Y.: CARBORHONE 4 cruise, RV Téthys II, <https://doi.org/10.17600/12450140>, 2012b.
1315
1316 Carter, B. R., Williams, N. L., Gray, A. R., and Feely, R. A.: Locally interpolated alkalinity regression for global
1317 alkalinity estimation, *Limnol. Oceanogr. Methods*, 14(4), 268–277, doi:10.1002/lom3.10087, 2016.
1318
1319 Chau, T.-T.-T., Gehlen, M., Metzl, N., and Chevallier, F.: CMEMS-LSCE: A global 0.25-degree, monthly
1320 reconstruction of the surface ocean carbonate system, *Earth Syst. Sci. Data Discuss.* [preprint],
1321 <https://doi.org/10.5194/essd-2023-146>, in review, 2023.
1322
1323 Chen, H., Haumann, F. A., Talley, L. D., Johnson, K. S., and Sarmiento, J. L.: The deep ocean's carbon exhaust.
1324 *Global Biogeochemical Cycles*. doi: <https://doi.org/10.1002/essoar.10507757.1>, 2022
1325
1326 Cheng, L. J., Abraham, J., Zhu, J., Trenberth, K. E., Fasullo, J., Boyer, T., Locarnini, R., Zhang, B., Yu, F. J.,
1327 Wan, L. Y., Chen, X. R., Song, X. Z., Liu, Y. L., and Mann, M. E.: Record-setting ocean warmth continued in
1328 2019, *Adv. Atmos. Sci.*, 37, 137–142. <https://doi.org/10.1007/s00376-020-9283-7>, 2020
1329
1330 Claustre, H., Johnson, K. S., and Takeshita, Y.: Observing the Global Ocean with Biogeochemical-Argo. *Annual*
1331 *Review of Marine Science*, 12: 23-48 | DOI: [10.1146/annurev-marine-010419-010956](https://doi.org/10.1146/annurev-marine-010419-010956), 2020.
1332
1333 Conan, P., Guieux, A., and Vuillemin, R.: MOOSE (MOLA), <https://doi.org/10.18142/234>, 2020.
1334
1335 Copin-Montégut, C.: Alkalinity and carbon budgets in the Mediterranean Sea, *Global Biogeochemical Cycles*,
1336 vol. 7, pp. 915–925, 1993.
1337
1338 Copin-Montégut, C., and Bégovic, M.: Distributions of carbonate properties and oxygen along the water column
1339 (0–2000 m) in the central part of the NW Mediterranean Sea (Dyfamed site): influence of the winter vertical
1340 mixing on air–sea CO₂ and O₂ exchanges. *Deep-Sea Research II* 49, 2049–2066, [https://doi.org/10.1016/S0967-](https://doi.org/10.1016/S0967-0645(02)00027-9)
1341 [0645\(02\)00027-9](https://doi.org/10.1016/S0967-0645(02)00027-9), 2002.
1342
1343 Coppola, L., and Diamond-Riquier, E.: MOOSE (DYFAMED), <https://doi.org/10.18142/131>, 2008.
1344
1345 Coppola, L., Raimbault, P., Mortier, L., and Testor, P.: Monitoring the environment in the northwestern
1346 Mediterranean Sea, *Eos*, 100, <https://doi.org/10.1029/2019EO125951>. Published on 25 July 2019.
1347
1348 Coppola, L., Boutin, J., Gattuso, J.-P., Lefèvre, D., and Metzl, N.: The Carbonate System in the Ligurian Sea. In
1349 *The Mediterranean Sea in the Era of Global Change: Evidence from 30 years of multidisciplinary study of the*
1350 *Ligurian Sea*, C. Migon, P. Nival, A. Sciandra, Eds. (ISTE Science Publishing LTD, London, UK, 2020), vol. 1,
1351 chap. 4, pp. 79–104. ISBN: 9781786304285. <https://doi.org/10.1002/9781119706960.ch4>, 2020.
1352
1353 Corbière, A., Metzl, N., Reverdin, G., Brunet, C., and Takahashi, T.: Interannual and decadal variability of the
1354 oceanic carbon sink in the North Atlantic subpolar gyre. *Tellus B*, Vol. 59, issue 2, 168–179, DOI:
1355 [10.1111/j.1600-0889.2006.00232](https://doi.org/10.1111/j.1600-0889.2006.00232), 2007.
1356
1357 D'Ortenzio, F. and Taillandier, V.: BIO-ARGO-MED-2018 cruise, RV Téthys II,
1358 <https://doi.org/10.17600/18000550>, 2018.



- 1359
1360 De Carlo, E. H., Mousseau, L., Passafiume, O., Drupp, P. and Gattuso J.-P.: Carbonate chemistry and air-sea
1361 CO₂ flux in a NW Mediterranean bay over a four-year period: 2007-2011. *Aquatic Geochemistry*
1362 doi:10.1007/s10498-013-9217-4, 2013.
1363
1364 Dickson, A. G., Sabine, C. L., and Christian, J. R.: Guide to best practices for ocean CO₂ measurements, North
1365 Pacific Marine Science Organization, Sidney, British Columbia, 191, <https://doi.org/10.25607/OBP-1342>, 2007.
1366
1367 Division Plans de DMI – SHOM: PROTEUS2010_LEG1 cruise, RV Pourquoi pas ?,
1368 <https://doi.org/10.17600/10030040>, 2010.
1369
1370 Division Plans de DMI – SHOM: PROTEUSMED_PERLE_2018 cruise, RV L'Atalante,
1371 <https://campagnes.flotteoceanographique.fr/campaign>, 2018.
1372
1373 Doney, S. C., Fabry, V. J., Feely, R. A., and Kleypas, J. A., Ocean acidification: The other CO₂ problem. *Annual*
1374 *Review of Marine Science*, 1(1), 169–192. 10.1146/annurev.marine.010908.163834, 2009
1375
1376 Doney, S. C., Busch, D. S., Cooley, S. R., and Kroeker, K. J.: The Impacts of Ocean Acidification on Marine
1377 Ecosystems and Reliant Human Communities. *Annual Review of Environment and Resources* 45:1,
1378 <https://doi.org/10.1146/annurev-environ-012320-083019>. 2020
1379
1380 Douville, E., Bourdin, G., Lombard, F., Gorsky, G., Fin, J., Metzl, N., Pesant, S., and Tara Pacific Consortium:
1381 Seawater carbonate chemistry dataset collected during the Tara Pacific Expedition 2016-2018. PANGAEA,
1382 <https://doi.org/10.1594/PANGAEA.944420>. 2022.
1383
1384 Durrieu de Madron, X.: CASCADE cruise, RV L'Atalante, <https://doi.org/10.17600/11010020>, 2011.
1385
1386 Durrieu de Madron, X., and Conan, P.: PERLE2 cruise, RV Pourquoi pas ?, <https://doi.org/10.17600/18000865>,
1387 2018
1388
1389 Edmond, J. M.: High precision determination of titration alkalinity and total carbon dioxide content of sea water
1390 by potentiometric titration, *Deep-Sea Res.*, 17, 737–750, [https://doi.org/10.1016/0011-7471\(70\)90038-0](https://doi.org/10.1016/0011-7471(70)90038-0), 1970.
1391
1392 Eldin, G. : PANDORA cruise, RV L'Atalante, <https://doi.org/10.17600/12010050>, 2012.
1393
1394 Eyring, V., Righi, M., Lauer, A., Evaldsson, M., Wenzel, S., Jones, C., Anav, A., Andrews, O., Cionni, I., Davin,
1395 E. L., Deser, C., Ehbrecht, C., Friedlingstein, P., Gleckler, P., Gottschaldt, K.-D., Hagemann, S., Juckes, M.,
1396 Kindermann, S., Krasting, J., Kunert, D., Levine, R., Loew, A., Mäkelä, J., Martin, G., Mason, E., Phillips, A. S.,
1397 Read, S., Rio, C., Roehrig, R., Senfleben, D., Sterl, A., van Ulft, L. H., Walton, J., Wang, S., and Williams, K.
1398 D.: ESMValTool (v1.0) – a community diagnostic and performance metrics tool for routine evaluation of Earth
1399 system models in CMIP, *Geosci. Model Dev.*, 9, 1747-1802, doi:10.5194/gmd-9-1747-2016, 2016.
1400
1401 Fabry, V. J., Seibel, B. A., Feely, R. A. and Orr, J. C.: Impacts of ocean acidification on marine fauna and
1402 ecosystem processes. *ICES J. Mar. Sci.* 65, 414–432. <https://doi.org/10.1093/icesjms/fsn048>, 2008.
1403
1404 Fassbender, A. J., Sabine, C. L., and Palevsky, H. I.: Nonuniform ocean acidification and attenuation of the
1405 ocean carbon sink, *Geophys. Res. Lett.*, 44, 8404–8413, doi:10.1002/2017GL074389., 2017.
1406
1407 Fassbender, A. J., Alin, S. R., Feely, R. A., Sutton, A. J., Newton, J. A., Krembs, C., Bos, J., Keyzers, M., Devol,
1408 A., Ruef, W., and Pelletier, G.: Seasonal carbonate chemistry variability in marine surface waters of the US
1409 Pacific Northwest, *Earth Syst. Sci. Data*, 10, 1367–1401, <https://doi.org/10.5194/essd-10-1367-2018>, 2018.
1410



- 1411 Feely, R. A., Sabine, C. L., Byrne, R. H., Millero, F. J., Dickson, A. G., Wanninkhof, R., et al.: Decadal changes
1412 in the aragonite and calcite saturation state of the Pacific Ocean. *Global Biogeochemical Cycles*, 26, GB3001.
1413 <https://doi.org/10.1029/2011GB004157>, 2012.
- 1414
1415 Fleury, E., Petton, S., Benabdelmouna, A., and Pouvreau, S., (coord.): Observatoire national du cycle de vie de
1416 l'huître creuse en France. Rapport annuel ECOSCOPA 2022. R.INT.BREST RBE/PFOM/PI 2023-1, 2023.
- 1417
1418 Fourier, M., Coppola, L., Claustre, H., D'Ortenzio, F., Sauzède, R. and Gattuso, J.-P.: A regional neural
1419 network approach to estimate water-column nutrient concentrations and carbonate system variables in the
1420 Mediterranean Sea: CANYON-MED. *Frontiers in Marine Science*, 7:620,
1421 <https://www.frontiersin.org/articles/10.3389/fmars.2020.00620>, 2020.
- 1422
1423 Fourier, M., Coppola, L., D'Ortenzio, F., Migon, C., and Gattuso, J.-P.: Impact of intermittent convection in the
1424 northwestern Mediterranean Sea on oxygen content, nutrients, and the carbonate system. *Journal of Geophysical*
1425 *Research: Oceans*, 127, e2022JC018615. <https://doi.org/10.1029/2022JC018615>, 2022
- 1426
1427 Friedlingstein, P., O'Sullivan, M., Jones, M. W., Andrew, R. M., Gregor, L., Hauck, J., Le Quééré, C., Luijkx, I.
1428 T., Olsen, A., Peters, G. P., Peters, W., Pongratz, J., Schwingshackl, C., Sitch, S., Canadell, J. G., Ciais, P.,
1429 Jackson, R. B., Alin, S. R., Alkama, R., Arneeth, A., Arora, V. K., Bates, N. R., Becker, M., Bellouin, N., Bittig,
1430 H. C., Bopp, L., Chevallier, F., Chini, L. P., Cronin, M., Evans, W., Falk, S., Feely, R. A., Gasser, T., Gehlen,
1431 M., Gkritzalis, T., Gloege, L., Grassi, G., Gruber, N., Gürses, Ö., Harris, I., Hefner, M., Houghton, R. A., Hurtt,
1432 G. C., Iida, Y., Ilyina, T., Jain, A. K., Jersild, A., Kadono, K., Kato, E., Kennedy, D., Klein Goldewijk, K.,
1433 Knauer, J., Korsbakken, J. I., Landschützer, P., Lefèvre, N., Lindsay, K., Liu, J., Liu, Z., Marland, G., Mayot, N.,
1434 McGrath, M. J., Metzl, N., Monacchi, N. M., Munro, D. R., Nakaoka, S.-I., Niwa, Y., O'Brien, K., Ono, T.,
1435 Palmer, P. I., Pan, N., Pierrot, D., Pockock, K., Poulter, B., Resplandy, L., Robertson, E., Rödenbeck, C.,
1436 Rodriguez, C., Rosan, T. M., Schwinger, J., Séférian, R., Shutler, J. D., Skjelvan, I., Steinhoff, T., Sun, Q.,
1437 Sutton, A. J., Sweeney, C., Takao, S., Tanhua, T., Tans, P. P., Tian, X., Tian, H., Tilbrook, B., Tsujino, H.,
1438 Tubiello, F., van der Werf, G. R., Walker, A. P., Wanninkhof, R., Whitehead, C., Willstrand Wranne, A.,
1439 Wright, R., Yuan, W., Yue, C., Yue, X., Zaehle, S., Zeng, J., and Zheng, B.: Global Carbon Budget 2022, *Earth*
1440 *Syst. Sci. Data*, 14, 4811–4900, <https://doi.org/10.5194/essd-14-4811-2022>, 2022.
- 1441
1442 Fröb, F., Olsen, A., Becker, M., Chafik, L., Johannessen, T., Reverdin, G., and Omar, A.: Wintertime fCO₂
1443 variability in the subpolar North Atlantic since 2004. *Geophysical Research Letters*, 46,
1444 <https://doi.org/10.1029/2018GL080554>, 2019.
- 1445
1446 Gac, J.-P., Marrec, P., Cariou, T., Guillerm, C., Macé, E., Vernet, M., and Bozec, Y.: Cardinal buoys: An
1447 opportunity for the study of air-sea CO₂ fluxes in coastal ecosystems. *Front. Mar. Sci.* doi:
1448 10.3389/fmars.2020.00712. 2020.
- 1449
1450 Gac, J.-P., Marrec, P., Cariou, T., Grosstefan, E., Macé, E., Rimmelin-Maury, P., Vernet, M., and Bozec, Y.:
1451 Decadal Dynamics of the CO₂ System and Associated Ocean Acidification in Coastal Ecosystems of the North
1452 East Atlantic Ocean. *Front. Mar. Sci.* 8:688008. doi:10.3389/fmars.2021.688008, 2021.
- 1453
1454 Ganachaud, A., Cravatte, S., Sprintall, J., Germineaud, C., Albery, M., Jeandel, C., Eldin, G., Metzl, N., Bonnet,
1455 S., Benavides, M., Heimburger, L.-E., Lefèvre, J., Michael, S., Resing, J., Quéroüé, F., Sarthou, G., Rodier, M.,
1456 Berthelot, H., Baurand, F., Grelet, J., Hasegawa, T., Kessler, W., Kilepak, M., Lacan, F., Privat, E., Send, U.,
1457 Van Beek, P., Souhaut, M. and Sonke, J. E.: The Solomon Sea: its circulation, chemistry, geochemistry and
1458 biology explored during two oceanographic cruises. *Elem Sci Anth*, 5: 33, DOI:
1459 <https://doi.org/10.1525/elementa.221>, 2017.
- 1460
1461 Gattuso, J.-P., Magnan, A., Billé, R., Cheung, W. W. L., Howes, E. L., Joos, F., Allemand, D., Bopp, L., Cooley,
1462 S., Eakin, M., Hoegh-Guldberg, O., Kelly, R. P., Pörtner, H.-O., Rogers, A. D., Baxter, J. M., Laffoley, D.,
1463 Osborn, D., Rankovic, A., Rochette, J., Sumaila, U. R., Treyer, S., and Turley, C.: Contrasting futures for ocean



- 1464 and society from different anthropogenic CO₂ emissions scenarios. *Science* 349:aac4722.doi:
1465 10.1126/science.aac4722, 2015.
1466
1467 Gattuso, J.-P., Alliouane, S., and Mousseau, L.: Seawater carbonate chemistry in the Bay of Villefranche, Point
1468 B (France), January 2007 - September 2020. PANGAEA, <https://doi.org/10.1594/PANGAEA.727120>, 2021.
1469
1470 Gattuso, J.-P., Alliouane, S., and Fischer, P.: High-frequency, year-round time series of the carbonate chemistry
1471 in a high-Arctic fjord (Svalbard), *Earth Syst. Sci. Data*, 15, 2809–2825, [https://doi.org/10.5194/essd-15-2809-](https://doi.org/10.5194/essd-15-2809-2023)
1472 [2023](https://doi.org/10.5194/essd-15-2809-2023), 2023.
1473
1474 Gattuso, J.-P., Alliouane, S., and Fischer, P.: High-frequency, year-round time series of the carbonate chemistry
1475 in a high-Arctic fjord (Svalbard) v2. PANGAEA, <https://doi.org/10.1594/PANGAEA.960131>, 2023.
1476
1477 Gemayel, E., Hassoun, A. E. R., Benallal, M. A., Goyet, C., Rivaro, P., Abboud-Abi Saab, M., Krasakopoulou,
1478 E., Touratier, F., and Ziveri, P.: Climatological variations of total alkalinity and total inorganic carbon in the
1479 Mediterranean Sea surface waters. *Earth Syst. Dynam.*, 6, 789–800, doi:10.5194/esd-6-789-2015, 2015.
1480
1481 Golbol, M., Vellucci, V., and Antoine, D.: BOUSSOLE, <https://doi.org/10.18142/1>, 2000.
1482
1483 Golbol M., Boutin J., Merlivat L., Vellucci, V., and Antoine, D.: Dissolved Inorganic Carbon and Total
1484 Alkalinity sampled at Boussole site in the Mediterranean Sea. SEANOE. <https://doi.org/10.17882/71911>, 2020.
1485
1486 Goris, N., Tjiputra, J. F., Olsen, A., Schwinger, J., Lauvset, S. K. and Jeansson, E.: Constraining projection-
1487 based estimates of the future North Atlantic carbon uptake, *J. Climate*, 31, 3959–3978,
1488 <https://doi.org/10.1175/JCLI-D-17-0564.1>, 2018.
1489
1490 Goyet, C., Beauverger, C., Brunet, C., and Poisson, A.: Distribution of carbon dioxide partial pressure in surface
1491 waters of the Southwest Indian Ocean, *Tellus B: Chemical and Physical Meteorology*, 43:1, 1–11, DOI:
1492 [10.3402/tellusb.v43i1.15242](https://doi.org/10.3402/tellusb.v43i1.15242), 1991.
1493
1494 Gregor, L. and Gruber, N.: OceanSODA-ETHZ: a global gridded data set of the surface ocean carbonate system
1495 for seasonal to decadal studies of ocean acidification, *Earth Syst. Sci. Data*, 13, 777–808,
1496 <https://doi.org/10.5194/essd-13-777-2021>, 2021.
1497
1498 Gruber, N., Clement, D., Carter, B. R., Feely, R. A., van Heuven, S., Hoppema, M., Ishii, M., Key, R. M.,
1499 Kozyr, A., Lauvset, S. K., Lo Monaco, C., Mathis, J. T., Murata, A., Olsen, A., Perez, F. F., Sabine, C. L.,
1500 Tanhua, T., and Wanninkhof, R.: The oceanic sink for anthropogenic CO₂ from 1994 to 2007, *Science* vol. 363
1501 (issue 6432), pp. 1193–1199. DOI: 10.1126/science.aau5153, 2019.
1502
1503 Guieu, C., Desboeufs, K., Albani, S., et al.: BIOGEOCHEMICAL dataset collected during the PEACETIME
1504 cruise. SEANOE. <https://doi.org/10.17882/75747>, 2020.
1505
1506 Hagens, M., and Middelburg, J. J.: Attributing seasonal pH variability in surface ocean waters to governing
1507 factors, *Geophys. Res. Lett.*, 43, doi:10.1002/2016GL071719, 2016.
1508
1509 Henson, S. A., Painter, S. C., Holliday, N. P., Stinchcombe, M. C., and Giering, S. L. C.: Unusual subpolar
1510 North Atlantic phytoplankton bloom in 2010: Volcanic fertilization or North Atlantic Oscillation?, *J. Geophys.*
1511 *Res. Oceans*, 118, 4771–4780, doi:10.1002/jgrc.20363, 2013.
1512
1513 Hoegh-Guldberg, O., Mumby, P.J., Hooten, A.J., Steneck, R.S., Greenfield, P., Gomez, E., Harvell, C.D., Sale,
1514 P.F., Edwards, A.J., Caldeira, K., Knowlton, N., Eakin, C.M., Iglesias-Prieto, R., Muthiga, N., Bradbury, R.H.,
1515 Dubi, A., and Hatzioiols, M.E.: Coral reefs under rapid climate change and ocean acidification. *Science* 14,
1516 1737–1742. <https://doi.org/10.1126/science.1152509>, 2007.
1517



- 1518 Hood, E.M., and Merlivat, L.: Annual to interannual variations of $f\text{CO}_2$ in the northwestern Mediterranean
1519 Sea: Results from hourly measurements made by CARIOCA buoys, 1995-1997, *Journal Of Marine Research*,
1520 59, 113-131, doi: 10.1357/002224001321237399. 2001
- 1521
- 1522 Howes, E., Stemmann, L., Assailly, C., Irsson, J.-O., Dima, M., Bijma, J., Gattuso, J.-P.: Pteropod time series
1523 from the North Western Mediterranean (1967-2003): impacts of pH and climate variability. *Mar Ecol Prog Ser*
1524 531: 193-206, doi: 10.3354/meps11322. 2015.
- 1525
- 1526 Howes, E. L., Eagle, R., Gattuso, J.-P., and Bijma, J.: Comparison of Mediterranean pteropod shell biometrics
1527 and ultrastructure from historical (1910 and 1921) and present day (2012) samples provides baseline for
1528 monitoring effects of global change. *PLoS ONE* 12:e0167891. 2017.
- 1529
- 1530 IPCC. Changing Ocean, Marine Ecosystems, and Dependent Communities. in *The Ocean and Cryosphere in a*
1531 *Changing Climate* 447–588 (Cambridge University Press, 2022). doi:10.1017/9781009157964.007. 2022
- 1532
- 1533 Jiang, Z.-P., Tyrrell, T., Hydes, D. J., Dai, M., and Hartman, S. E.: Variability of alkalinity and the alkalinity-
1534 salinity relationship in the tropical and subtropical surface ocean, *Global Biogeochem. Cycles*, 28, 729–742,
1535 doi:10.1002/2013GB004678, 2014.
- 1536
- 1537 Jiang, L.-Q., Feely, R. A., Carter, B. R., Greeley, D. J., Gledhill, D. K., and Arzayus K. M.: Climatological
1538 distribution of aragonite saturation state in the global oceans, *Global Biogeochem. Cycles*, 29, 1656–1673,
1539 doi:10.1002/2015GB005198, 2015.
- 1540
- 1541 Jiang, L.-Q., Carter, B. R., Feely, R. A., Lauvset, S. K. and Olsen, A.: Surface ocean pH and buffer capacity:
1542 past, present and future, *Sci Rep*, 9(1), 1–11, doi:10.1038/s41598-019-55039-4. 2019.
- 1543
- 1544 Jiang, L.Q., Feely, R. A., Wanninkhof, R., et al.: Coastal Ocean Data Analysis Product in North America
1545 (CODAP-NA, Version 2021) (NCEI Accession 0219960). [indicate subset used]. NOAA National Centers for
1546 Environmental Information. Dataset. <https://doi.org/10.25921/531n-c230>. Accessed [date]. 2020.
- 1547
- 1548 Jiang, L.-Q., Dunne, J., Carter, B. R., Tjiputra, J. F., Terhaar, J., Sharp, J. D., et al.: Global surface ocean
1549 acidification indicators from 1750 to 2100. *Journal of Advances in Modeling Earth Systems*, 15,
1550 e2022MS003563. <https://doi.org/10.1029/2022MS003563>, 2023a
- 1551
- 1552 Jiang, L.Q., Kozyr, A., Relph, J.M. *et al.* The Ocean Carbon and Acidification Data System. *Sci Data* 10, 136.
1553 <https://doi.org/10.1038/s41597-023-02042-0>, 2023b
- 1554
- 1555 Johnson, K. S., Mazloff, M. R., Bif, M. B., Takeshita, Y., Jannasch, H. W., Maurer, T. L., et al.: Carbon to
1556 nitrogen uptake ratios observed across the Southern Ocean by the SOCCOM profiling float array. *Journal of*
1557 *Geophysical Research: Oceans*, 127, e2022JC018859. <https://doi.org/10.1029/2022JC018859>, 2022.
- 1558
- 1559 Joos, F., Hameau, A., Frölicher, T. L., and Stephenson, D. B.: Anthropogenic attribution of the
1560 increasing seasonal amplitude in surface ocean $p\text{CO}_2$. *Geophysical Research Letters*, 50, e2023GL102857.
1561 <https://doi.org/10.1029/2023GL102857>, 2023.
- 1562
- 1563 Joyce, T. and Corry, C., eds: Requirements for WOCE Hydrographic Programme Data Reporting. WHPO
1564 Publication 90-1 Revision 2, WOCE Report 67/91, Woods Hole, Mass., USA, May 1994.
- 1565
- 1566 Kapsenberg, L., Alliouane, S., Gazeau, F., Mousseau, L., and Gattuso, J.-P.: Coastal ocean acidification and
1567 increasing total alkalinity in the northwestern Mediterranean Sea, *Ocean Sci.*, 13, 411-426, doi:10.5194/os-13-
1568 411-2017, 2017.
- 1569
- 1570 Keppler, L., Landschützer, P., Gruber, N., Lauvset, S. K., and Stemmler, I.: Seasonal carbon dynamics in the
1571 near-global ocean. *Global Biogeochemical Cycles*, 34, e2020GB006571. doi:10.1029/2020GB006571, 2020.



- 1572
1573 Keppler, L., Landschützer, P., Lauvset, S.K., and Gruber, N.: Recent trends and variability in the oceanic storage
1574 of dissolved inorganic carbon. *Global Biogeochemical Cycles*, 37, e2022GB007677. Doi:
1575 10.1029/2022GB007677, 2023.
1576
1577 Keraghel, M. A., Louanchi, F., Zerrouki, M., Kaci, M. A., Aït-Ameur, N., Labaste, M., Legoff, H., Taillandier,
1578 V., Harid, R., and Mortier, L.: Carbonate system properties and anthropogenic carbon inventory in the Algerian
1579 Basin during SOMBA cruise (2014): Acidification estimate, *Marine Chemistry*,
1580 <https://doi.org/10.1016/j.marchem.2020.103783>. 2020.
1581
1582 Key, R. M., Kozyr, A., Sabine, C. L., Lee, K., Wanninkhof, R., Bullister, J. L., Feely, R. A., Millero, F. J.,
1583 Mordy, C., and Peng, T. H.: A global ocean carbon climatology: Results from Global Data Analysis Project
1584 (GLODAP), *Global Biogeochemical Cycles*, 18, GB4031, <https://doi.org/10.1029/2004GB002247>, 2004.
1585
1586 Key, R. M., Tanhua, T., Olsen, A., Hoppema, M., Jutterström, S., Schirnick, C., van Heuven, S., Kozyr, A., Lin,
1587 X., Velo, A., Wallace, D. W. R., and Mintrop, L.: The CARINA data synthesis project: introduction and
1588 overview, *Earth Syst. Sci. Data*, 2, 105–121, <https://doi.org/10.5194/essd-2-105-2010>, 2010.
1589
1590 Khatiwala, S., Tanhua, T., Mikaloff Fletcher, S., Gerber, M., Doney, S. C., Graven, H. D., Gruber, N.,
1591 McKinley, G. A., Murata, A., Ríos, A. F., and Sabine, C. L.: Global ocean storage of anthropogenic carbon,
1592 *Biogeosciences*, 10, 2169–2191, <https://doi.org/10.5194/bg-10-2169-2013>, 2013.
1593
1594 Kitidis, V., Shutler, J. D., Ashton, I., Warren, M., Brown, I., Findlay, H., Hartman, S. E., Sanders, R.,
1595 Humphreys, M., Kivimäe, C., Greenwood, N., Hull, T., Pearce, D., McGrath, T., Stewart, B. M., Walsham, P.,
1596 McGovern, E., Bozec, Y., Gac, J.-P., van Heuven, S., Hoppema, M., Schuster, U., Johannessen, T., Omar, A.,
1597 Lauvset, S. K., Skjelvan, I., Olsen, A., Steinhoff, T., Körtzinger, A., Becker, M., Lefèvre, N., Diverrès, D.,
1598 Gkritzalis, T., Cattrijsse, A., Petersen, W., Voynova, Y., Chapron, B., Grouazel, A., Land, P. E., Sharples, J., and
1599 Nightingale, P. D.: Winter weather controls net influx of atmospheric CO₂ on the north-west European shelf. *Sci*
1600 *Rep* 9, 20153, doi:10.1038/s41598-019-56363-5. 2019.
1601
1602 Koffi U., Lefevre, N., Kouadio, G., and Boutin, J.: Surface CO₂ parameters and air-sea CO₂ fluxes distribution
1603 in the eastern equatorial Atlantic Ocean. *J. Marine Systems*, doi:10.1016/j.jmarsys/2010.04.010. 2010.
1604
1605 Koffi, U., Georges, K., and Boutin, J.: Partial pressure (or fugacity) of carbon dioxide, dissolved inorganic
1606 carbon, alkalinity, temperature, salinity and other variables collected from Surface underway, discrete sample
1607 and profile observations using CTD, Carbon dioxide (CO₂) gas analyzer and other instruments from ANTEA
1608 and L'ATALANTE in the Gulf of Guinea, North Atlantic Ocean and South Atlantic Ocean from 2005-06-09 to
1609 2007-09-30 (NCEI Accession 0108086). [indicate subset used]. NOAA National Centers for Environmental
1610 Information. Dataset. https://doi.org/10.3334/cdiac/otg.egee1_6. Accessed [date]., 2013
1611
1612 Koseki, S., Tjiputra, J., Fransner, F. et al.: Disentangling the impact of Atlantic Niño on sea-air CO₂ flux. *Nat*
1613 *Commun* 14, 3649. <https://doi.org/10.1038/s41467-023-38718-9>, 2023.
1614
1615 Kwiatkowski, L., Torres, O., Bopp, L., Aumont, O., Chamberlain, M., Christian, J. R., Dunne, J. P., Gehlen, M.,
1616 Ilyina, T., John, J. G., Lenton, A., Li, H., Lovenduski, N. S., Orr, J. C., Palmieri, J., Santana-Falcón, Y.,
1617 Schwinger, J., Séférian, R., Stock, C. A., Tagliabue, A., Takano, Y., Tjiputra, J., Toyama, K., Tsujino, H.,
1618 Watanabe, M., Yamamoto, A., Yool, A., and Ziehn, T.: Twenty-first century ocean warming, acidification,
1619 deoxygenation, and upper-ocean nutrient and primary production decline from CMIP6 model projections,
1620 *Biogeosciences*, 17, 3439–3470, <https://doi.org/10.5194/bg-17-3439-2020>, 2020.
1621
1622 Land, P. E., Findlay, H. S., Shutler, J. D., Ashton, I. G., Holding, T., Grouazel, A., Girard-Ardhuin, F., Reul, N.,
1623 Piolle, J. F., Chapron, B., and Quilfen, Y.: Optimum satellite remote sensing of the marine carbonate system
1624 using empirical algorithms in the global ocean, the Greater Caribbean, the Amazon Plume and the Bay of
1625 Bengal. *Remote Sensing of Environment*, 235, p.111469, doi: 10.1016/j.rse.2019.111469, 2019.



- 1626
1627 Lange, N., Fiedler, B., Álvarez, M., Benoit-Cattin, A., Benway, H., Buttigieg, P. L., Coppola, L., Currie, K.,
1628 Flecha, S., Honda, M., Huertas, I. E., Lauvset, S. K., Muller-Karger, F., Körtzinger, A., O'Brien, K. M.,
1629 Ólafsdóttir, S. R., Pacheco, F. C., Rueda-Roa, D., Skjelvan, I., Wakita, M., White, A., and Tanhua, T.: Synthesis
1630 Product for Ocean Time-Series (SPOTS) – A ship-based biogeochemical pilot, *Earth Syst. Sci. Data Discuss.*
1631 [preprint], <https://doi.org/10.5194/essd-2023-238>, in review, 2023.
1632
1633 Lauvset, S. K., Gruber, N., Landschützer, P., Olsen, A., and Tjiputra, J.: Trends and drivers in global surface
1634 ocean pH over the past 3 decades. *Biogeosciences*, 12, 1285-1298, doi:10.5194/bg-12-1285-2015, 2015
1635
1636 Lauvset, S. K., Carter, B. R., Perez, F. F., Jiang, L.-Q., Feely, R. A., Velo, A., and Olsen, A.: Processes Driving
1637 Global Interior Ocean pH Distribution, *Global Biogeochem. Cycles*, 34, e2019GB006 229,
1638 <https://doi.org/10.1029/2019GB006229>, 2020.
1639
1640 Lauvset, S. K., Lange, N., Tanhua, T., Bittig, H. C., Olsen, A., Kozyr, A., Álvarez, M., Becker, S., Brown, P. J.,
1641 Carter, B. R., Cotrim da Cunha, L., Feely, R. A., van Heuven, S., Hoppema, M., Ishii, M., Jeansson, E.,
1642 Jutterström, S., Jones, S. D., Karlsen, M. K., Lo Monaco, C., Michaelis, P., Murata, A., Pérez, F. F., Pfeil, B.,
1643 Schirnack, C., Steinfeldt, R., Suzuki, T., Tilbrook, B., Velo, A., Wanninkhof, R., Woosley, R. J., and Key, R. M.:
1644 An updated version of the global interior ocean biogeochemical data product, GLODAPv2.2021, *Earth Syst. Sci.*
1645 *Data*, 13, 5565–5589, <https://doi.org/10.5194/essd-13-5565-2021>, 2021.
1646
1647 Lebehot, A. D., Halloran, P. R., Watson, A. J., McNeill, D., Ford, D. A., Landschützer, P., Lauvset, S. K.,
1648 and Schuster, U.: Reconciling Observation and Model Trends in North Atlantic Surface CO₂, *Global*
1649 *Biogeochem. Cy.*, 33, 1204–1222, <https://doi.org/10.1029/2019GB006186>, 2019.
1650
1651 Lee, K., Wanninkhof, R., Feely, R. A., Millero, F. J., and Peng, T.-H.: Global relationships of total inorganic
1652 carbon with temperature and nitrate in surface seawater, *Global Biogeochem. Cy.*, 14, 979–994,
1653 <https://doi.org/10.1029/1998GB001087>, 2000.
1654
1655 Lee, K., Tong, L.T., Millero, F.J., Sabine, C.L., Dickson, A.G., Goyet, C., Park, G.H., Wanninkhof, R., Feely,
1656 R.A., and Key, R.M.: Global relationships of total alkalinity with salinity and temperature in surface waters of
1657 the world's oceans. *Geophys. Res. Lett.* 33, L19605. doi10.1029/2006GL027207. 2006.
1658
1659 Lefèvre, D.: MOOSE (ANTARES), <https://doi.org/10.18142/233>, 2010.
1660
1661 Lefèvre, N., Guillot, A., Beaumont, L., and Danguy, T.: Variability of fCO₂ in the Eastern Tropical Atlantic
1662 from a moored buoy. *J. of Geophysical Research-Oceans*, Volume: 113 Issue: C1, DOI:
1663 10.1029/2007JC004146. 2008.
1664
1665 Lefèvre N., and Merlivat, L.: Carbon and oxygen net community production in the eastern tropical Atlantic
1666 estimated from a moored buoy. *Global biogeochemical cycles*, 26(1), 1-14.
1667 <https://doi.org/10.1029/2010GB004018>. 2012.
1668
1669 Lefèvre, N., Diverres, D., and Gallois, F.: Origin of CO₂ undersaturation in the western tropical Atlantic: *Tellus*
1670 *Series B Chemical and Physical Meteorology*. Volume: 62 Issue: 5 Special Issue: SI Pages: 595-607 DOI:
1671 10.1111/j.1600-0889.2010.00475.x, 2010.
1672
1673 Lefèvre N.: Carbon parameters along a zonal transect. SEANOE. <https://doi.org/10.17882/58575>, 2010.
1674
1675 Lefèvre, N., Veleda, D., Araujo, M., Caniaux, G.: Variability and trends of carbon parameters at a time series in
1676 the eastern tropical Atlantic. *Tellus B*, Co-Action Publishing, 68, pp.30305. 10.3402/tellusb.v68.30305. 2016.
1677



- 1678 Lefèvre, N., Mejia, C., Khvorostyanov, D., Beaumont, L., and Koffi, U.: Ocean Circulation Drives the
1679 Variability of the Carbon System in the Eastern Tropical Atlantic. *Oceans*, 2021, 2, 126–148.
1680 <https://doi.org/10.3390/oceans2010008>, 2021.
- 1681
1682 Lefèvre, N.: Discrete profile measurements of dissolved inorganic carbon, total alkalinity, temperature and
1683 salinity collected from R/V Antea French PIRATA cruise in Eastern Tropical Atlantic Ocean from 2009-07-10
1684 to 2010-10-01 (NCEI Accession 0171193), 2018a.
- 1685
1686 Lefèvre, N.: Discrete surface measurements of dissolved inorganic carbon, total alkalinity, temperature and
1687 salinity collected from R/V Le Suroit French PIRATA cruise in Eastern Tropical Atlantic Ocean from 2011-05-
1688 03 to 2011-05-25 (NCEI Accession 0171197), 2018b.
- 1689
1690 Lefèvre, N.: Discrete profile measurements of dissolved inorganic carbon, total alkalinity, temperature and
1691 salinity collected from R/V Le Suroit French PIRATA cruise in Eastern Tropical Atlantic Ocean from 2012-03-
1692 21 to 2012-04-30 (NCEI Accession 0171195), 2018c.
- 1693
1694 Lefèvre, N.: Discrete surface measurements of dissolved inorganic carbon, total alkalinity, temperature and
1695 salinity collected from R/V Le Suroit French PIRATA cruise in Eastern Tropical Atlantic Ocean from 2013-05-
1696 11 to 2013-06-18 (NCEI Accession 0171189), 2018d.
- 1697
1698 Lefèvre, N.: Discrete profile measurements of dissolved inorganic carbon, total alkalinity, temperature and
1699 salinity collected from R/V Le Suroit French PIRATA cruise in Eastern Tropical Atlantic Ocean from 2014-04-
1700 10 to 2014-05-19 (NCEI Accession 0171194), 2018e.
- 1701
1702 Lefèvre, N.: Discrete surface measurements of dissolved inorganic carbon, total alkalinity, temperature and
1703 salinity collected from R/V Thalassa French PIRATA cruise in Eastern Tropical Atlantic Ocean from 2015-03-
1704 18 to 2015-04-15 (NCEI Accession 0171196), 2018f.
- 1705
1706 Lefèvre, N.: Discrete surface measurements of dissolved inorganic carbon, total alkalinity, temperature and
1707 salinity collected from R/V Thalassa French PIRATA cruise in Eastern Tropical Atlantic Ocean from 2016-03-
1708 08 to 2016-04-11 (NCEI Accession 0171190), 2018g.
- 1709
1710 Lefèvre, N.: Discrete surface measurements of dissolved inorganic carbon, total alkalinity, temperature and
1711 salinity collected from R/V Thalassa French PIRATA cruise in Eastern Tropical Atlantic Ocean from 2017-02-
1712 26 to 2017-03-30 (NCEI Accession 0171191), 2018h.
- 1713
1714 Le Quéré, C., Moriarty, R., Andrew, R. M., Canadell, J. G., Sitch, S., Korsbakken, J. I., Friedlingstein, P., Peters,
1715 G. P., Andres, R. J., Boden, T. A., Houghton, R. A., House, J. I., Keeling, R. F., Tans, P., Arneeth, A., Bakker, D.
1716 C. E., Barbero, L., Bopp, L., Chang, J., Chevallier, F., Chini, L. P., Ciais, P., Fader, M., Feely, R. A., Gkritzalis,
1717 T., Harris, I., Hauck, J., Ilyina, T., Jain, A. K., Kato, E., Kitidis, V., Klein Goldewijk, K., Koven, C.,
1718 Landschützer, P., Lauvset, S. K., Lefèvre, N., Lenton, A., Lima, I. D., Metzl, N., Millero, F., Munro, D. R.,
1719 Murata, A., Nabel, J. E. M. S., Nakaoka, S., Nojiri, Y., O'Brien, K., Olsen, A., Ono, T., Pérez, F. F., Pfeil, B.,
1720 Pierrot, D., Poulter, B., Rehder, G., Rödenbeck, C., Saito, S., Schuster, U., Schwinger, J., Séférian, R., Steinhoff,
1721 T., Stocker, B. D., Sutton, A. J., Takahashi, T., Tilbrook, B., van der Laan-Luijkx, I. T., van der Werf, G. R., van
1722 Heuven, S., Vandemark, D., Viovy, N., Wiltshire, A., Zaehle, S., and Zeng, N.: Global Carbon Budget 2015,
1723 *Earth Syst. Sci. Data*, 7, 349–396, <https://doi.org/10.5194/essd-7-349-2015>, 2015.
- 1724
1725 Lerner, P., Romanou, A., Kelley, M., Romanski, J., Ruedy, R., and Russell, G.: Drivers of Air-Sea CO₂ Flux
1726 Seasonality and its Long-Term Changes in the NASA-GISS model CMIP6 submission. *Journal of Advances in*
1727 *Modeling Earth Systems*, 13, e2019MS002028. [Doi:10.1029/2019MS002028](https://doi.org/10.1029/2019MS002028), 2021.
- 1728
1729 Leseurre, C., Lo Monaco, C., Reverdin, G., Metzl, N., Fin, J., Olafsdottir, S., and Racapé, V.: Ocean carbonate
1730 system variability in the North Atlantic Subpolar surface water (1993–2017), *Biogeosciences*, 17, 2553–2577,
1731 <https://doi.org/10.5194/bg-17-2553-2020>, 2020
- 1732
1733 Leseurre, C., Lo Monaco, C., Reverdin, G., Metzl, N., Fin, J., Mignon, C., and Benito, L.: Summer trends and
1734 drivers of sea surface fCO₂ and pH changes observed in the southern Indian Ocean over the last two decades
1735 (1998–2019), *Biogeosciences*, 19, 2599–2625, <https://doi.org/10.5194/bg-19-2599-2022>, 2022.



- 1736
1737 Lherminier, P., Mercier, H., Gourcuff, C., Alvarez, M., Bacon, S., and Kermabon, C.: Transports across the 2002
1738 Greenland-Portugal OVIDE section and comparison with 1997. *J. Geophys. Res.*, 112(C7), C07003,
1739 [doi:10.1029/2006JC003716](https://doi.org/10.1029/2006JC003716). 2007
1740
1741 Li, B. F., Watanabe, Y. W., Hosoda, S., Sato, K., and Nakano, Y.: Quasireal-time and high-resolution
1742 spatiotemporal distribution of ocean anthropogenic CO₂. *Geophysical Research Letters*, 46, 4836–4843.
1743 <https://doi.org/10.1029/2018GL081639>. 2019.
1744
1745 Lo Monaco, C., Álvarez, M., Key, R. M., Lin, X., Tanhua, T., Tilbrook, B., Bakker, D. C. E., van Heuven, S.,
1746 Hoppema, M., Metzl, N., Ríos, A. F., Sabine, C. L., and Velo, A.: Assessing the internal consistency of the
1747 CARINA database in the Indian sector of the Southern Ocean, *Earth Syst. Sci. Data*, 2, 51–70,
1748 <https://doi.org/10.5194/essd-2-51-2010>, 2010.
1749
1750 Lo Monaco, C., Metzl, N., Fin, J., and Tribollet, A.: Sea surface measurements of dissolved inorganic carbon
1751 (DIC) and total alkalinity (TALK), temperature and salinity during the R/V Marion-Dufresne cruise CLIM-
1752 EPARSE (EXPOCODE 35MV20190405) in the Indian Ocean and Mozambique Channel from 2019-04-04 to
1753 2019-04-30. (NCEI Accession 0212218). [indicate subset used]. NOAA National Centers for Environmental
1754 Information. Dataset. <https://doi.org/10.25921/26rw-w185>. Accessed [date]. 2020.
1755
1756 Lo Monaco, C., Metzl, N., Fin, J., Mignon, C., Cuet, P., Douville, E., Gehlen, M., Trang Chau, T.T., and
1757 Tribollet, A.: Distribution and long-term change of the sea surface carbonate system in the Mozambique Channel
1758 (1963-2019), *Deep-Sea Research Part II*, <https://doi.org/10.1016/j.dsr2.2021.104936>, 2021
1759
1760 Lombard, F., Bourdin, G., Pesant, S., Agostini, S., Baudena, A., Boissin, E., Cassar, N., Clampitt, M., Conan,
1761 P., Da Silva, O., Dimier, C., Douville, E., Elineau, A., Fin, J., Flores, J.-M., Ghiglione, J.-F., Hume, B. C. C.,
1762 Jalabert, L., John, S. G., Kelly, R. L., Koren, I., Lin, Y., Marie, D., McMinds, R., Méridet, Z., Metzl, N., Paz-
1763 García, D. A., Luiza Pedrotti, M., Poulain, J., Pujo-Pay, M., Ras, J., Reverdin, G., Romac, S., Röttinger, E.,
1764 Vardi, A., Voolstra, C. R., Moulin, C., Iwankow, G., Banaigs, B., Bowler, C., de Vargas, C., Forcioli, D., Furla,
1765 P., Galand, P. E., Gilson, E., Reynaud, S., Sunagawa, S., Thomas, O., Troublé, R., Vega Thurber, R., Wincker,
1766 P., Zoccola, D., Allemand, D., Planes, S., Boss, E., and Gorsky, G.: Open science resources from the Tara
1767 Pacific expedition across the surface ocean and coral reef ecosystems. *Sci Data* 10, 324 (2023).
1768 <https://doi.org/10.1038/s41597-022-01757-w>, 2022.
1769
1770 Ma, D., Gregor, L., and Gruber, N.: Four decades of trends and drivers of global surface ocean acidification.
1771 *Global Biogeochemical Cycles*, 37, e2023GB007765. [10.1029/2023GB007765](https://doi.org/10.1029/2023GB007765), 2023.
1772
1773 Maier, C., Watremez, P., Taviani, M., Weinbauer, M. G., and Gattuso, J.-P.: Calcification rates and the effect of
1774 ocean acidification on Mediterranean cold-water corals. *Proceedings of the Royal Society B-Biological Sciences*,
1775 279(1734), 1716-1723, [doi:10.1098/rspb.2011.1763](https://doi.org/10.1098/rspb.2011.1763). 2012.
1776
1777 Margirier, F., Testor, P., Heslop, E. et al. : Abrupt warming and salinification of intermediate waters interplays
1778 with decline of deep convection in the Northwestern Mediterranean Sea. *Sci Rep* 10, 20923. [10.1038/s41598-020-77859-5](https://doi.org/10.1038/s41598-020-77859-5), 2020.
1779
1780
1781 Marrec, P., Cariou, T., Collin, E., Durand, A., Latimier, M., Macé, E., Morin, P., Raimund, S., Vernet, M., and
1782 Bozec, Y.: Seasonal and latitudinal variability of the CO₂ system in the western English Channel based on
1783 Voluntary Observing Ship (VOS) measurements. *Marine Chemistry*, 155 (2013): 29–41. 2013.
1784
1785 Marrec, P., Cariou, T., Latimier, M., Macé, E., Morin, P., Vernet, M., and Bozec, Y.: Spatio-temporal dynamics
1786 of biogeochemical processes and air–sea CO₂ fluxes in the Western English Channel based on two years of
1787 FerryBox deployment. *Journal of Marine Systems*, Special Issue: 5th FerryBox Workshop.
1788 [10.1016/j.jmarsys.2014.05.010](https://doi.org/10.1016/j.jmarsys.2014.05.010). 2014.
1789



- 1790 Marrec, P., Cariou, T., Macé, E., Morin, P., Salt, L. A., Vernet, M., Taylor, B., Paxman, K., and Y. Bozec:
1791 Dynamics of air–sea CO₂ fluxes in the northwestern European shelf based on voluntary observing ship and
1792 satellite observations, *Biogeosciences*, 12, 5371–5391, doi:10.5194/bg-12-5371-2015. 2015
1793
1794 Marrec, P., and Bozec, Y.: Partial pressure (or fugacity) of carbon dioxide, dissolved inorganic carbon, alkalinity
1795 and salinity collected from Surface underway observations using Carbon dioxide (CO₂) gas analyzer and other
1796 instruments from ARMORIQUE in the English Channel from 2012-04-25 to 2013-01-03 (NCEI Accession
1797 0157472). Version 1.1. NOAA National Centers for Environmental Information. Dataset. doi:10.3334/CDIAC/OTG.COAST_FERRYBOX_ROSCOFF_PLYMOUTH_2012 [access date]. 2016a.
1798
1799
1800 Marrec, P., and Bozec, Y.: Partial pressure (or fugacity) of carbon dioxide, dissolved inorganic carbon, alkalinity
1801 and salinity collected from Surface underway observations using Carbon dioxide (CO₂) gas analyzer and other
1802 instruments from ARMORIQUE in the English Channel from 2013-03-15 to 2013-12-22 (NCEI Accession
1803 0157444). Version 1.1. NOAA National Centers for Environmental Information. Dataset. doi:10.3334/CDIAC/OTG.COAST_FERRYBOX_ROSCOFF_PLYMOUTH_2013 [access date]. 2016b.
1804
1805
1806 Marrec, P., and Bozec, Y.: Partial pressure (or fugacity) of carbon dioxide, dissolved inorganic carbon, alkalinity
1807 and salinity collected from surface underway observations using Carbon dioxide (CO₂) gas analyzer and other
1808 instruments from ARMORIQUE in the English Channel from 2014-03-18 to 2014-10-09 (NCEI Accession
1809 0163193). Version 1.1. NOAA National Centers for Environmental Information. Dataset. doi:10.3334/CDIAC/OTG.COAST_FERRYBOX_ROSCOFF_PLYMOUTH_2014 [access date]. 2017.
1810
1811
1812 Mazloff, M. R., Verdy, A., Gille, S. T., Johnson, K. S., Cornuelle, B. D., and Sarmiento, J.: Southern Ocean
1813 acidification revealed by biogeochemical-Argo floats. *Journal of Geophysical Research: Oceans*, 128,
1814 e2022JC019530. <https://doi.org/10.1029/2022JC019530>, 2023.
1815
1816 McCulloch, M., Trotter, J., Montagna, P., Falter, J., Dunbar, R., Freiwald, A., Försterra, G., López Correa, M.,
1817 Maier, C., Rüggeberg, A., and Taviani, M.: Resilience of cold-water scleractinian corals to ocean acidification:
1818 Boron isotopic systematics of pH and saturation state up-regulation. *Geochimica et Cosmochimica Acta*, Volume
1819 87, 21–34. <http://dx.doi.org/10.1016/j.gca.2012.03.027>. 2012
1820
1821 McKinley, G. A., Fay, A. R., Takahashi, T., and Metzl, N.: Convergence of atmospheric and North Atlantic
1822 carbon dioxide trends on multidecadal timescales. *Nature Geoscience*. doi:10.1038/NGEO1193. 2011.
1823
1824 McKinley, G. A., Ritzer, A. L. and Lovenduski, N. S.: Mechanisms of northern North Atlantic biomass
1825 variability, *Biogeosciences*, 15(20), 6049–6066, doi:<https://doi.org/10.5194/bg-15-6049-2018>, 2018.
1826
1827 Meier, K. J. S., Beaufort, L., Heussner, S., and Ziveri, P.: The role of ocean acidification in *Emiliania huxleyi*
1828 coccolith thinning in the Mediterranean Sea, *Biogeosciences*, 11, 2857–2869, [https://doi.org/10.5194/bg-11-](https://doi.org/10.5194/bg-11-2857-2014)
1829 2857-2014, 2014.
1830
1831 Mercier, H., Lherminier, P., Sarafanov, A., Gaillard, F., Daniault, N., Desbruyères, D., Falina, A., Ferron, B.,
1832 Huck, T., and Thierry, V.: Variability of the meridional overturning circulation at the Greenland-Portugal Ovide
1833 section from 1993 to 2010. *Progress in Oceanography*, 132, 250–261, doi:10.1016/j.pocean.2013.11.001. 2015
1834
1835 Merlivat, L., Boutin, J., Antoine, D., Beaumont, L., Golbol, M., and Vellucci, V.: Increase of dissolved inorganic
1836 carbon and decrease in pH in near-surface waters in the Mediterranean Sea during the past two decades,
1837 *Biogeosciences*, 15, 5653–5662, <https://doi.org/10.5194/bg-15-5653-2018>, 2018.
1838
1839 Metzl, N., Brunet, C., Jabaud-Jan, A., Poisson, A., and Schauer, B.: Summer and winter air–sea CO₂ fluxes in
1840 the Southern Ocean *Deep Sea Res I*, 53, 1548–1563, doi:10.1016/j.dsr.2006.07.006. 2006.
1841



- 1842 Metzl, N., Tilbrook, B., Bakker, D., Le Quééré, C., Doney, S., Feely, R., Hood M., and Dargaville, R.: Global
1843 Changes in Ocean Carbon: Variability and Vulnerability. *Eos, Transactions of the American Geophysical Union*
1844 88 (28): 286-287. doi: 10.1029/2007EO280005, 2007.
- 1845
1846 Metzl, N., Corbière, A., Reverdin, G., Lenton, A., Takahashi, T., Olsen, A., Johannessen, T., Pierrot, D.,
1847 Wanninkhof, R., Ólafsdóttir, S. R., Ólafsson, J., and Ramonet, M.: Recent acceleration of the sea surface fCO₂
1848 growth rate in the North Atlantic subpolar gyre (1993-2008) revealed by winter observations, *Global*
1849 *Biogeochem. Cycles*, 24, GB4004, doi:10.1029/2009GB003658, 2010.
- 1850
1851 Metzl, N., and Lo Monaco, C.: OISO - OCÉAN INDIEN SERVICE D'OBSERVATION,
1852 <https://doi.org/10.18142/228>, 1998.
- 1853
1854 Metzl, N., Pierre, C., and Vangriesheim, A.: Hydrographic and Chemical measurements during the R/V
1855 L'Atalante BIOZAIRE III Cruise in the Atlantic Ocean (14 December, 2003 - 7 January 2004).
1856 <http://cdiac.esd.ornl.gov/ftp/oceans/BIOZAIRE3>. Carbon Dioxide Information Analysis Center, Oak Ridge
1857 National Laboratory, US Department of Energy, Oak Ridge, Tennessee. doi:
1858 10.3334/CDIAC/OTG.BIOZAIRE3, 2016.
- 1859
1860 Metzl, N., Ferron, B. Lherminier, P. Sarthou, G. Thierry, V.: Discrete profile measurements of dissolved
1861 inorganic carbon (DIC), total alkalinity (TALK), temperature and salinity during the multiple ships Observatoire
1862 de la variabilité interannuelle et décennale en Atlantique Nord (OVIDE) project, OVIDE-2006, OVIDE-2008,
1863 OVIDE-2010, OVIDE-2012, OVIDE-2014 cruises in the North Atlantic Ocean from 2006-05-23 to 2014-06-30
1864 (NCEI Accession 0177219). Version 1.1. NOAA National Centers for Environmental Information. Dataset.
1865 doi:10.25921/v0qt-ms48 [access date], 2018.
- 1866
1867 Metzl, N., Fin, J., Lo Monaco, C., et al.: SNAPO-CO₂ data-set: A synthesis of total alkalinity and total dissolved
1868 inorganic carbon observations in the global ocean (1993-2022). *SEANOE*. <https://doi.org/10.17882/95414>, 2023.
- 1869
1870 Mignot, A., Claustre, H., Cossarini, G., D'Ortenzio, F., Gutknecht, E., Lamouroux, J., Lazzari, P., Perruche, C.,
1871 Salon, S., Sauzède, R., Taillandier, V., and Teruzzi, A.: Using machine learning and Biogeochemical-Argo
1872 (BGC-Argo) floats to assess biogeochemical models and optimize observing system design, *Biogeosciences*, 20,
1873 1405–1422, <https://doi.org/10.5194/bg-20-1405-2023>, 2023.
- 1874
1875 Millero, F. J., Lee, K. and Roche, M.: Distribution of alkalinity in the surface waters of the major oceans. *Mar.*
1876 *Chem.* **60**, 111–130. [https://doi.org/10.1016/S0304-4203\(97\)00084-4](https://doi.org/10.1016/S0304-4203(97)00084-4), 1998.
- 1877
1878 Mongwe, N. P., Vichi, M., and Monteiro, P. M. S: The seasonal cycle of pCO₂ and CO₂ fluxes in the Southern
1879 Ocean: Diagnosing anomalies in CMIP5 earth system models. *Biogeosciences*, 15(9), 2851–2872.
1880 <https://doi.org/10.5194/bg-15-2851-2018>, 2018.
- 1881
1882 Mortier, L., Ait Ameer, N., and Taillandier, V.: SOMBA-GE-2014 cruise, RV Téthys II,
1883 <https://doi.org/10.17600/14007500>, 2014.
- 1884
1885 Moutin, T., and Bonnet, S.: OUTPACE cruise, RV L'Atalante, <https://doi.org/10.17600/15000900>, 2015.
- 1886
1887 Moutin, T., Wagener, T., Caffin, M., Fumenia, A., Gimenez, A., Baklouti, M., Bouruet-Aubertot, P., Pujo-Pay,
1888 M., Leblanc, K., Lefevre, D., Helias Nunige, S., Leblond, N., Grosso, O., and de Verneil, A.: Nutrient
1889 availability and the ultimate control of the biological carbon pump in the western tropical South Pacific Ocean,
1890 *Biogeosciences*, 15, 2961-2989, <https://doi.org/10.5194/bg-15-2961-2018>, 2018.
- 1891
1892 Newton, J.A., Feely, R. A., Jewett, E. B., Williamson, P. and Mathis, J.: Global Ocean Acidification Observing
1893 Network: Requirements and Governance Plan. Second Edition, GOA-ON, http://www.goa-on.org/docs/GOA-ON_plan_print.pdf, 2015.
- 1894



- 1895 Nykjaer, L.: Mediterranean Sea surface warming 1985–2006. *Clim. Res.* 39, 11–17. doi: 10.3354/cr00794, 2009.
- 1896
- 1897 Obnerosterer, I.: MOBYDICK-THEMISTO cruise, RV Marion-Dufresne, <https://doi.org/10.17600/18000403>, 2018.
- 1898
- 1899
- 1900 OCADS: Coastal Carbon Data, https://www.ncei.noaa.gov/access/ocean-carbon-acidification-data-system/oceans/coastal_carbon_data.html, 2023
- 1901
- 1902
- 1903 Olafsson, J., Olafsdottir, S.R., Benoit-Cattin, A., Danielsen, M., Arnarson, T.S., and Takahashi, T.: Rate of
- 1904 Iceland Sea acidification from time series measurements. *Biogeosciences* 6, 2661–2668.
- 1905 <https://doi.org/10.5194/bg-6-2661-2009>, 2009.
- 1906
- 1907 Olivier, L., Boutin, J., Reverdin, G., Lefèvre, N., Landschützer, P., Speich, S., Karstensen, J., Labaste, M.,
- 1908 Noisel, C., Ritschel, M., Steinhoff, T., and Wanninkhof, R.: Wintertime process study of the North Brazil
- 1909 Current rings reveals the region as a larger sink for CO₂ than expected, *Biogeosciences*, 19, 2969–2988,
- 1910 <https://doi.org/10.5194/bg-19-2969-2022>, 2022.
- 1911
- 1912 Olsen, A., Key, R. M., van Heuven, S., Lauvset, S. K., Velo, A., Lin, X., Schirnack, C., Kozyr, A., Tanhua, T.,
- 1913 Hoppema, M., Jutterström, S., Steinfeldt, R., Jeansson, E., Ishii, M., Pérez, F. F., and Suzuki, T.: The Global
- 1914 Ocean Data Analysis Project version 2 (GLODAPv2) – an internally consistent data product for the world ocean,
- 1915 *Earth Syst. Sci. Data*, 8, 297–323, <https://doi.org/10.5194/essd-8-297-2016>, 2016.
- 1916
- 1917 Olsen, A., Lange, N., Key, R. M., Tanhua, T., Álvarez, M., Becker, S., Bittig, H. C., Carter, B. R., Cotrim da
- 1918 Cunha, L., Feely, R. A., van Heuven, S., Hoppema, M., Ishii, M., Jeansson, E., Jones, S. D., Jutterström, S.,
- 1919 Karlsen, M. K., Kozyr, A., Lauvset, S. K., Lo Monaco, C., Murata, A., Pérez, F. F., Pfeil, B., Schirnack, C.,
- 1920 Steinfeldt, R., Suzuki, T., Telszewski, M., Tilbrook, B., Velo, A., and Wanninkhof, R.: GLODAPv2.2019 – an
- 1921 update of GLODAPv2, *Earth Syst. Sci. Data*, 11, 1437–1461, <https://doi.org/10.5194/essd-11-1437-2019>, 2019.
- 1922
- 1923 Olsen, A., Lange, N., Key, R. M., Tanhua, T., Bittig, H. C., Kozyr, A., Álvarez, M., Azetsu-Scott, K., Becker, S.,
- 1924 Brown, P. J., Carter, B. R., Cotrim da Cunha, L., Feely, R. A., van Heuven, S., Hoppema, M., Ishii, M.,
- 1925 Jeansson, E., Jutterström, S., Landa, C. S., Lauvset, S. K., Michaelis, P., Murata, A., Pérez, F. F., Pfeil, B.,
- 1926 Schirnack, C., Steinfeldt, R., Suzuki, T., Tilbrook, B., Velo, A., Wanninkhof, R., and Woosley, R. J.: An updated
- 1927 version of the global interior ocean biogeochemical data product, GLODAPv2.2020, *Earth Syst. Sci. Data*, 12,
- 1928 3653–3678, <https://doi.org/10.5194/essd-12-3653-2020>, 2020.
- 1929
- 1930 Orr, J. C., Epitalon, J.-M., and Gattuso, J.-P.: Comparison of ten packages that compute ocean carbonate
- 1931 chemistry, *Biogeosciences*, 12(5), 1483–1510, doi:10.5194/bg-12-1483-2015, 2015.
- 1932
- 1933 Parard, G., Lefèvre, N., and Boutin, J.: Sea water fugacity of CO₂ at the PIRATA mooring at 6°S, 10°W. *Tellus-*
- 1934 *B*, DOI: 10.1111/j.1600-0889.2010.00503.x. 2010.
- 1935
- 1936 Pérez F. F., Vázquez-Rodríguez, M., Mercier, H., Velo, A., Lherminier, P. and Ríos, A. F.: Trends of
- 1937 anthropogenic CO₂ storage in North Atlantic water masses. *Biogeosciences*, 7, 1789–1807, doi:10.5194/bg-7-
- 1938 [1789-2010](https://doi.org/10.5194/bg-7-1789-2010), 2010.
- 1939
- 1940 Pérez, F. F., Mercier, H., Vazquez-Rodriguez, M., Lherminier, P., Velo, A., Pardo, P., Roson, G., and Rios, A.:
- 1941 Reconciling air-sea CO₂ fluxes and anthropogenic CO₂ budgets in a changing North Atlantic. *Nature*
- 1942 *Geosciences*, 6, 146–152, doi:10.1038/ngeo1680, 2013.
- 1943
- 1944 Pérez, F., Fontela, M., García-Ibáñez, M. et al. : Meridional overturning circulation conveys fast acidification to
- 1945 the deep Atlantic Ocean. *Nature* 554, 515–518. Doi: 10.1038/nature25493, 2018.
- 1946
- 1947 Pesant, S., Not, F., Picheral, M., Kandels-Lewis, S., Le Bescot, N., Gorsky, G., Iudicone, D., Karsenti, E.,
- 1948 Speich, S., Troublé, R., Dimier, C., Searson, S., and Tara Oceans Consortium Coordinators: Open science



- 1949 resources for the discovery and analysis of Tara Oceans data. *Scientific Data* 2:150023. doi:
1950 10.1038/sdata.2015.23, 2015.
1951
1952 Petrenko, A.: LATEX10 cruise, RV Téthys II, <https://doi.org/10.17600/10450150>, 2010.
1953
1954 Petrenko, A.A., Doglioli, A.M., Nencioli, F., Kersalé, M., Hu, Z., and d'Ovidio, F.: A review of the LATEX
1955 project: mesoscale to submesoscale processes in a coastal environment. *Ocean Dynam.*, doi: 10.1007/s10236-
1956 017-1040-9, 2017.
1957
1958 Petton, S., Pouvreau, S., and Fleury, E.: ECOSCOPA network : high frequency environmental database.
1959 SEANOE. <https://doi.org/10.17882/86131>, 2023.
1960
1961 Pfeil, B., Olsen, A., Bakker, D. C. E., Hankin, S., Koyuk, H., Kozyr, A., Malczyk, J., Manke, A., Metzl, N.,
1962 Sabine, C. L., Akl, J., Alin, S. R., Bates, N., Bellerby, R. G. J., Borges, A., Boutin, J., Brown, P. J., Cai, W.-J.,
1963 Chavez, F. P., Chen, A., Cosca, C., Fassbender, A. J., Feely, R. A., González-Dávila, M., Goyet, C., Hales,
1964 B., Hardman-Mountford, N., Heinze, C., Hood, M., Hoppema, M., Hunt, C. W., Hydes, D., Ishii, M.,
1965 Johannessen, T., Jones, S. D., Key, R. M., Körtzinger, A., Landschützer, P., Lauvset, S. K., Lefèvre, N.,
1966 Lenton, A., Laurantou, A., Merlivat, L., Midorikawa, T., Mintrop, L., Miyazaki, C., Murata, A., Nakadate, A.,
1967 Nakano, Y., Nakaoka, S., Nojiri, Y., Omar, A. M., Padin, X. A., Park, G.-H., Paterson, K., Perez, F. F., Pierrot,
1968 D., Poisson, A., Ríos, A. F., Santana-Casiano, J. M., Salisbury, J., Sarma, V. V. S. S., Schlitzer, R.,
1969 Schneider, B., Schuster, U., Sieger, R., Skjelvan, I., Steinhoff, T., Suzuki, T., Takahashi, T., Tedesco, K.,
1970 Telszewski, M., Thomas, H., Tilbrook, B., Tjiputra, J., Vandemark, D., Veness, T., Wanninkhof, R., Watson,
1971 A. J., Weiss, R., Wong, C. S., and Yoshikawa-Inoue, H.: A uniform, quality controlled Surface Ocean CO₂
1972 Atlas (SOCAT), *Earth Syst. Sci. Data*, 5, 125-143, doi:10.5194/essd-5-125-2013, 2013.
1973
1974 Picheral, M., Searson, S., Taillandier, V., Bricaud, A., Boss, E., Ras, J., Claustre, H., Ouhssain, M., Morin, P.,
1975 Coppola, L., Gattuso, J.-P., Metzl, N., Thuillier, D., Gorsky, G., Tara Oceans Consortium, Coordinators; Tara
1976 Oceans Expedition, Participants: Vertical profiles of environmental parameters measured on discrete water
1977 samples collected with Niskin bottles during the Tara Oceans expedition 2009-2013.
1978 doi:10.1594/PANGAEA.836319, 2014.
1979
1980 Pilcher, D. J., Brody, S. R., Johnson, L., and Bronselaer, B.: Assessing the abilities of CMIP5 models to
1981 represent the seasonal cycle of surface ocean pCO₂, *J. Geophys. Res. Oceans*, 120, 4625–4637,
1982 doi:10.1002/2015JC010759, 2015.
1983
1984 Poisson, A., Culkin, F., and Ridout, P.: Intercomparison of CO₂ measurements. *Deep Sea Research Part A.*
1985 *Oceanographic Research Papers*, 37, 10, 1647-1650, [https://doi.org/10.1016/0198-0149\(90\)90067-6](https://doi.org/10.1016/0198-0149(90)90067-6), 1990.
1986
1987 Pujo-Pay, M., Durrieu de Madron, X., and Conan, P.: PERLE3 cruise, RV Pourquoi pas ?,
1988 <https://doi.org/10.17600/18001342>, 2020.
1989
1990 Pujo-Pay, M., Durrieu de Madron, X., and Conan, P.: PERLE4 cruise, RV L'Atalante,
1991 <https://doi.org/10.17600/18001980>, 2021.
1992
1993 Rabouille C.: AMOR-BFLUX cruise, RV Téthys II, <https://doi.org/10.17600/15008700>, 2015.
1994
1995 Racapé, V., Metzl, N., Pierre, C., Reverdin, G., Quay, P.D., and Olafsdottir, S. R.: The seasonal cycle of the
1996 d13C_{DIC} in the North Atlantic Subpolar Gyre. *Biogeosciences*, 11, 6, 1683-1692, doi:10.5194/bg-11-1683-2014,
1997 2014.
1998
1999 Revelle, R., and Suess, H. E.: Carbon dioxide exchange between atmosphere and ocean and the question of an
2000 increase of atmospheric CO₂ during the past decades. *Tellus* 9, 18–27. doi:10.1111/j.2153-
2001 3490.1957.tb01849.x., 1957.
2002



- 2003 Reverdin, G.: STRASSE cruise, RV Thalassa, <https://doi.org/10.17600/12040060>, 2012.
- 2004
- 2005 Reverdin, G., Metzl, N., Olafsdottir, S., Racapé, V., Takahashi, T., Benetti, M., Valdimarsson, H., Benoit-Cattin,
- 2006 A., Danielsen, M., Fin, J., Naamar, A., Pierrot, D., Sullivan, K., Bringas, F., and Goni, G.: SURATLANT: a
- 2007 1993–2017 surface sampling in the central part of the North Atlantic subpolar gyre, *Earth Syst. Sci. Data*, 10,
- 2008 1901-1924, <https://doi.org/10.5194/essd-10-1901-2018>, 2018.
- 2009
- 2010 Reverdin, G., Metzl, N., Olafsdottir, S., Racapé, V., Takahashi, T., Benetti, M., Valdimarsson, H., Quay, P. D.,
- 2011 Benoit-Cattin, A., Danielsen, M., Fin, J., Naamar, A., Pierrot, D., Sullivan, K., Bringas, F., and Goni, G.:
- 2012 SURATLANT: a surface dataset in the central part of the North Atlantic subpolar gyre. *SEANOE*.
- 2013 <https://doi.org/10.17882/54517>, 2022.
- 2014
- 2015 Ridame, C., Dekaezemacker, J., Guieu, C., Bonnet, S., L'Helguen, S., and Malien, F.: Contrasted Saharan dust
- 2016 events in LNLC environments: impact on nutrient dynamics and primary production, *Biogeosciences*, 11, 4783–
- 2017 4800, <https://doi.org/10.5194/bg-11-4783-2014>, 2014.
- 2018
- 2019 Robertson, J. E., Robinson, C., Turner, D. R., Holligan, P., Watson, A. J., Boyd, P., Fernandez, E., and Finch,
- 2020 M.: The impact of a coccolithophore bloom on oceanic carbon uptake in the northeast Atlantic during summer
- 2021 1991, *Deep Sea Res., Part I*, 41(2), 297–314, 1994.
- 2022
- 2023 Rödenbeck, C., Keeling, R. F., Bakker, D. C. E., Metzl, N., Olsen, A., Sabine, C., and Heimann, M.: Global
- 2024 surface-ocean pCO₂ and sea–air CO₂ flux variability from an observation-driven ocean mixed-layer scheme,
- 2025 *Ocean Sci.*, 9, 193–216, <https://doi.org/10.5194/os-9-193-2013>, 2013.
- 2026
- 2027 Rödenbeck, C., Bakker, D. C. E., Gruber, N., Iida, Y., Jacobson, A.R., Jones, S., Landschützer, P., Metzl, N.,
- 2028 Nakaoka, S., Olsen, A., Park, G.-H., Peylin, P., Rodgers, K. B., Sasse, T. P., Schuster, U., Shutler, J. D., Valsala,
- 2029 V., Wanninkhof, R., Zeng, J. Data-based estimates of the ocean carbon sink variability – First results of the
- 2030 Surface Ocean pCO₂ Mapping intercomparison (SOCOM). *Biogeosciences* 12: 7251-7278. doi:10.5194/bg-12-
- 2031 7251-2015, 2015.
- 2032
- 2033 Sabine, C. L., Feely, R. A., Gruber, N., Key, R. M., Lee, K., Bullister, J. L., Wanninkhof, R., Wong, C. S.,
- 2034 Wallace, D. W. R., Tilbrook, B., Millero, F. J., Peng, T.-H., Kozyr, A., Ono, T., and Rios, A. F.: The Oceanic
- 2035 Sink for Anthropogenic CO₂, *Science*, 305, 367-371, <https://doi.org/10.1126/science.1097403>, 2004.
- 2036
- 2037 Sabine, C. L., Hankin, S., Koyuk, H., Bakker, D. C. E., Pfeil, B., Olsen, A., Metzl, N., Kozyr, A., Fassbender,
- 2038 A., Manke, A., Malczyk, J., Akl, J., Alin, S. R., Bellerby, R. G. J., Borges, A., Boutin, J., Brown, P. J., Cai, W.-
- 2039 J., Chavez, F. P., Chen, A., Cosca, C., Feely, R.A., González-Dávila, M., Goyet, C., Hardman-Mountford, N.,
- 2040 Heinze, C., Hoppema, M., Hunt, C. W., Hydes, D., Ishii, M., Johannessen, T., Key, R. M., Körtzinger, A.,
- 2041 Landschützer, P., Lauvset, S. K., Lefèvre, N., Lenton, A., Lourantou, A., Merlivat, L., Midorikawa, T.,
- 2042 Mintrop, L., Miyazaki, C., Murata, A., Nakadate, A., Nakano, Y., Nakaoka, S., Nojiri, Y., Omar, A. M., Padin,
- 2043 X. A., Park, G.-H., Paterson, K., Perez, F. F., Pierrot, D., Poisson, A., Ríos, A. F., Salisbury, J., Santana-
- 2044 Casiano, J. M., Sarma, V. V. S. S., Schlitzer, R., Schneider, B., Schuster, U., Sieger, R., Skjelvan, I., Steinhoff,
- 2045 T., Suzuki, T., Takahashi, T., Tedesco, K., Telszewski, M., Thomas, H., Tilbrook, B., Vandemark, D., Veness,
- 2046 T., Watson, A. J., Weiss, R., Wong, C. S., and Yoshikawa-Inoue, H.: Surface Ocean CO₂ Atlas (SOCAT)
- 2047 gridded data products, *Earth Syst. Sci. Data*, 5, 145-153, doi:10.5194/essd-5-145-2013, 2013.
- 2048
- 2049 Salt, L. A., Beaumont, L., Blain, S., Bucciarelli, E., Grosstefan, E., Guillot, A., L'Helguen, S., Merlivat, L.,
- 2050 Répécaud, M., Quémener, L., Rimmelin-Maury, P., Tréguer, P., and Bozec, Y.: The annual and seasonal
- 2051 variability of the carbonate system in the Bay of Brest (Northwest Atlantic Shelf, 2008–2014). *Marine*
- 2052 *Chemistry*, doi:10.1016/j.marchem.2016.09.003. 2016.
- 2053
- 2054 Sasse, T. P., McNeil, B. I., and Abramowitz, G.: A novel method for diagnosing seasonal to inter-annual surface
- 2055 ocean carbon dynamics from bottle data using neural networks, *Biogeosciences*, 10, 4319–4340,
- 2056 <https://doi.org/10.5194/bg-10-4319-2013>, 2013.



- 2057
2058 Sauzède, R., Claustre, H., Pasqueron de Fommervault, O., Bittig, H., Gattuso, J.-P., Legendre, L. and Johnson,
2059 K. S.: Estimates of water-column nutrients and carbonate system parameters in the global ocean: A novel
2060 approach based on neural networks. *Front. Mar. Sci.* 4:128. doi:10.3389/fmars.2017.00128, 2017.
2061
2062 Seelmann, K., Steinhoff, T., Aßmann, S., and Körtzinger, A.: Enhance Ocean Carbon Observations: Successful
2063 Implementation of a Novel Autonomous Total Alkalinity Analyzer on a Ship of Opportunity. *Front. Mar. Sci.*
2064 7:571301. doi: 10.3389/fmars.2020.571301, 2020.
2065
2066 Schlitzer, R.: Ocean Data View, Ocean Data View, <http://odv.awi.de> (last access: 13 March 2019), 2018.
2067
2068 Schneider, A., Wallace, D. W. R., and Körtzinger, A.: Alkalinity of the Mediterranean Sea, *Geophys. Res. Lett.*,
2069 34, L15608, doi:10.1029/2006GL028842, 2007.
2070
2071 Schuster, U., Watson, A.J., Bates, N., Corbière, A., Gonzalez-Davila, M., Metzl, N., Pierrot, D. and Santana-
2072 Casiano, M.: Trends in North Atlantic sea surface pCO₂ from 1990 to 2006. *Deep-Sea Res II*,
2073 doi:10.1016/j.dsr2.2008.12.011, 2009.
2074
2075 Schuster, U., McKinley, G. A., Bates, N., Chevallier, F., Doney, S. C., Fay, A. R., González-Dávila, M., Gruber,
2076 N., Jones, S., Krijnen, J., Landschützer, P., Lefèvre, N., Manizza, M., Mathis, J., Metzl, N., Olsen, A., Rios, A.
2077 F., Rödenbeck, C., Santana-Casiano, J. M., Takahashi, T., Wanninkhof, R., and Watson, A. J.: An assessment of
2078 the Atlantic and Arctic sea-air CO₂ fluxes, 1990–2009, *Biogeosciences*, 10, 607–627,
2079 <https://doi.org/10.5194/bg-10-607-2013>, 2013.
2080
2081 Sims, R. P., Holding, T. M., Land, P. E., Piolle, J.-F., Green, H. L., and Shutler, J. D.: OceanSODA-UNEXE: a
2082 multi-year gridded Amazon and Congo River outflow surface ocean carbonate system dataset, *Earth Syst. Sci.*
2083 *Data*, 15, 2499–2516, <https://doi.org/10.5194/essd-15-2499-2023>, 2023.
2084
2085 Skjelvan, I., Lauvset, S.K., Johannessen, T., et al.: Decadal trends in Ocean Acidification from the Ocean
2086 Weather Station M in the Norwegian Sea, *Journal of Marine Systems*,
2087 <https://doi.org/10.1016/j.jmarsys.2022.103775>, 2022.
2088
2089 Speich, S., and The Embarked Science Team: EUREC4A-OA. Cruise Report. 19 January – 19 February 2020.
2090 Vessel: L'ATALANTE. <https://doi.org/10.13155/80129>, 2021
2091
2092 Takahashi, T., Sutherland, S. C., Sweeney, C., Poisson, A., Metzl, N., Tilbrook, B., Bates, N., Wanninkhof, R.,
2093 Feely, R. A., Sabine, C., Olafsson, J., and Nojiri, Y.: Global Sea-Air CO₂ Flux Based on Climatological Surface
2094 Ocean pCO₂, and Seasonal Biological and Temperature Effect. *Deep-Sea Res. II*, 49, 9-10, 1601-1622,
2095 [https://doi.org/10.1016/S0967-0645\(02\)00003-6](https://doi.org/10.1016/S0967-0645(02)00003-6). 2002
2096
2097 Takahashi, T., Sutherland, S. C., Wanninkhof, R., Sweeney, C., Feely, R. A., Chipman, D. W., Hales, B.,
2098 Friederich, G., Chavez, F., Sabine, C., Watson, A. J., Bakker, D. C., Schuster, U., Metzl, N., Yoshikawa-Inoue,
2099 H., Ishii, M., Midorikawa, T., Nojiri, Y., Körtzinger, A., Steinhoff, T., Hoppema, M., Olafsson, J., Arnarson, T.
2100 S., Tilbrook, B., Johannessen, T., Olsen, A., Bellerby, R., Wong, C., Delille, B., Bates, N., and de Baar, H. J.:
2101 Climatological mean and decadal change in surface ocean pCO₂, and net sea air CO₂ flux over the global
2102 oceans. *Deep-Sea Res. II*, 56 (8-10), 554–577, <http://dx.doi.org/10.1016/j.dsr2.2008.12.009>. 2009.
2103
2104 Takahashi, T., Sutherland, S. C., Chipman, D. W., Goddard, J. G., Ho, C., Newberger, T., Sweeney, C. and
2105 Munro, D. R.: Climatological distributions of pH, pCO₂, total CO₂, alkalinity, and CaCO₃ saturation in the
2106 global surface ocean, and temporal changes at selected locations. *Marine Chemistry*, 164, 95–125,
2107 doi:10.1016/j.marchem.2014.06.004. 2014.
2108
2109 Tanhua, T., Pouliquen, S., Hausman, J., O'Brien, K., Bricher, P., de Bruin, T., Buck, J. J. H., Burger, E. F.,
2110 Carval, T., Casey, K. S., Diggs, S., Giorgetti, A., Glaves, H., Harscoat, V., Kinkade, D., Muelbert, J. H.,



- 2111 Novellino, A., Pfeil, B., Pulsifer, P. L., Van de Putte, A., Robinson, E., Schaap, D., Smirnov, A., Smith, N.,
2112 Snowden, D., Spears, T., Stall, S., Tacoma, M., Thijsse, P., Tronstad, S., Vandenberghe, T., Wengren, M.,
2113 Wyborn, L. and Zhao, Z.: Ocean FAIR Data Services. *Front. Mar. Sci.* 6:440. doi: 10.3389/fmars.2019.00440,
2114 2019.
2115
2116 Tanhua, T., Lauvset, S.K., Lange, N. et al.: A vision for FAIR ocean data products. *Commun Earth Environ* 2,
2117 136. <https://doi.org/10.1038/s43247-021-00209-4>, 2021
2118
2119 Testor, P., Bosse, A., and Coppola, L.: MOOSE-GE, <https://doi.org/10.18142/235>, 2010.
2120
2121 Testor, P.: DEWEX-MERMEX 2013 LEG1 cruise, RV Le Suroît, <https://doi.org/10.17600/13020010>, 2013.
2122
2123 Tilbrook, B., Jewett, E. B., DeGrandpre, M. D., Hernandez-Ayon, J. M., Feely, R. A., Gledhill, D. K., Hansson,
2124 L., Isensee, K., Kurz, M. L., Newton, J. A., Siedlecki, S. A., Chai, F., Dupont, S., Graco, M., Calvo, E., Greeley,
2125 D., Kapsenberg, L., Lebec, M., Pelejero, C., Schoo, K. L., and Telszewski, M.: An Enhanced Ocean
2126 Acidification Observing Network: From People to Technology to Data Synthesis and Information Exchange.
2127 *Frontiers in Marine Science*, 6, 337, DOI:10.3389/fmars.2019.00337, 2019.
2128
2129 Touratier, F., Azouzi, L. and Goyet, C.: CFC-11, $\Delta 14C$ and 3H tracers as a means to assess anthropogenic CO₂
2130 concentrations in the ocean. *Tellus B*, 59(2), 318–325, doi:10.1111/j.1600-0889.2006.00247.x, 2007.
2131
2132 Touratier, F., and Goyet, C.: Decadal evolution of anthropogenic CO₂ in the north western Mediterranean Sea
2133 from the mid-1990's to the mid-2000's. *Deep Sea Research Part I*.doi:10.1016/j.dsr.2009.05.015, 2009.
2134
2135 Touratier, F., Goyet, C., Houpert, L., Durrieu de Madron, X., Lefèvre, D., Stabholz, M., and Guglielmi, V.: Role
2136 of deep convection on anthropogenic CO₂ sequestration in the Gulf of Lions (northwestern Mediterranean Sea).
2137 *Deep-Sea Research Part I*. doi.org/10.1016/j.dsr.2016.04.003, 2016.
2138
2139 Turk, D., Dowd, M., Lauvset, S. K., Koelling, J., Alonso-Pérez, F. and Pérez, F. F.: Can Empirical Algorithms
2140 Successfully Estimate Aragonite Saturation State in the Subpolar North Atlantic? *Front. Mar. Sci.* 4:385. doi:
2141 10.3389/fmars.2017.00385, 2017.
2142
2143 Ulses, C., Estournel, C., Marsaleix, P., Soetaert, K., Fourier, M., Coppola, L., Lefèvre, D., Touratier, F., Goyet,
2144 C., Guglielmi, V., Kessouri, F., Testor, P., and Durrieu de Madron, X.: Seasonal dynamics and annual budget of
2145 dissolved inorganic carbon in the northwestern Mediterranean deep convection region, *Biogeosciences Discuss.*
2146 [preprint], <https://doi.org/10.5194/bg-2022-219>, in review, 2022.
2147
2148 UNESCO: Intercomparison of total alkalinity and total inorganic carbon determinations in seawater. UNESCO
2149 Tech. Pap. Mar. Sci. 59., 1990
2150
2151 UNESCO: Reference materials for oceanic carbon dioxide measurements. UNESCO Tech. Pap. Mar. Sci. 60.,
2152 1991
2153
2154 United Nations. The Sustainable Development Goals 2020, 68pp. <https://unstats.un.org/sdgs/report/2020/>, 2020
2155
2156 Vangriesheim A., Pierre, C., Aminot, A., Metzl, N., Baurand, F., and Caprais, J.-C.: The influence of Congo
2157 river discharges in the surface and deep layers of the Gulf of Guinea. *Deep-Sea Res. II*, doi:
2158 10.1016/j.dsr2.2009.04.002, 2009.
2159
2160 Vazquez-Rodriguez, M., Perez, F., Velo, A., Rios, A., and Mercier, H.: Observed acidification trends in the
2161 North Atlantic water masses. *Biogeosciences*, 9, 5217-5230, doi:10.5194/bg-9-5217-2012, 2012.
2162
2163 Velo, A., Perez, F. F., Brown, P., Tanhua, T., Schuster, U., and Key, R. M.: CARINA alkalinity data in the
2164 Atlantic Ocean, *Earth Syst. Sci. Data*, 1, 45–61, <https://doi.org/10.5194/essd-1-45-2009>, 2009.



- 2165
2166 von Schuckmann, K., Cheng, L., Palmer, M. D., Hansen, J., Tassone, C., Aich, V., Adusumilli, S., Beltrami, H.,
2167 Boyer, T., Cuesta-Valero, F. J., Desbruyères, D., Domingues, C., García-García, A., Gentine, P., Gilson, J.,
2168 Gorfer, M., Haimberger, L., Ishii, M., Johnson, G. C., Killick, R., King, B. A., Kirchengast, G., Kolodziejczyk,
2169 N., Lyman, J., Marzeion, B., Mayer, M., Monier, M., Monselesan, D. P., Purkey, S., Roemmich, D., Schweiger,
2170 A., Seneviratne, S. I., Shepherd, A., Slater, D. A., Steiner, A. K., Straneo, F., Timmermans, M.-L., and Wijffels,
2171 S. E.: Heat stored in the Earth system: where does the energy go?, *Earth Syst. Sci. Data*, 12, 2013–2041,
2172 <https://doi.org/10.5194/essd-12-2013-2020>, 2020.
2173
2174 von Schuckmann, K., Minière, A., Gues, F., Cuesta-Valero, F. J., Kirchengast, G., Adusumilli, S., Straneo, F.,
2175 Ablain, M., Allan, R. P., Barker, P. M., Beltrami, H., Blazquez, A., Boyer, T., Cheng, L., Church, J.,
2176 Desbruyeres, D., Dolman, H., Domingues, C. M., García-García, A., Giglio, D., Gilson, J. E., Gorfer, M.,
2177 Haimberger, L., Hakuba, M. Z., Hendricks, S., Hosoda, S., Johnson, G. C., Killick, R., King, B., Kolodziejczyk,
2178 N., Korosov, A., Krinner, G., Kuusela, M., Landerer, F. W., Langer, M., Lavergne, T., Lawrence, I., Li, Y.,
2179 Lyman, J., Marti, F., Marzeion, B., Mayer, M., MacDougall, A. H., McDougall, T., Monselesan, D. P., Nitzbon,
2180 J., Otosaka, I., Peng, J., Purkey, S., Roemmich, D., Sato, K., Sato, K., Savita, A., Schweiger, A., Shepherd, A.,
2181 Seneviratne, S. I., Simons, L., Slater, D. A., Slater, T., Steiner, A. K., Suga, T., Szekely, T., Thiery, W.,
2182 Timmermans, M.-L., Vanderkelen, I., Wijffels, S. E., Wu, T., and Zemp, M.: Heat stored in the Earth system
2183 1960–2020: where does the energy go?, *Earth Syst. Sci. Data*, 15, 1675–1709, [https://doi.org/10.5194/essd-15-](https://doi.org/10.5194/essd-15-1675-2023)
2184 [1675-2023](https://doi.org/10.5194/essd-15-1675-2023), 2023.
2185
2186 Wagener, T., Metzl, N., Caffin, M., Fin, J., Helias Nunige, S., Lefevre, D., Lo Monaco, C., Rougier, G., and
2187 Moutin, T.: Carbonate system distribution, anthropogenic carbon and acidification in the western tropical South
2188 Pacific (OUTPACE 2015 transect), *Biogeosciences*, 15, 5221–5236, <https://doi.org/10.5194/bg-15-5221-2018>,
2189 2018a.
2190
2191 Wagener, T., Metzl, N., Caffin, M., Fin, J., Helias Nunige, S., Lefevre, D., Lo Monaco, C., Rougier, G., and
2192 Moutin, T.: Discrete profile measurements of dissolved inorganic carbon (DIC), total alkalinity (TALK),
2193 temperature, salinity and other parameters during the R/V L'Atalante "Oligotrophy from Ultra-oligoTrophy
2194 PACific Experiment" (OUTPACE) cruise (EXPCODE 35A320150218) in the South Pacific Ocean from 2015-
2195 02-18 to 2015-04-03 (NCEI Accession 0177706). Version 1.1. NOAA National Centers for Environmental
2196 Information. Dataset. doi:10.25921/wbkb-0q19 [access date], 2018b.
2197
2198 Walton, D. W. H., and Thomas, J.: Cruise Report - Antarctic Circumnavigation Expedition (ACE) 20th
2199 December 2016 - 19th March 2017 (1.0). Zenodo. <https://doi.org/10.5281/zenodo.1443511>, 2018.
2200
2201 Wanninkhof, R., Park, G.-H., Takahashi, T., Sweeney, C., Feely, R., Nojiri, Y., Gruber, N., Doney, S. C.,
2202 McKinley, G. A., Lenton, A., Le Quééré, C., Heinze, C., Schwinger, J., Graven, H., and Khatiwala, S.: Global
2203 ocean carbon uptake: magnitude, variability and trends, *Biogeosciences*, 10, 1983–2000, doi:10.5194/bg-10-
2204 1983-2013, 2013.
2205
2206 Watson, A. J., Schuster, U., Bakker, D. C. E., Bates, N., Corbiere, A., Gonzalez-Davila, M., Freidrich, T.,
2207 Hauck, J., Heinze, C., Johannessen, T., Koertzinger, A., Metzl, N., Olafsson, J., Olsen, A., Oschlies, A., Padin,
2208 X., Pfeil, B., Rios, A., Santana-Casiano, M., Steinhoff, T., Telszewski, M., Wallace, D. W. R., and Wanninkhof,
2209 R.: Tracking the variable North Atlantic sink for atmospheric CO₂, *Science*, 326, 1391,
2210 doi:10.1126/science.1177394, 2009.
2211
2212 Watson, A. J., Schuster, U., Shutler, J.D. et al.: Revised estimates of ocean-atmosphere CO₂ flux are consistent
2213 with ocean carbon inventory. *Nat Commun* 11, 4422, <https://doi.org/10.1038/s41467-020-18203-3>, 2020.
2214
2215 Williams, N. L., Juranek, L. W., Johnson, K. S., Feely, R. A., Riser, S. C., Talley, L. D., et al.: Empirical
2216 algorithms to estimate water column pH in the Southern Ocean. *Geophysical Research Letters*, 43, 3415–3422.
2217 <https://doi.org/10.1002/2016GL068539>, 2016.
2218



- 2219 Williams, N. L., Juranek, L. W., Feely, R. A., Johnson, K. S., Sarmiento, J. L., Talley, L. D., Dickson,
2220 A. G., Gray, A. R., Wanninkhof, R., Russell, J. L., Riser, S. C., and Takeshita, Y.: Calculating surface
2221 ocean pCO₂ from biogeochemical Argo floats equipped with pH: An uncertainty analysis, *Global Biogeochem.*
2222 *Cycles*, 31, 591–604, doi:10.1002/2016GB005541., 2017.
2223
- 2224 Williams, N. L., Juranek, L. W., Feely, R. A., Russell, J. L., Johnson, K. S., and Hales, B.: Assessment of the
2225 carbonate chemistry seasonal cycles in the Southern Ocean from persistent observational platforms. *Journal of*
2226 *Geophysical Research: Oceans*, 123. <https://doi.org/10.1029/2017JC012917>, 2018.
2227
- 2228 Wimart-Rousseau, C., Lajaunie-Salla, K., Marrec, P., Wagener, T., Raimbault, P., Lagadec, V., Lafont, M.,
2229 Garcia, N., Diaz, F., Pinazo, C., Yohia, C., Garcia, F., Xueref-Remy, I., Blanc, P.-E., Armengaud, A., and
2230 Lefèvre, D.: Temporal variability of the carbonate system and air-sea CO₂ exchanges in a Mediterranean human-
2231 impacted coastal site. *Estuarine, Coastal and Shelf Science*. <https://doi.org/10.1016/j.ecss.2020.106641>, 2020a.
2232
- 2233 Wimart-Rousseau, C., Wagener, T., Raimbault, P., Lagadec, V., Lafont, M., Garcia, N., and Lefèvre, D.:
2234 Oceanic carbonate chemistry measurements from discrete samples collected at the SOLEMIO station (Bay of
2235 Marseille - North western Mediterranean Sea) between 2016 and 2019. *SEANOE*.
2236 <https://doi.org/10.17882/72356>, 2020b.
2237
- 2238 Wimart-Rousseau, C., Wagener, T., Álvarez, M., Moutin, T., Fourier, M., Coppola, L., Niclas-Chirurgien, L.,
2239 Raimbault, P., D'Ortenzio, F., Durrieu de Madron, X., Taillandier, V., Dumas, F., Conan, P., Pujo-Pay, M. and
2240 Lefèvre, D.: Seasonal and Interannual Variability of the CO₂ System in the Eastern Mediterranean Sea: A Case
2241 Study in the North Western Levantine Basin. *Front. Mar. Sci.* 8:649246. doi: 10.3389/fmars.2021.649246, 2021
2242
- 2243 WMO/GCOS, 2018: <https://gcos.wmo.int/en/global-climate-indicators>, 2018
2244
- 2245 Wu, Y., Hain, M. P., Humphreys, M. P., Hartman, S., and Tyrrell, T.: What drives the latitudinal gradient in
2246 open-ocean surface dissolved inorganic carbon concentration?, *Biogeosciences*, 16, 2661-2681,
2247 <https://doi.org/10.5194/bg-16-2661-2019>, 2019.
2248